CANADIAN THESES ON MICROFICHE

20983

THÈSES CANADIENNES SUR MICROFICHE

AUTHOR/AUTEUR

CHENG, E.H.-C.

TITLE/TITRE

ACTIVE FILTER SYNTHESIS.

20983

NATIONAL LIBRARY
OTTAWA

BIBLIOTHÈQUE NATIONALE
OTTAWA

NAME OF AUTHOR....Ephrem Hiu-Chung CHENG

TITLE OF THESIS.....ACTIVE FILTER SYNTHESIS

.....

.....

UNIVERSITY.....of Alberta, Edmonton

DEGREE FOR WHICH THESIS WAS PRESENTED.....Ph.D.....

YEAR THIS DEGREE GRANTED.....Spring 1974.....

Permission is hereby granted to THE NATIONAL LIBRARY OF CANADA to microfilm this thesis and to lend or sell copies of the film.

The author reserves other publication rights, and neither the thesis nor extensive extracts from it may be printed or otherwise reproduced without the author's written permission.

(Signed) E. H. C. Cheng

PERMANENT ADDRESS:

65 Fairway Heights Drive
Thornhill
Ont.

DATED..Nov. 19.....1973

NL-91 (10-68)

THE UNIVERSITY OF ALBERTA

ACTIVE FILTER SYNTHESIS

by

© EPHREM HIU-CHUNG CHENG

A THESIS

SUBMITTED TO THE FACULTY OF GRADUATE STUDIES

AND RESEARCH IN PARTIAL FULFILMENT OF THE

REQUIREMENTS FOR THE DEGREE OF

DOCTOR OF PHILOSOPHY

DEPARTMENT OF ELECTRICAL ENGINEERING

EDMONTON, ALBERTA

SPRING, 1974

THE UNIVERSITY OF ALBERTA

FACULTY OF GRADUATE STUDIES AND RESEARCH

The undersigned certify that they have read, and recommend to the Faculty of Graduate Studies and Research, for acceptance, a thesis entitled "ACTIVE FILTER SYNTHESIS" submitted by Ephrem Hiu-Chung CHENG in partial fulfilment of the requirements for the degree of Doctor of Philosophy.

Keith A. Stammore

Supervisor

D. Routledge

External Examiner

Date. 14 Nov 1973

ABSTRACT

In this dissertation, some general procedures for synthesizing filters using only R-C elements, unity-gain amplifiers, and operational amplifiers are discussed. Two approaches are taken. In Chapter II, second-order voltage transfer functions are realized by various methods to yield minumum sensitivity to parameter variations. Theories due to Calahan and Horowitz for optimal decomposition of the denominator polynomial are applied in the synthesis. The state-variable technique is also used to give the optimal result in terms of the number of capacitors used and the spread of element values. Two other methods, the coefficient-matching technique and the simulation of grounded inductances, lead to a low-sensitivity result with only three active elements. Transistor circuits are introduced to construct the unity-gain amplifiers. Experimental circuits using state-variable techniques and grounded-inductance simulation are constructed and tested. Practical results indicate a close relationship with the theory.

A different approach is taken for synthesis in Chapters III and IV. A high-order function is realized directly in one section. Operational amplifiers are employed to realize the negative immittance inverters which are used to replace the floating inductors in the filter configurations derived by conventional design. A sixth-order Chebyshev low-pass filter and a twelfth-order Butterworth band-pass filter are built with favorable results. A band-stop filter of the Cauer type with sharp frequency cutoff is designed in Chapter IV. All practical high-order filter circuits in these two chapters are also

tested with respect to temperature variations. Measured data indicate that the performance of these filters does not change significantly.

ACKNOWLEDGEMENTS

The author wishes to extend his appreciation to

- Dr. K. A. Stromsmoe for his inspirational supervision and guidance of this dissertation,
- Prof. Y. J. Kingma for his assistance, encouragement and permission to use laboratory equipment,
- Department of Electrical Engineering, University of Alberta, and the National Research Council of Canada for financial support throughout the years,
- Mr. W. K. Chan for drawing most of the figures,
- Mr. J. O. E. Gurke for reading the manuscript,
- His wife for her patience in typing the complete thesis,
- His parents and wife for their constant encouragement and support.

TABLE OF CONTENTS

		Page
Chapter 1	INTRODUCTION	
1.1	Background	1
1.2	Scope of the Thesis	15
Chapter II	SYNTHESIS OF INTEGRABLE SECOND-ORDER HIGH-Q FILTERS AND GROUNDED DRIVING-POINT ADMITTANCES USING GROUNDED UNITY-GAIN AMPLIFIERS	
2.1	Background	16
2.2	Ideal Models of Grounded Unity-Gain Amplifiers (GUGA's)	18
2.3	Active RC Filter Synthesis	18
	2.3.1 Calahan RC-RL Decomposition	20
	2.3.2 Synthesis of Horowitz RC-NIC Decomposition	26
	2.3.3 Synthesis of RC Filters by State-Variable Technique	29
	2.3.4 Synthesis of RC Active Filters by Coefficient-Matching Technique	35
2.4	Synthesis of Grounded Driving-point Admittance Functions	38
	2.4.1 Realizing a Grounded Inductance	39
	2.4.2 Realizing Grounded One-Port Negative R-L-C	41

		Page
2.5	Synthesis of the Second-Order Band-Pass Filter from a Passive Configuration	42
2.6	Experimental Circuits for Synthesizing Second-Order Band-Pass Filters	44
	2.6.1 Transistor Circuitry Using State-Variable Technique	45
	2.6.2 Experimental Second-Order Band-Pass Filter Synthesis Using a CUGA and Riordan's Gyrator	47
Chapter III	HIGH-ORDER INDUCTORLESS FILTERS SYNTHESIZED BY NEGATIVE IMMITTANCE INVERTERS (NIV'S)	
3.1	Background	58
3.2	Simulation of the Floating Inductor by NIV's	59
3.3	Realizing High-Order Transfer Functions by NIV's	62
	3.3.1 Realizing the Negative Resistance in the NIV by Operational Amplifier	64
3.4	Synthesis of a Sixth-Order Chebyshev Low-Pass Filter	65
3.5	Realizing a Grounded Inductor by a NIV	72
3.6	Synthesis of Fourth-Order Butterworth Band-Pass Filter	73

		Page
3.7	A Twelfth-Order Butterworth Band-Pass Filter Realized by NIV's	84
Chapter IV	ACTIVE INDUCTORLESS CAUER FILTERS	
4.1	Background	90
4.2	Active Synthesis of High-Order Cauer Band-Stop Filters	94
4.3	Realizing a Sixth-Order Cauer Band-Stop Filter	100
Chapter V	CONCLUDING REMARKS	
5.1	Conclusions	106
5.2	Suggestions for Further Research	107
	BIBLIOGRAPHY	109
	APPENDIX A	117
	APPENDIX B	122
	APPENDIX C	123
	APPENDIX D	124
	APPENDIX E	130
	APPENDIX F	132
	APPENDIX G	135
	APPENDIX H	138
	APPENDIX I	140
	APPENDIX J	141

LIST OF TABLES

Table	Title	Page
2.1	Realizing various Y_{21A}	25

LIST OF ILLUSTRATIONS

Figure	Title	Page
1.1	Third-order Cauer low-pass filter	3
1.2	Frequency response in magnitude of the third-order Cauer low-pass filter with the quality factor as a parameter	4
1.3	Frequency response of the filter given in Fig. (1.1) in the transition region	5
1.4	Fifth-order Cauer low-pass filter	6
1.5	Frequency response in magnitude of the fifth-order Cauer low-pass filter with the quality factor as a parameter	7
1.6	Frequency response of the filter given in Fig. (1.4) in the transition region	8
2.1	Ideal models of UGA's: (a) a non-inverting GVUGA, (b) an inverting GVUGA, (c) a GCUGA	19
2.2	General configuration for Calahan RC-RL decomposition	20
2.3	Band-pass filter by Calahan RC-RL decomposition	24
2.4	General configuration for Horowitz RC-NIC decomposition	26
2.5	General filter realization by Horowitz RC-NIC decomposition	29
2.6	A summing device	30
2.7	An integrating device	31
2.8	A general configuration by state-variable technique	32

Figure	Title	Page
2.9	Configuration to account for biasing resistance	35
2.10	Configuration realizing filters by coefficient-matching technique	36
2.11	Synthesis of grounded driving-point admittance from t_V ($t_V = V_2/V_1$).	38
2.12	Realization of $Y_{in} = (4P^2 - 5)/(4P^2 - 3)$ by $t_V = 2/(4P^2 - 3)$ and $Y = 1$	39
2.13	Simulation of a grounded inductance	40
2.14	Simulation of grounded one-port negative R-L-C	41
2.15	A passive Butterworth second-order band-pass filter	42
2.16	Simulation of L_X and C_X in parallel	42
2.17	An active second-order Butterworth band-pass filter	43
2.18	Schematic transistor circuit of band-pass filter for $Q = 30$, $\omega_0 = 10^5$ rad/sec	46
2.19	Frequency response of the second-order Butterworth band-pass active filter with a Q of 30, center frequency of 10^5 rad/sec	48
2.20	Frequency response of the second-order band-pass filter with a Q of 30, center frequency of 10^5 rad/sec in the neighborhood of resonance	49
2.21	Frequency response of the second-order Butterworth band-pass active filter with a Q of 200, center frequency of 200 K Hz	50

Figure	Title	Page
2.22	Frequency response of the second-order band-pass filter with a Q of 200, center frequency of 200 KHz in the neighborhood of resonance	51
2.23	Very high-Q band-pass filter	52
2.24a	Simulation of L_X, C_X, R_X; $S_C = S_R = Q$	54
2.24b	Simulation of L_X and R_X; $S_C = \sqrt{Q}$, $S_R = Q$	54
2.24c	Riordan's gyrator to simulate L_X; $S_C = 1$, $S_R = Q$, $L_X = G_2C/G_1G_3G_5$	54
2.25	Schematic diagram for very high-Q band-pass filter	55
2.26	Frequency response of filter using Riordan's gyrator for $Q = 500$, $\omega_0 = 10^4$	56
2.27	Frequency response of filter in the neighborhood of resonance	57
3.1	Two reciprocal, resistive NIV networks	59
3.2	A simpler notation for NIV	60
3.3	Cascading two NIV's	61
3.4	An admittance in cascade with an ideal transformer	61
3.5	Nth-order polynomial filters	62
3.6	Four equivalent two-port networks	63
3.7	An operational-amplifier circuit to simulate a negative grounded resistance	64
3.8	A passive R-L-C sixth-order Chebyshev low-pass filter	66
3.9	Transformation by NIV's	67
3.10	Simplification of Fig. (3.9)	67

Figure	Title	Page
3.11	An active sixth-order Chebyshev low-pass filter; f_{-3db} = 795.774 Hz	69
3.12	Frequency response of the active sixth-order Chebyshev low-pass filter; f_{-3db} = 795.774 Hz	70
3.13	Frequency response of the sixth-order Chebyshev low-pass filter in the neighborhood of the half-power point f_{-3db} = 795.774 Hz	71
3.14	Simulating a grounded inductor	72
3.15	Non-ideal realization of a grounded inductor	73
3.16	A second-order Butterworth low-pass filter	73
3.17	A fourth-order Butterworth band-pass filter	74
3.18	An equivalent fourth-order band-pass filter ($- R_y = - Q/2$, $- C_y = - 1/Q$, $- L_y = - Q$)	75
3.19	Simulation of negative R-L-C in parallel	75
3.20	Simulation of parallel-connected R-L-C by one operational amplifier	76
3.21	Active fourth-order Butterworth band-pass filter, f_0 = 795.774 Hz, Q = 5.0	77
3.22	Frequency response of a fourth-order Butterworth band-pass filter; Q = 5.0, f_0 = 795.774 Hz	79
3.23	Frequency response of a fourth-order Butterworth band-pass filter in the pass-band region; Q = 5.0, f_0 = 795.774 Hz	80

Figure	Title	Page
3.24	An active fourth-order Butterworth band-pass filter; $Q = 31.6$, $\omega_0 = 5 \times 10^3$	81
3.25	Frequency response of a fourth-order Butterworth band-pass filter; $Q = 31.6$, $\omega_0 = 5 \times 10^3$	82
3.26	Frequency response of a fourth-order Butterworth band-pass filter in the pass-band region; $Q = 31.6$, $\omega_0 = 5 \times 10^3$	83
3.27	A twelfth-order Butterworth band-pass filter	84
3.28	A twelfth-order Butterworth band-pass filter realized by NIV's	85
3.29	An active twelfth-order band-pass Butterworth filter, $Q = 10$, $f_0 = 795.774$	87
3.30	Frequency response of the active twelfth-order band-pass Butterworth filter; $Q = 10$, $f_0 = 795.774$ Hz	88
3.31	Frequency response of the active twelfth-order band-pass Butterworth filter in the pass-band region; $Q = 10$, $f_0 = 795.774$ Hz	89
4.1	The frequency-dependent negative-resistance (conductance) element realized by two operational amplifiers	90
4.2	A Cauer low-pass filter	91
4.3	A Cauer low-pass filter using FDNC's	92
4.4	A Cauer band-pass filter by using FDNC and FDNR elements	93
4.5	A Cauer band-stop high-order filter using FDNC and FDNR elements	94

Figure	Title	Page
4.6	Realization of a series combination of a resistor, a FDNC and a FDNR element by realizing two FDNR elements	96
4.7	An equivalent circuit to that in Fig. (4.6)	96
4.8	Realization of a series combination of a resistor, a FDNC and a FDNR element by realizing two FDNC elements	98
4.9	An equivalent circuit to that in Fig. (4.8)	98
4.10	A Cauer third-order low-pass filter	100
4.11	An equivalent circuit to that in Fig. (4.10)	101
4.12	The equivalent low-pass filter containing a FDNC element	102
4.13	A sixth-order Cauer band-stop filter	102
4.14	The active sixth-order Cauer band-stop filter for a minimum attenuation of 30db between f = 2100 and 2300 Hz	104
4.15	Frequency response of the band-stop filter with respect to temperature variations	105
A.1	Realizing an inverse-L of inductors	117
A.2	Realizing a π of inductors	120
A.3	Realizing a π of inductors and an inverse-polarity ideal transformer by NIV's	121
A.4	A second-order polynomial band-pass filter	122

CHAPTER I

INTRODUCTION

1.1 *BACKGROUND*

In conventional filter design the non-ideal characteristics of inductors result in a degradation of the filter performance. Many early attempts were made to overcome the problems associated with inductors by using R-C active filters with vacuum tubes originally used as the active elements. Cost, power consumption, size, weight among many factors were obstacles that limited the practical use of such filters. The invention of the transistor in 1948 helped to overcome some of these problems. The further development in manufacturing technology led to the availability of integrated-circuit operational amplifiers which are now widely used as the active element. The advancement in the performance of available active circuit elements has been paralleled by research in synthesis techniques that can be used for the construction of R-C active filters.

Many of the problems inherent to active filter design such as sensitivity and stability have been overcome. It is now both economical and practical in many applications to replace conventional filters by their active counterparts. As better active elements are developed the areas where active filters can be used to replace conventional filters will increase.

The advantages of active filters over conventional filters are multifold. Weight and space requirements are reduced. The output impedance of the amplifiers used as the active device is usually

low and thus the load impedance does not become a condition which must be satisfied in the design of the filter. Buffer amplifiers are not normally required, and insertion gain is possible without the use of additional amplifiers. Filters can be designed with a high input impedance and the source impedance is no longer a factor that must be considered.

The R-C active filter is not without disadvantages. The active elements require a power supply and power dissipation is greater than that in a passive structure. Resistors and capacitors are limited to moderate values. Performance of the active components limits the practical use of active filters to the audio range of frequencies. Stability and sensitivity are two serious problems; however, with proper design they can be brought under control. The dynamic range of the active filter is another limitation and moreover the active elements add additional noise to any system.

In practice, active filters are found most useful in the low frequency range where large inductances are usually required in the conventional filter design. Large-value inductors are difficult to manufacture, bulky, expensive and poor in quality. It is not just an alternative to use active design in the low frequency range but a necessity, especially for filters with a sharp-cutoff frequency characteristic. The following two examples will demonstrate the problems associated with inductors used in a conventional design.

Example 1:

Design objectives: Low-pass filter, Cauer type, third-

order, pass-band ripple of 1.25 db, minumum attenuation is 31.3 db and it occurs at the normalized radian frequency of 1.7434.

Conventional design of such a filter is given in Fig. (1.1).

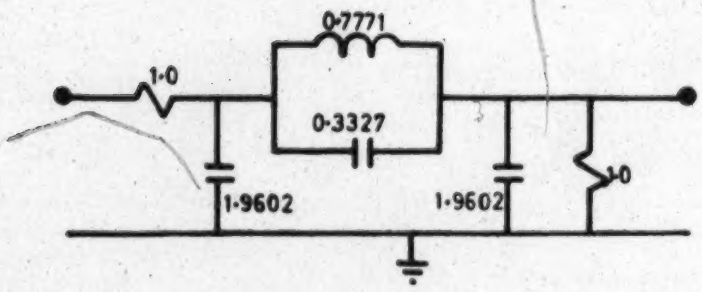

Figure (1.1) Third-order Cauer low-pass filter.

A family of normalized frequency response curves are shown in Fig. (1.2) and Fig. (1.3) where the quality factor for the inductor ($Q_L = \omega_n L/r$) is given as curve parameter ($\omega_n = 1$ in normalized value, r = internal resistance).

As the quality factor decreases the response curves deviate from the desired value and the transition region especially shows a marked deviation from the desired curve. In addition, the insertion loss is increased in the pass-band. It is, therefore, estimated that for $Q_L \leq 3.0$ approximately, the response deviates too much from the ideal case to be practically useful.

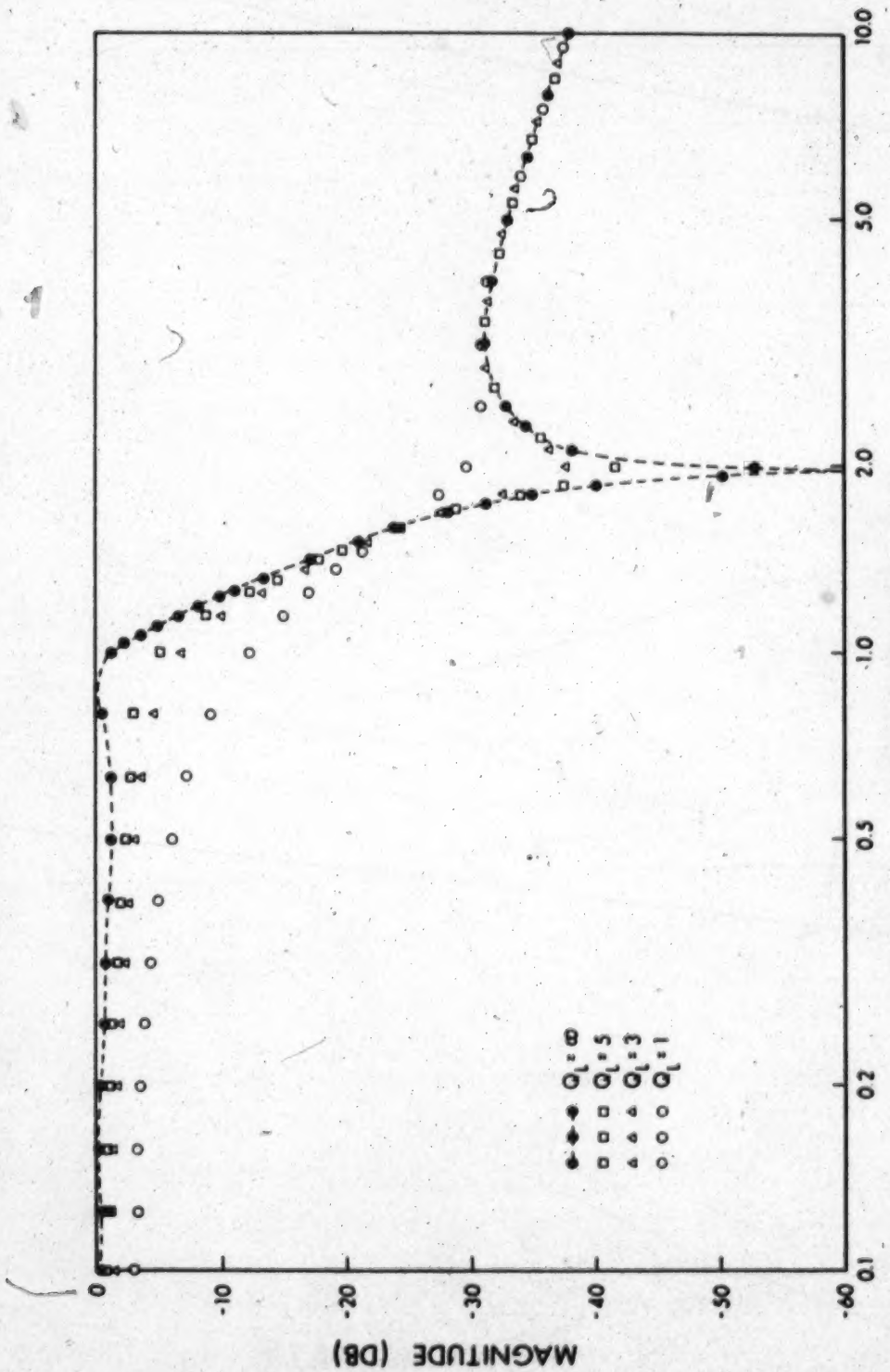

Figure (1.2) Frequency response in magnitude of the third-order Cauer low-pass filter with the quality factor as a parameter.

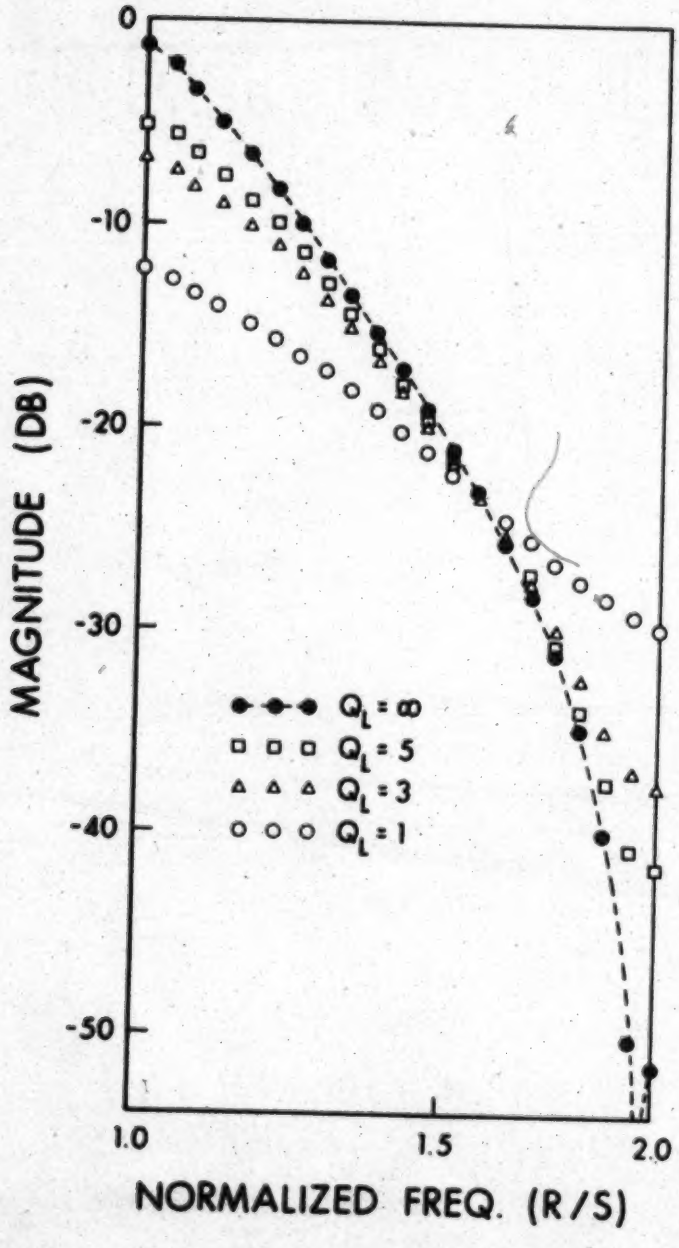

Figure (1.3) Frequency response of the filter given in Fig. (1.1) in the transition region.

Example 2:

Design objectives: low-pass filter, Cauer's type, fifth-order, pass-band ripple is 0.18 db, minimum attenuation is 61.43 db and it occurs at the normalized radian frequency of 2.0.

R-L-C filter by conventional design is given in Fig. (1.4).

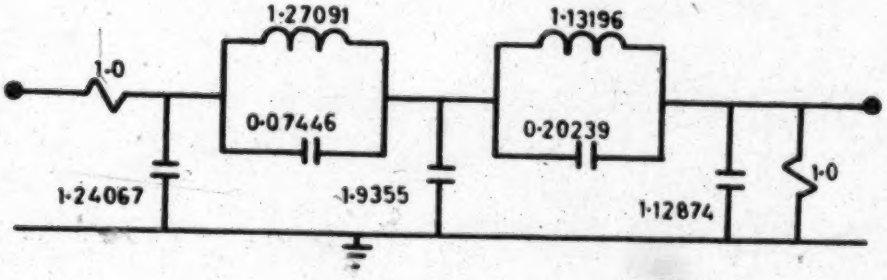

Figure (1.4) Fifth-order Cauer low-pass filter.

For convenience, all inductors in the circuit are assumed to have the same quality factor.

Again, Fig. (1.5) and Fig. (1.6) indicate that for $Q_L \leq 5.0$ approximately, the filter has too poor a response to be practically acceptable. It is estimated that inductors of even better quality are required for more severe conditions.

From these two examples, one can see that the low quality factor of inductors at low-frequency ranges causes very poor filter performance. That is why active inductorless filters are necessary in situations like these.

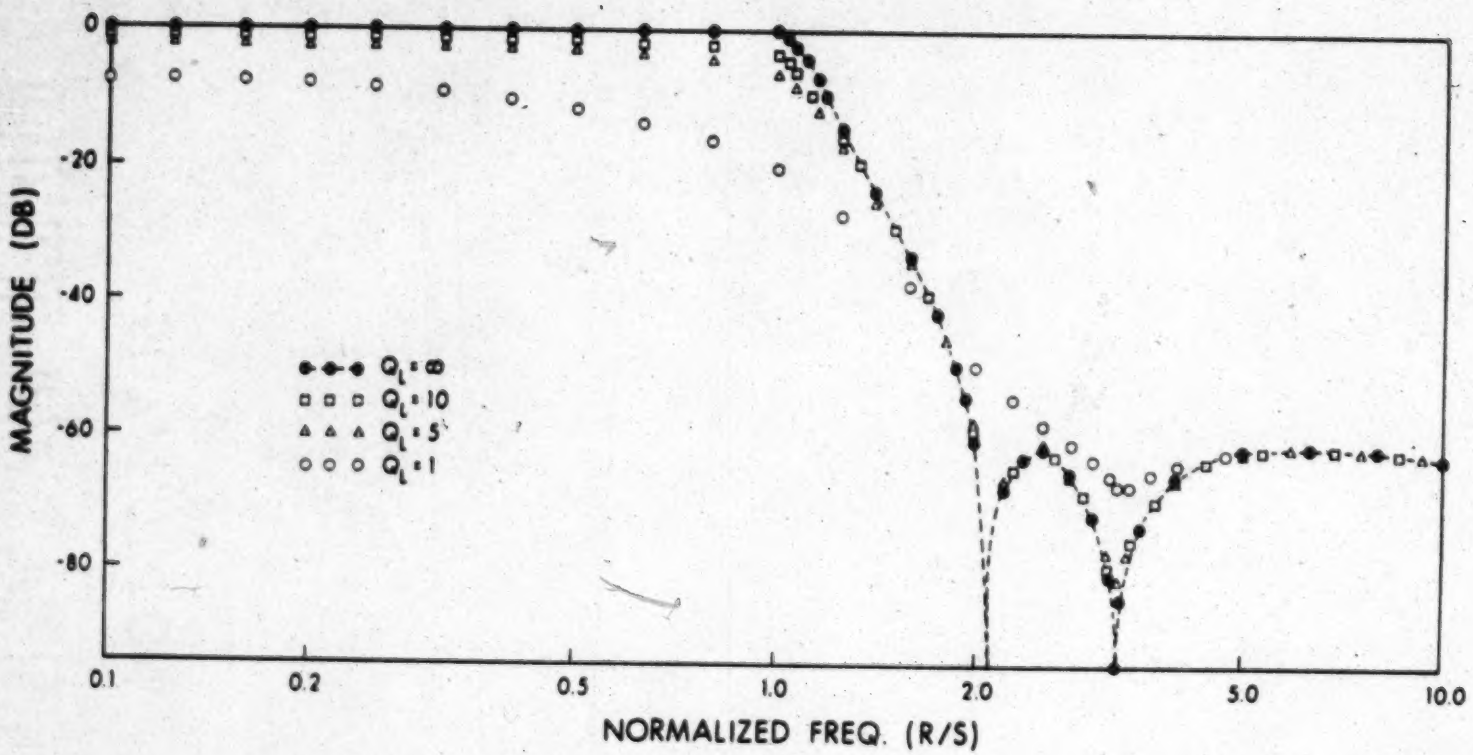

Figure (1.5) Frequency response in magnitude of the fifth-order Cauer low-pass filter with the quality factor as a parameter.

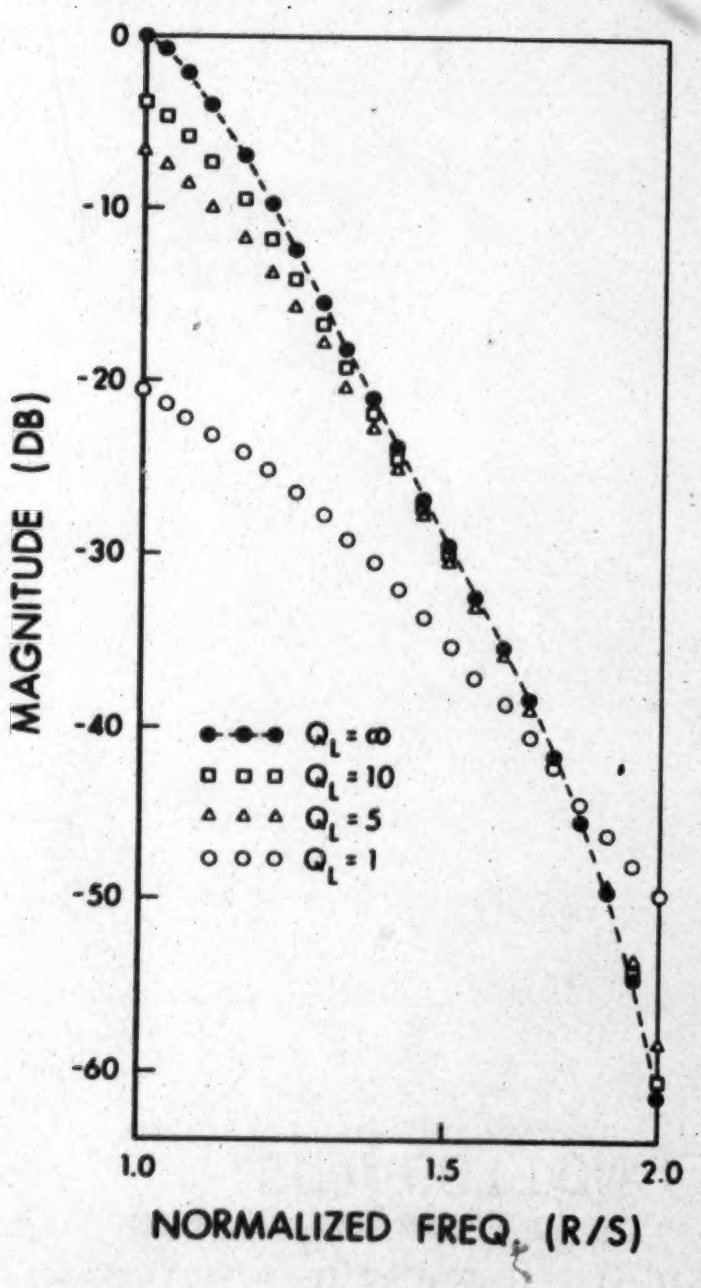

Figure (1.6) Frequency response of the filter given in Fig. (1.4) in the transition region.

There are many approaches used to synthesize R-C active networks, and the methods presented in this thesis can either be classified as the synthesis of basic second-order sections which are cascaded to form higher sections, or the direct synthesis where the passive structure is replaced by an equivalent circuit. Within this somewhat narrowed field, the following brief survey of the literature is selected to give representative approaches, since the contributions over the years have become too numerous to be listed completely. The references are listed in chronological order so as to give a broad overview of the directions and trends that have developed.

In 1955, Sallen and Key [1] published some twenty-five circuits for realizing various types of second-order voltage transfer functions using R-C passive elements and active amplifiers. In many cases, the active elements were simple cathode-followers with stable gain, high input impedance, low output impedance, and large dynamic range. Two experimental circuits using vacuum-tubes were constructed and tested. These filters operated well in the low frequency range below 30 Hz where the dissipation factors of available inductors were too large to permit the practical design of conventional filters. This paper is considered one of the significant contributions and some of their circuits are still in use. Hakim [2] proposed a new synthesis technique for low-pass filters which involved a voltage amplifier with a gain of two. The root sensitivity to parameter variations was minimized using the optimum decomposition of the denominator polynomial. Transistor circuits were used to realize the voltage and current

amplifiers.

In 1966, a sixth-order band-pass active filter with independent adjustment of poles and $j\omega$ axis zeros was proposed by Kerwin and Huelsman [3]. Three second-order filters were cascaded together. A low-gain amplifier was used in each section in which the output signal was fedback through a properly designed two-port R-C network.

One year later, Riordan [4] advanced a novel and effective method for synthesizing a grounded inductor using two operational amplifiers. High inductances and quality factors at low frequency were made possible. Grounded inductors in conventional filter design are simply replaced by the active realization. This circuit was found very useful in many later applications in active filter design. In the same year, Deboo [5] also reported a three-operational-amplifier design to realize a floating inductor by a gyrator circuit. An experimental third-order, low-pass, Cauer filter was constructed accordingly. The analog simulation of a second-order voltage transfer function had been well-known. However, Kerwin, Huelsman and Newcomb [6] formally published their result using state-variable synthesis for insensitive integrated circuit transfer functions. For second-order functions three operational amplifiers were used. In the same circuit, band-pass, low-pass and high-pass functions with the same denominator could be realized. The main advantages were very low sensitivity with respect to parameter changes, and independent adjustments of center frequency and quality factor. No more than the canonic number of capacitors (two) was required. The versatility and high performance of this design is the main reason why

commercially available active filters in the past few years have been based on this synthesis technique.

The idea was initiated by Bruton in 1968 [7] that a frequency-dependent negative resistor could be realized by positive-impedance-convertor-type networks. The concept was used to synthesize new types of inductorless selective networks. This work started a new trend of design ideas in later years. Geffe [8] introduced what was called a resonator which was realized by two operational amplifiers using the dual-integrator concept. One circuit was taken from Sallen and Key's catalogue and its usefulness was extended by active Q multiplication. Hilberman and Joseph [9] dealt with analysis and synthesis of admittance matrices of R-L-C and active common-ground networks. The concept was further extended by Hilberman [10] in realizing rational transfer and admittance matrices with unity-gain voltage amplifiers. However, the common terminal of the amplifiers was not necessarily connected to ground.

Holmes and Heinlein in 1969 [11] reported some capacitor-loaded semi-floating gyrator circuits for realizing sharp-cutoff low-pass filters. Temperature independence was tested and found to be satisfactory over a wide range. The theory of realizing gyrators with floating ports, gyrator Q-enhance, and component tolerances in filters was also discussed. Bruton [12] further developed his own ideas of using frequency-dependent negative resistance to realize the elliptic ladder low-pass filters. A two operational amplifier circuit was introduced to realize this active component. Tow [13] reported a new approach of active filter design by

following the described five-step process. Design methods using single-loop feedback or multi-loop feedback approach were critically examined by Mitra [14] with particular emphasis on sensitivity and construction problems. Soderstrand and Mitra [15] proposed a low-sensitivity second-order structure which had the minimum number of capacitors. Capacitor values were inversely proportional to the system Q.

In 1970, Moschytz [16] made a thorough study of the network characteristics of a nonideal operational amplifier which was used in most linear active filter synthesis. Cheung [17] advanced a new synthesis procedure using only unity-gain controlled-sources. The denominator could be decomposed in two ways: one with prescribed pole sensitivity, the other by Calahan's RC-RL decomposition. Moschytz [18] reported a versatile design approach by decomposing a given second-order function into a low-Q approximation of this function in cascade with an active frequency emphasizing network. Generalized immittance converters were used by Antoniou [19] to yield low-sensitivity for synthesis. A direct synthesis approach was taken to realize an eigth-order Butterworth transfer function. A circuit with a Q-invariant property obtained by optimizing the gains of amplifiers was published by Geffe [20]. However, the center frequency and band-width could still shift. The research reported by Orchard and Sheahan [21] made intensive use of Riordan's gyrator. Several experimental high-order band-pass filters were made to meet the severe requirements of telephone channel filters. Inigo [22] presented a circuit realizing a band-elimination second-order filter using a finite-gain voltage amplifier. Tarmy and Ghausi [23]

reported a second-order filter which was capable of very high-Q results by using differential-input differential-output finite gain amplifiers. Stable Q's up to about five thousand were obtained. Moschytz [24] found that proper selection of pole-zero pairs for the second-order realization of prescribed Nth-order network yielded minimum sensitivity.

The idea of using frequency dependent negative-resistance elements as the active devices was further extended by Antoniou [25] in 1971 for the synthesis of elliptic band-pass functions. Thomas [26] presented a new kind of active element called the biquad by using operational amplifiers. A compensation technique was derived to allow high-Q operation at several hundred kilohertz with high signal capacity and wide dynamic range.

In 1972, some new configurations for realizing second-order functions were introduced by Hamilton and Sedra [27]. The method was based on pole-zero cancellation of a twin-T network. Two operational amplifiers were used in the filter for a Q of about five hundred. Sensitivity of active-cascade and inductance-simulation schemes was compared in a paper by Holt and Lee [28]. Analytical results indicated that doubly terminated LC filters realized with simulated inductances had a limited improvement in sensitivity as compared with filters realized with a cascade of second-order active sections. Apart from all previously mentioned design methods using only linear active elements Bruton [29] recently reported some interesting results of using the analog multiplier as the basic nonlinear active element in the realization of an elliptic, high-order, low-pass function with tunable cutoff frequency. Realizations were simulated by

means of impedance scaling networks. A survey on the practical and economical aspects of active filters was made by Mattera [30]. Filter realizations by various methods were presented by Cheng and Stromsmoe [31] using current and voltage grounded unity-gain amplifiers.

1.2 *SCOPE OF THE THESIS*

This thesis deals with the synthesis of linear, lumped filters by passive R-C and linear active components only. Band-pass and band-stop filters are the main design objectives as they are usually more difficult to realize. Techniques are developed for filters to be used in the audio frequency range. Operation of such filters in a higher frequency range is limited by the design methods and performance of active devices. Furthermore, relative lower costs and satisfactory performance of passive R-L-C filters do not justify the use of their active counterparts [30]. Practical filters constructed in this dissertation do not require the use of high-performance operational amplifiers.

Six new methods discussed in Chapter II for realizing second-order functions are directly applicable to realizing polynomial filters such as those of Butterworth, Gaussian response, and Legendre response.

High-order polynomial filters realizable by a new direct synthesis technique are reported in Chapter III.

In Chapter IV, the Cauer band-stop filters are synthesized by a novel method which requires only a small number of active components. High-order direct synthesis is also possible in this case.

Experimental circuits based on the proposed design techniques are constructed and tested in most cases. Temperature effects on the performance of the filters are observed for several cases within the range of 22° C (72° F) to 70° C (158° F).

CHAPTER II

SYNTHESIS OF INTEGRABLE SECOND-ORDER HIGH-Q FILTERS AND GROUNDED DRIVING-POINT ADMITTANCES USING GROUNDED UNITY-GAIN AMPLIFIERS

2.1 *BACKGROUND*

Since high-order high-Q voltage transfer functions whether they be of Butterworth, Chebyshev, Cauer or other type can be broken down into those consisting of at most second-order functions, it is natural that one approach to realize all the poles and zeros of such a high-order function is to synthesize each complex pole-pair in second-order sub-functions. Cascading all the sub-sections (first-order functions for real poles), a very complex filter of high order can be synthesized. It is an easier problem because there are fewer variables to control. In addition, in many cases, the location of the complex pole-pair can easily be controlled just by changing some resistances which tune the filter in terms of center frequency ω_n and quality factor Q. In fact, most of the earlier work in this field has taken this approach instead of realizing the complex transfer function as a whole.

The most serious problem is that of sensitivity. It is not uncommon to find second-order filters to have a very high coefficient sensitivity of the denominator polynomial. Some are in the order of Q itself or even Q^2. In other words, one percent change in component values which may be due to component tolerances will give rise to 100% or even 10000% change in the coefficients for a given Q of one hundred. The location of poles will be altered roughly by the same order.

Temperature effects due to environmental changes and aging will also play an important role in slightly varying the characteristics of all the passive and active components. Thus, it is impossible to put such highly sensitive filters into practical use. High sensitivity appears often as a result of having two terms subtracting in the denominator polynomial. In other words, the result of subtraction of two very close and large numbers is a very sensitive one. It is mainly this reason that makes the design of a high-Q second-order filter difficult.

Various kinds of active device, such as controlled sources, negative values of resistance, inductance and capacitance, generalized immittance converters, gyrators, etc., have been used in the design [45],[49],[50],[51]. A unique kind of low-gain amplifier, the voltage and current unity-gain amplifiers (VUGA's and CUGA's) have become popular as the active element for synthesis [9],[10],[32],[33], [34],[35],[36],[47]. It has been found that the unity-gain amplifier is just as powerful as other commonly used active devices in many respects. Although it is considered as an amplifier, its isolating property is much more important than its amplifying property. Some of the many practical advantages for using such an element as the active device are simple construction, low cost, and high frequency response. In addition, using operational amplifiers, voltage unity gain amplifiers can be constructed with a highly stable gain.

By properly arranging the admittances at the output and input of the unity-gain amplifiers and the various amplifier sections, several methods are proposed to overcome the problem of sensitivity. Experimentally measured data from some hardware implementations constructed according to theory prove to be suitable for high Q

and very high Q requirements.

2.2 *IDEAL MODELS OF GROUNDED UNITY-GAIN AMPLIFIERS (GUGA'S)*

One can define two kinds of UGA's: the non-inverting and inverting VUGA's and the CUGA. Their ideal models are defined in Fig. (2.1). Referring to Fig. (2.1a), an ideal non-inverting VUGA is shown as a voltage controlled-voltage source amplifier having a gain (K) of unity with infinite input impedance and output admittance. An ideal inverting VUGA, as shown in Fig. (2.1b), differs only in the sign of the gain. Figure (2.1c) defines an ideal CUGA which is a current controlled-current source amplifier with current gain (I_2/I_1) of negative unity and infinite output impedance and input admittance. Note that the input and output voltages of these amplifiers are at a common ground.

The actual devices may deviate from the corresponding ideal models by having finite input and output impedances and a gain slightly different from unity. Practical UGA's have been built successfully [32],[35],[37],[48]. Alternatively, one may choose a one-transistor arrangement in a common-collector (emitter-follower), bootstrapping fashion, for the non-inverting GVUGA [38]. The GCUGA can be built to good approximation by using the superalpha Darlington configuration [39].

2.3 *ACTIVE RC FILTER SYNTHESIS*

R-C filters using GUGA's are realized by the following four methods: Calahan's [40],[41] and Horowitz's [42],[43] optimal decom-

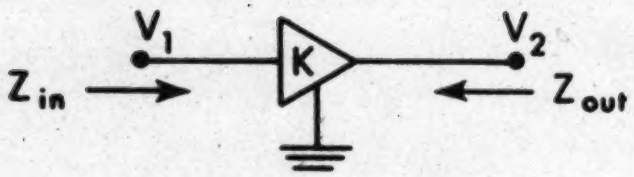

(a)

$V_2 = KV_1$, $Z_{in} = \infty$, $Z_{out} = 0$

NOMINAL $K = \bar{K} = 1.0$

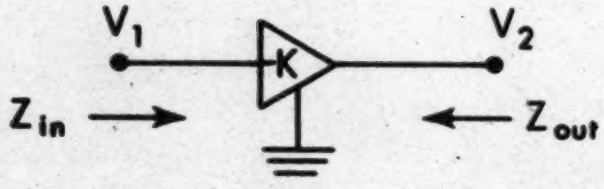

(b)

$V_2 = -KV_1$, $Z_{in} = \infty$, $Z_{out} = 0$

NOMINAL $K = \bar{K} = 1.0$

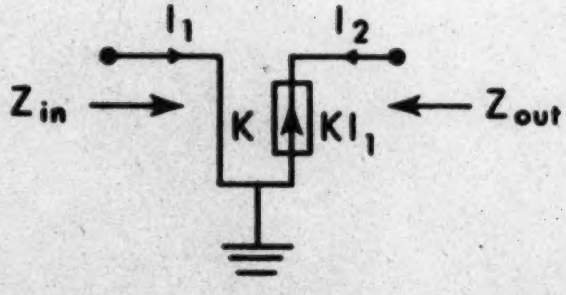

(c)

$I_2 = -KI_1$, $Z_{in} = 0$, $Z_{out} = \infty$

NOMINAL $K = \bar{K} = 1.0$

Figure (2.1) Ideal models of UGA's: (a) a non-inverting GVUGA, (b) an inverting GVUGA, (c) a GCUGA.

position of a given polynomial, state-variable and coefficient-matching techniques. It is well known that transfer functions of higher orders are better realized by cascading sections of, at most, second-order functions to obtain a lower sensitivity. For this reason, only the important case of realizing second-order voltage transfer functions is discussed. The first-order case, being obvious, is not treated.

2.3.1 Calahan RC-RL Decomposition

Consider the configuration in Fig. (2.2). The voltage transfer function is given by

$$-t_V = \frac{V_2}{V_1} = \frac{N(P)}{D(P)} = \frac{Y_{21A}\alpha}{(Y_F Y_C / Y_E) + \alpha Y_D} \qquad (2.1)$$

where $\alpha = K_{1234} = K_1 K_2 K_3 K_4$ and P is the complex frequency.

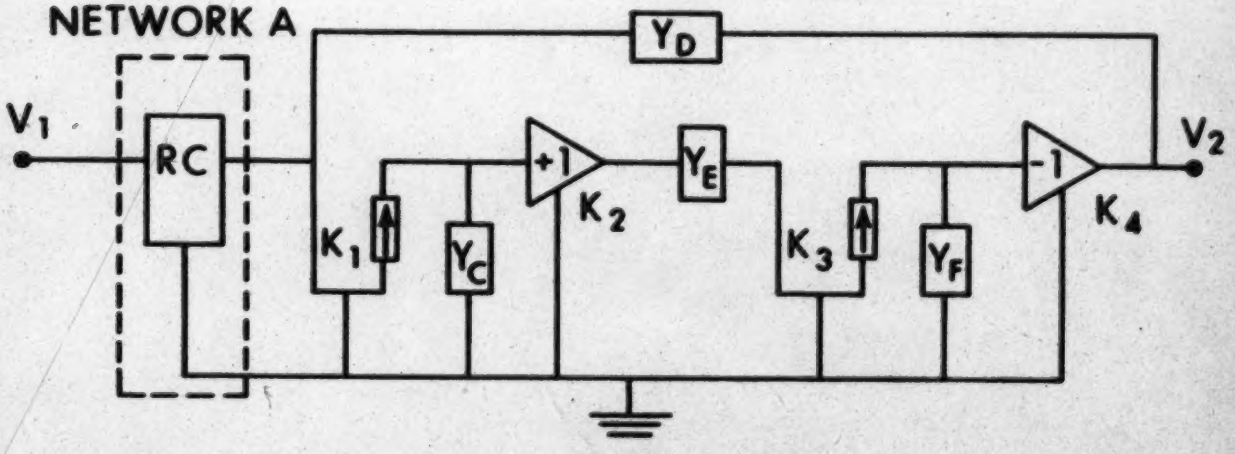

Figure (2.2) General configuration for Calahan RC-RL decomposition.

For an arbitrary polonomial $Q(P)$ one can write

$$-t_V = \frac{N(P)/Q(P)}{D(P)/Q(P)} \tag{2.2}$$

To apply Calahan's technique for optimal decomposition of the denominator polonomial one must express $D(P)/Q(P)$ as a sum of driving point RC and RL admittances. If one takes

$$Y_F = G_F = 1 \quad \text{and} \quad Y_C = G_C = 1,$$

then

$$\frac{D(P)}{Q(P)} = \frac{1}{Y_E} + {}_{\alpha}Y_D \tag{2.3}$$

and the denominator has the required form.

For the case of a second-order system t_V has the form

$$-t_V = \frac{N(P)}{P^2 + b_1P + b_2} = \frac{N(P)}{P^2 + 2\zeta P + 1} \tag{2.4}$$

where ζ = damping ratio ($\zeta < 1$), and the natural frequency ω_n has been normalized to unity. A convenient choice for $Q(P)$ that satisfies Calahan's decomposition requirements is

$$Q(P) = P + \zeta, \tag{2.5}$$

so that

$$-t_V = \frac{\frac{N(P)}{P+\zeta}}{\frac{P^2 + 2\zeta P + 1}{P + \zeta}} = \frac{\frac{N(P)}{P+\zeta}}{P + \zeta + \frac{1-\zeta^2}{P+\zeta}} \tag{2.6}$$

where

$$\frac{D(P)}{Q(P)} = P + \zeta + \frac{1-\zeta^2}{P+\zeta}. \tag{2.7}$$

Comparing (2.7) and (2.3), Y_E and Y_D can be specified as follows:

$$Y_D = P + \zeta = G_D + C_D P \ , \tag{2.8}$$

$$Y_E = \frac{P + \zeta}{1 - \zeta^2} = G_E + C_E P \ , \quad \text{provided} \quad \alpha = 1.0 \ . \tag{2.9}$$

Using (2.8), (2.9) and (2.1)

$$- t_V = \frac{- Y_{21A}(G_E S_E + P) S_D}{P^2 + P(G_E S_E + G_D S_D) + [G_D G_E S_D S_E + (G_C G_F S_D S_E/\alpha)]} \tag{2.10}$$

where

$S_D = 1/C_D$, $G_D = 1/R_D$, $S_E = 1/C_E$ and $G_E = 1/R_E$.

Investigation of the sensitivity of the denominator can be carried out by means of the sensitivity matrix [44], [45] . It relates the normalized sensitivity of the coefficients b_1, b_2 to all the normalized parameter variations in the circuit. The sensitivity matrix is computed in the following. One first defines a row vector of all the normalized parameter variations as

$$\Delta^{(n)}\chi = \underbrace{\Delta^{(n)} G_E \Delta^{(n)} S_E \Delta^{(n)} G_D \Delta^{(n)} S_D \Delta^{(n)} G_F \Delta^{(n)} G_C \Delta^{(n)} K_1 \Delta^{(n)} K_2 \Delta^{(n)} K_3 \Delta^{(n)} K_4}_{} \ .$$

In matrix form, one can express the sensitivity matrix as

$$\Delta^{(n)} b_{1,2} = S^{b1,b2}{}_{\Delta^{(n)}}{}^{T} \chi \tag{2.11}$$

where

$$\Delta^{(n)}b_{1,2} = \begin{bmatrix} \Delta^{(n)}b_1 \\ \\ \Delta^{(n)}b_2 \end{bmatrix}, \quad \Delta^{(n)T}X = \text{transpose of } \Delta^{(n)}X,$$

$$S^{b_1,b_2} = \begin{bmatrix} \frac{1}{2} & \frac{1}{2} & \frac{1}{2} & \frac{1}{2} & 0 & 0 & 0 & 0 & 0 & 0 \\ \\ \zeta^2 & 1 & \zeta^2 & 1 & 1-\zeta^2 & 1-\zeta^2 & -(1-\zeta^2) & -(1-\zeta^2) & -(1-\zeta^2) & -(1-\zeta^2) \end{bmatrix}. \quad (2.12)$$

The normalized Q sensitivity, S_X, with respect to any parameter variation is defined by

$$\frac{\Delta Q}{Q} = \frac{\Delta b_2}{2b_2} - \frac{\Delta b_1}{b_1} \quad . \quad (2.13)$$

From (2.11) and (2.12) one obtains

$$\Delta^{(n)}Q = S^Q \Delta^{(n)T}X$$

where

$$S^Q = \left[-\tfrac{1}{2}(1-\zeta^2) \;\; 0 \;\; -\tfrac{1}{2}(1-\zeta^2) \;\; 0 \;\; \frac{1-\zeta^2}{2} \;\; \frac{1-\zeta^2}{2} \;\; -\left(\frac{1-\zeta^2}{2}\right) \;\; -\left(\frac{1-\zeta^2}{2}\right) \;\; -\left(\frac{1-\zeta^2}{2}\right) \;\; -\left(\frac{1-\zeta^2}{2}\right) \right] . \quad (2.14)$$

From (2.12) and (2.14) one can see that all expressions for the sensitivity coefficients are independent of the element values, and low for high-Q values. Thus high-Q bandpass filters are realizable.

The spread of element values is defined as the ratio of two elements of the same kind of extremal values. The spreads of resistance (S_R) and capacitance (S_C) are found to be

$$S_R = 1/\zeta = 2Q \quad \text{(for high Q)} ,$$

$$S_C = 1/(1-\zeta^2) = 1.0 \quad \text{(for high Q)} .$$

For a given voltage transfer function,

$$-t_V = -\frac{V_2}{V_1} = \frac{HP}{P^2 + 2\zeta P + 1} \quad (\omega_n=1,\ \zeta < 1) ,$$

the bandpass filter is realized in Fig. (2.3). Synthesis of other types of filters follow the same procedure with changes only in the realizations of Network A as summarized in the table. With other choices of the factor Q(P) different realizations would be possible.

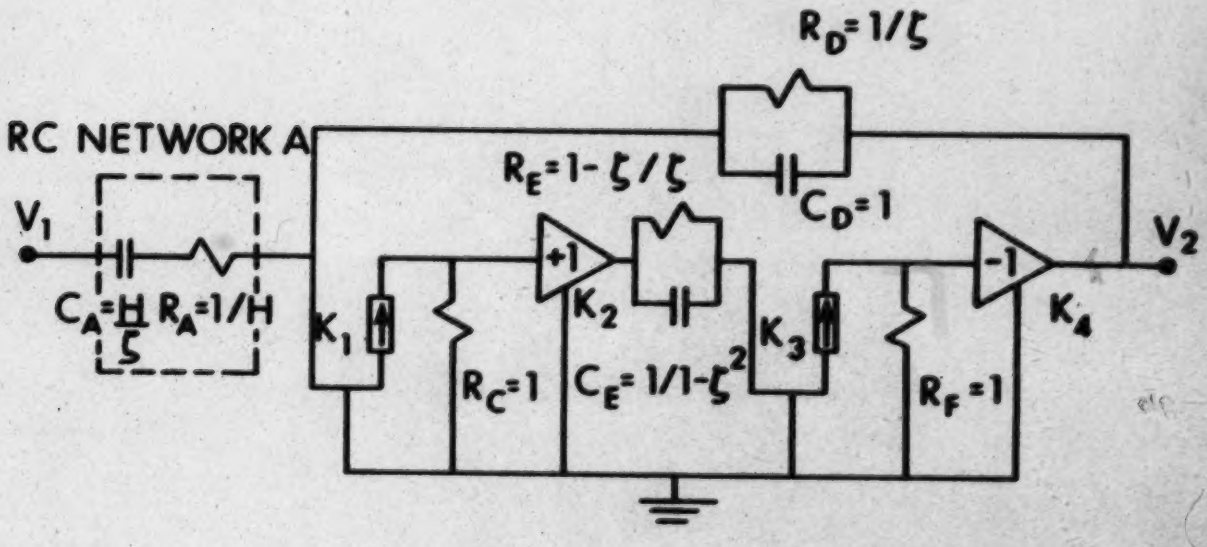

Figure (2.3) Bandpass filter by Calahan RC-RL decomposition.

TRANSFER FUNCTION	NETWORK A
$-t_v = \dfrac{Hp^2}{p^2+2\zeta p+1}$	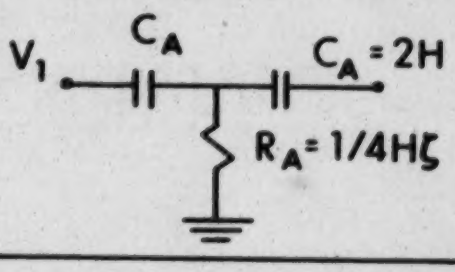
$-t_v = \dfrac{H}{p^2+2\zeta p+1}$	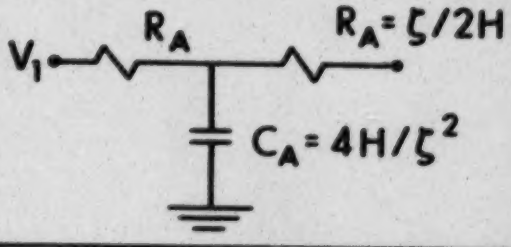
$-t_v = \dfrac{H(p-a)}{p^2+2\zeta p+1}$ $(a>0)$	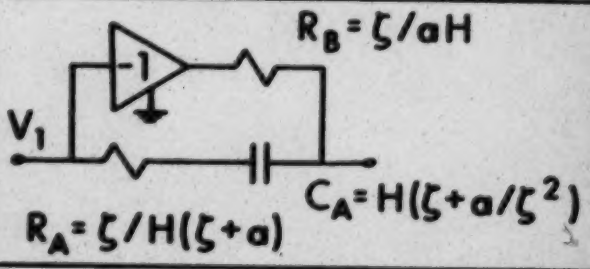
$-t_v = \dfrac{H(p^2-2\zeta p+1)}{p^2+2\zeta p+1}$	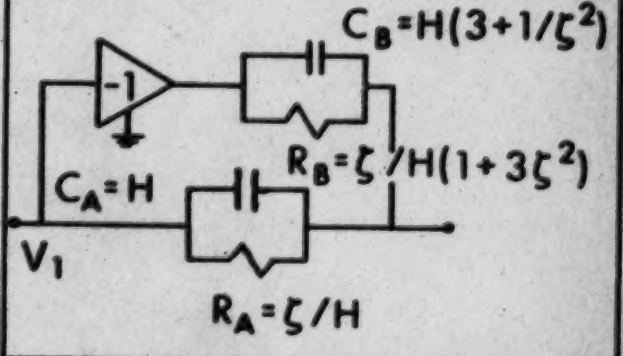

Table (2.1) Realizing various Y_{21A} .

2.3.2 Synthesis Of Horowitz RC-NIC Decomposition

If sensitivity requirement is not severe, a configuration with basically only two GUGA's is found suitable for realizing filters with application of Horowitz RC-NIC minimum-sensitivity decomposition of the denominator polynomial.

Consider the configuration in Fig. (2.4). Straightforward analysis yields

$$t_V = \frac{V_2}{V_1} = \frac{N(P)}{D(P)} = \frac{-K_{12}Y_{21A}}{Y_C - K_{12}Y_D} \qquad (2.15)$$

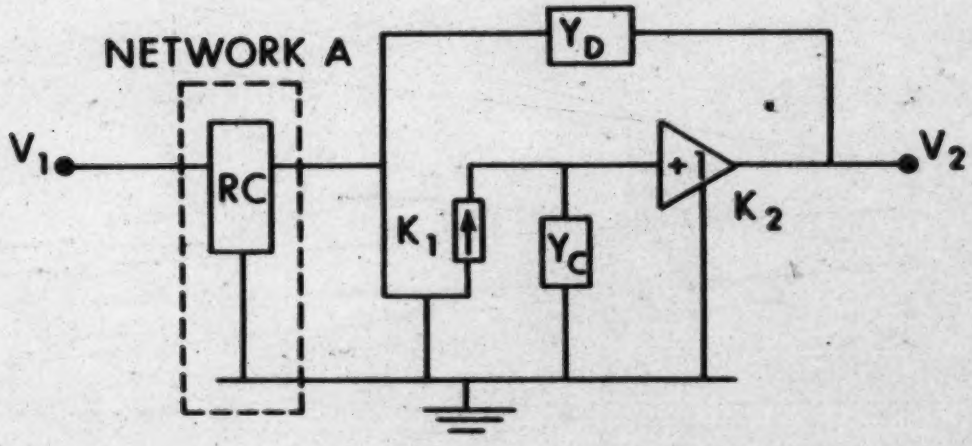

Figure (2.4) General configuration for Horowitz RC-NIC decomposition.

where

$$K_{12} = K_1 K_2 \ , \ \bar{K}_i = 1.0 \ , \ i=1, 2 \ .$$

Again making a simple choice for $Q(P)$ let

$$Q(P) = P + 1 \quad (1 < 0)$$

such that

$$t_V = \frac{N(P)/Q(P)}{D(P)/Q(P)} \quad .$$

According to Horowitz for the second-order case, minmum sensitivity will result if $D(P)/Q(P)$ is expressed as the difference of two RC driving-point admittances. Thus for the $Q(P)$ selected,

$$Y_C = G_C + C_C P \ , \quad Y_D = \frac{PG_D}{P + G_D S_D}$$

Equation (2.15) becomes

$$t_V = \frac{-K_{12} Y_{21A} S_C (P + G_D S_D)}{P^2 + P(G_D S_D + G_C S_C - K_{12} G_D S_C) + G_C G_D S_C S_D}$$

where

$$S_X = 1/C_X \ , \quad G_X = 1/R_X \ , \quad X = C \ , \ D \quad .$$

To realize a given voltage transfer function of the form

$$t_V = \frac{V_2}{V_1} = \frac{N(P)}{D(P)} = \frac{N(P)}{P^2 + b_1 P + b_2} = \frac{N(P)}{P^2 + 2\zeta P + 1} \quad .$$

By Horowitz's theory, with $Q(P) = P + 1 = P + \omega_n = P + 1$,

$$t_V = \frac{\frac{N(P)}{P+1}}{\frac{P^2 + 2\zeta P + 1}{P+1}} = \frac{\frac{N(P)}{P+1}}{(P+1) - \frac{2(1-\zeta)P}{P+1}} \tag{2.16}$$

where

$$\frac{D(P)}{Q(P)} = (P+1) - \frac{2(1-\zeta)P}{P+1} .$$

Comparing (2.15) and (2.16)

$$Y_C = P + 1 , \quad Y_D = \frac{2(1-\zeta)P}{P+1} , \tag{2.17}$$

where the nominal value of $\bar{K}_{12} = 1.0$ is assumed.

From (2.17) one has

$$G_C = 1.0 , \quad C_C = 1.0 , \quad G_D = 2(1-\zeta) , \quad C_D = 2(1-\zeta) .$$

The normalized sensitivity matrix is computed as

$$S^{b1,b2} = \begin{bmatrix} \frac{-1+2\zeta}{2\zeta} & \frac{1}{2\zeta} & \frac{1}{2\zeta} & \frac{-1+2\zeta}{2\zeta} & \frac{-(1-\zeta)}{\zeta} & \frac{-(1-\zeta)}{\zeta} \\ 1 & 1 & 1 & 1 & 0 & 0 \end{bmatrix}$$

where

$$\Delta^{(n)}X = \underbrace{\Delta^{(n)}G_D\ \Delta^{(n)}S_D\ \Delta^{(n)}G_C\ \Delta^{(n)}S_C\ \Delta^{(n)}K_1\ \Delta^{(n)}K_2}\ .$$

The maximum sensitivity coefficient is

$$\max\ |S_X^{b1,b2}| = |S^{b1}_{K1,K2}| = 1/\zeta = 2Q \quad \text{(for high Q)}\ .$$

Therefore, the configuration yields much higher sensitivity when compared to the previous one. Consequently, filters so designed are suitable for moderate or low Q-values. The Q-sensitivity can be readily obtained by using (2.9). Spread of resistance and capacitance is low; $S_R = S_C = 2(1-\zeta)$. A general configuration is shown in Fig. (2.5).

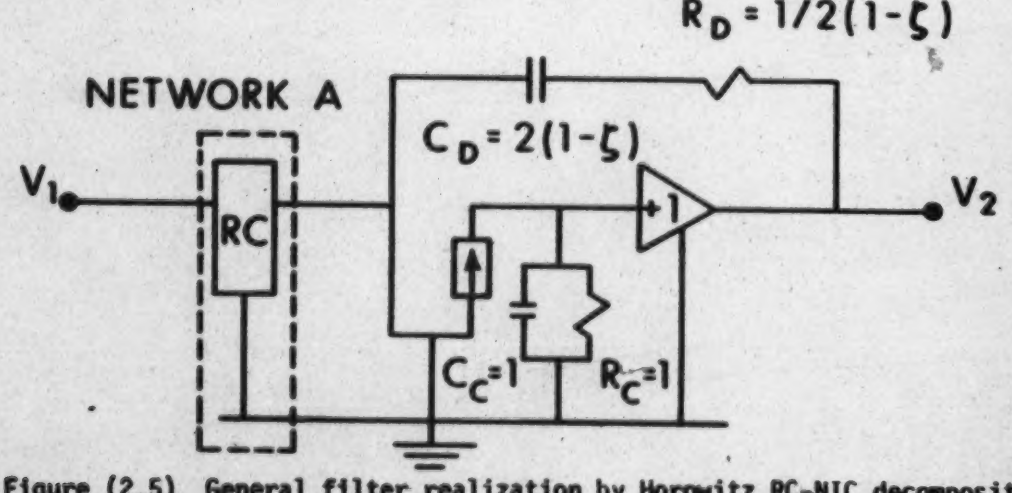

Figure (2.5) General filter realization by Horowitz RC-NIC decomposition.

2.3.3 Synthesis Of RC Filters By State-Variable Technique

State-variable technique has proven very effective for realizing low-sensitivity filters using operational amplifiers [6]. The main idea

lies in the fact that realization of voltage transfer functions by this technique yields coefficients (b_1, b_2) containing only product (or division) expressions of parameters concerned. Thus the sensitivity coefficient is either ± 1.0 or zero [45]. This method is easily applicable and general in nature. Devices that perform the two basic functions necessary in state variable technique are shown in Figs. (2.6) and (2.7). Referring to Fig. (2.6),

$$V_2' = V_1 \frac{G_1}{G_F} + V_2 \frac{G_2}{G_F} + \ldots + V_N \frac{G_N}{G_F} \quad .$$

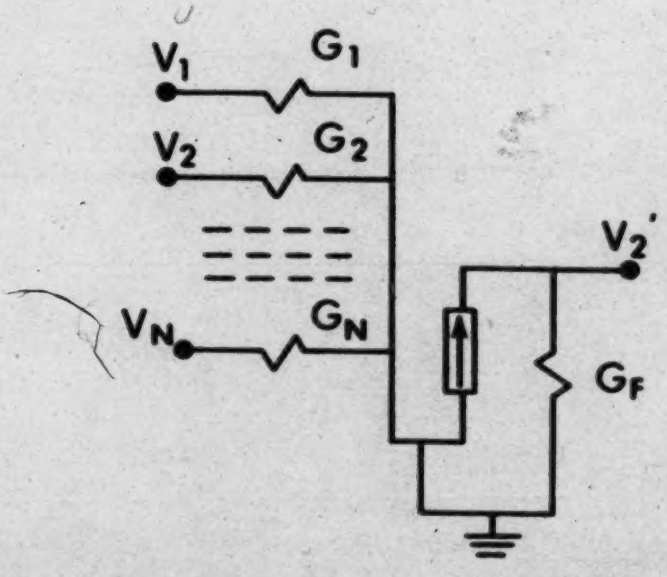

Figure (2.6) A summing device.

A summing device is formed with gains independently adjusted by various admittances. Figure (2.7) indicates a pure integrator

$$\frac{V_2}{V_1} = \frac{1}{R_1 C_F p} \quad .$$

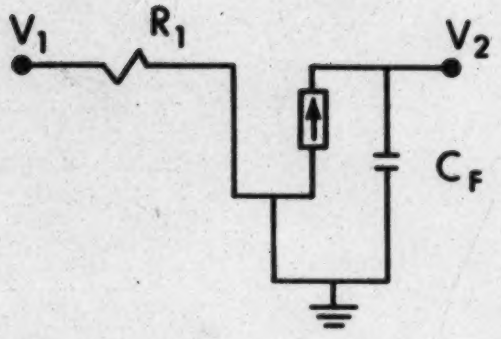

Figure (2.7) An integrating device.

The two functions can be combined as shown in the configuration of Fig. (2.8). The various types of filters at different locations of Fig. (2.8) can be computed as

$$\frac{V_A}{V_1} = \frac{R_4}{R_1} \frac{P^2}{\left(P^2 + P\frac{R_4 K_{234}}{R_2 R_5 C_1} + \frac{R_4}{R_3 R_5 R_6 C_1 C_2} K_{23456} \right)}$$

which is a high-pass voltage transfer function;

$$-\frac{V_B}{V_1} = \frac{R_4}{R_1 R_5 C_1} \frac{K_{234} P}{\left(P^2 + P \frac{R_4}{R_2 R_5 C_1} K_{234} + \frac{R_4}{R_3 R_5 R_6 C_1 C_2} K_{23456} \right)}$$

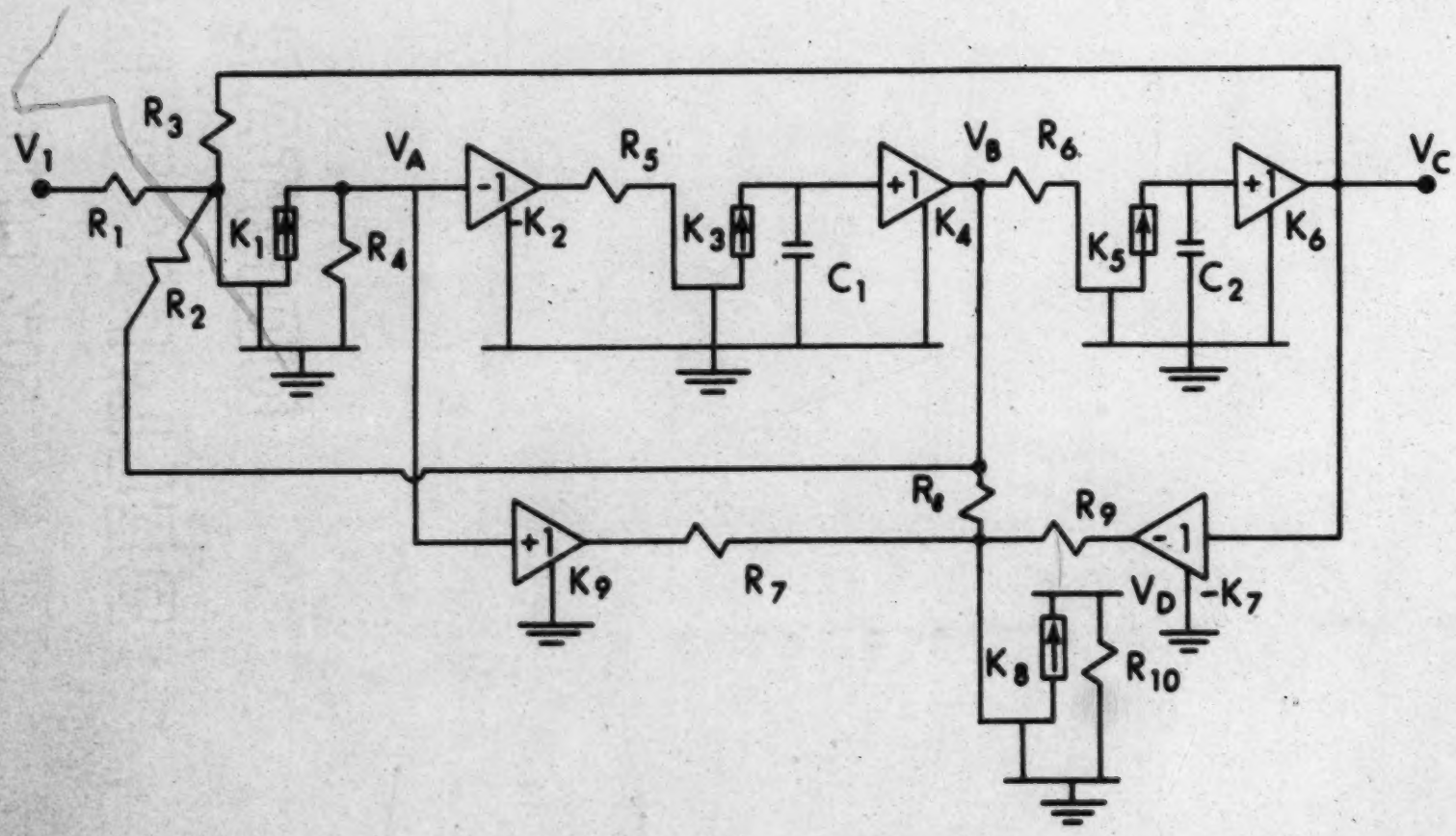

Figure (2.8) A general configuration by state-variable technique.

which is a bandpass voltage transfer function;

$$\frac{-V_C}{V_1} = \frac{R_4}{R_1R_5R_6C_1C_2} \frac{K_{23456}}{\left(P^2 + P \frac{R_4}{R_2R_5C_1} K_{234} + \frac{R_4}{R_3R_5R_6} \frac{K_{23456}}{C_1C_2} \right)}$$

which is a low-pass voltage transfer function;

$$\frac{V_D}{V_1} = \frac{R_4R_{10}}{R_1R_7} K_{89} \frac{\left(P^2 - \frac{R_7}{R_5R_8C_1} \frac{K_{234}}{K_9} P + \frac{R_7}{R_5R_6R_9C_1C_2} \frac{K_{234567}}{K_9} \right)}{\left(P^2 + P \frac{R_4}{R_2R_5C_1} K_{234} + \frac{R_4}{R_3R_5R_6C_1C_2} K_{23456} \right)}$$

which is an all-pass voltage transfer function.

The normalized sensitivity matrix of coefficients (b_1, b_2) of the denominator can be given by inspection as

$$S^{b_1, b_2} = \begin{bmatrix} 0 & -1 & 0 & 1 & -1 & 0 & 0 & 0 & 0 & 0 & -1 & 0 & 0 & 1 & 1 & 1 & 0 & 0 & 0 & 0 & 0 \\ 0 & 0 & -1 & 1 & -1 & -1 & 0 & 0 & 0 & 0 & -1 & -1 & 0 & 1 & 1 & 1 & 1 & 1 & 0 & 0 & 0 \end{bmatrix}$$

and the Q-sensitivity is

$$S^Q = \underbrace{0 \; 1 \; -\tfrac{1}{2} \; -\tfrac{1}{2} \; \tfrac{1}{2} \; -\tfrac{1}{2} \; 0 \; 0 \; 0 \; 0 \; \tfrac{1}{2} \; -\tfrac{1}{2} \; 0 \; -\tfrac{1}{2} \; -\tfrac{1}{2} \; -\tfrac{1}{2} \; \tfrac{1}{2} \; \tfrac{1}{2} \; 0 \; 0 \; 0}$$

where

$$\Delta^{(n)}X = \underbrace{\Delta^{(n)}R_1 \ldots \Delta^{(n)}R_{10}\ \Delta^{(n)}C_1\ \Delta^{(n)}C_2\ \Delta^{(n)}K_1 \ldots \Delta^{(n)}K_9}\ .$$

All sensitivity coefficients are independent of Q and element values. Sensitivity can be further reduced by properly arranging the temperature coefficients of all active and passive elements as indicated by the above two matrices. As it is shown in Fig. (2.8), in order to realize a high-Q bandpass filter, six active UGA's, six resistors and only two capacitors are used. Usually, in integrated circuits, capacitors are the more critical elements compared to transistors and resistors. Besides one can get rid of amplifiers K_4, K_6, K_9 provided R_2, R_6, $R_8 >> 1/C_1P$, $R_3 >> 1/C_2P$ and $R_7 >> R_4$ in the frequency range of interest. Element values can be conveniently chosen to satisfy

$$b_1 = 2\zeta = \frac{R_4}{R_2R_5C_1} \quad \text{and} \quad b_2 = \frac{R_4}{R_3R_5R_6C_1C_2} = 1.0\ .$$

Hence, resistors can be used advantageously to tune each section, and the spread of resistance and capacitance is low. Sometimes, in order to account for biasing resistance at the output of each GCUGA, it is convenient to realize the filter by blocks of transfer functions of $1/(P + M)$ $(M > 0)$ types instead of those of pure integrators, $1/P$. This is easily done for the case of low-pass filters. However, in view of Fig. (2.9), the pure integrator can be replaced by one with transfer function of $1/(P + M)$ as illustrated in the following:

$$\frac{V_2}{V_1} = \frac{Y_A}{Y_C - Y_D} .$$

Let $Y_A = G'$, $Y_D = G$, $Y_C = G + C_P$; the above equation then becomes

$$\frac{V_2}{V_1} = \frac{G'}{C_P} .$$

Any finite output impedance of the GCUGA and finite input impedance of the following GVUGA can also be easily absorbed into Y_C in Fig. (2.9).

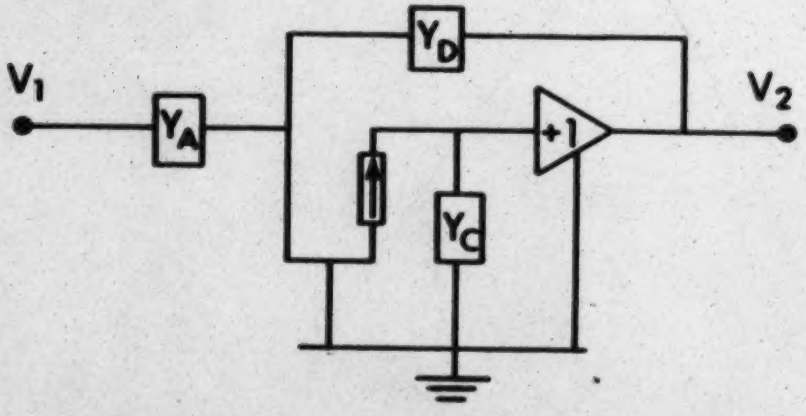

Figure (2.9) Configuration to account for biasing resistance.

2.3.4 Synthesis Of RC Active Filters By Coefficient-Matching Technique

Consider the configuration shown in Fig. (2.10). Analysis gives

$$-t_V = -\frac{V_2}{V_1} = \frac{K_{123}\, Y_A\, Y_E}{Y_F(Y_C + Y_F) + K_{123} Y_D\, Y_E} . \qquad (2.18)$$

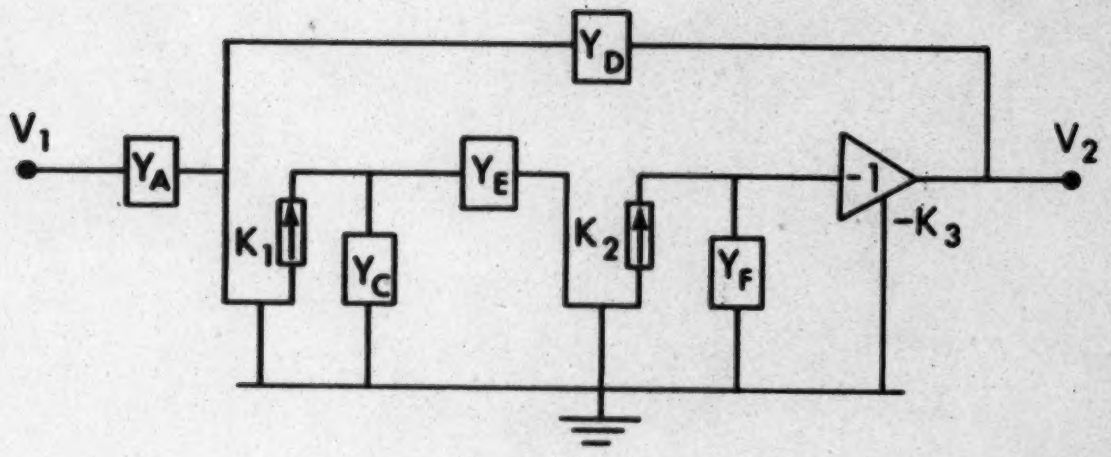

Figure (2.10) Configuration realizing filters by coefficient-matching technique.

Let $Y_D = C_D P$, $Y_E = C_E P$, $Y_F = G_F$, $Y_C = G_C$. Equation (2.18) then becomes

$$- t_V = - \frac{V_2}{V_1} = \frac{Y_A S_D P}{P^2 + P \frac{G_F S_D}{K_{123}} + \frac{G_C G_F S_D S_E}{K_{123}}} .$$

The normalzied sensitivity is given by inspection as

$$S^{b1, b2} = \begin{bmatrix} 0 & 0 & 1 & 1 & 0 & -1 & -1 & -1 \\ 0 & 1 & 1 & 1 & 1 & -1 & -1 & -1 \end{bmatrix}$$

$$S^{Q} = \underbrace{0 \quad \tfrac{1}{2} \quad -\tfrac{1}{2} \quad -\tfrac{1}{2} \quad \tfrac{1}{2} \quad \tfrac{1}{2} \quad \tfrac{1}{2} \quad \tfrac{1}{2}}$$

where

$$\Delta^{(n)}X = \underbrace{\Delta^{(n)}G_A\ \Delta^{(n)}G_C\ \Delta^{(n)}G_F\ \Delta^{(n)}S_D\ \Delta^{(n)}S_E\ \Delta^{(n)}K_1\ \Delta^{(n)}K_2\ \Delta^{(n)}K_3}\ .$$

Again, sensitivity coefficients are all independent of Q and element values. If we assume $Y_A = G_A$, a bandpass filter results. Its element values are given by $G_F S_D = b_1$, $G_A S_D = H$, $G_C S_E = 1/b_1$. Spread of resistance and capacitance is low, $S_R = S_C = Q$. If the resistors and capacitors are replaced by each other, a new bandpass filter is obtained. Choosing $Y_A = C_A P$ would lead to a high-pass realization. Element values are given as before except $C_A S_D = H$. If one chooses $Y_A = G_A$, $Y_E = G_E$, $Y_D = G_D$, $Y_C = C_C P$, $Y_F = C_F P$, one has

$$-t_V = -\frac{V_2}{V_1} = \frac{K_{123} G_A G_E S_C S_F}{P^2 + P G_E S_C + K_{123} G_E G_D S_C S_F}\ .$$

A low-pass filter is realized with element values determined by $G_E S_C = b_1$, $G_D S_F = 1/b_1$, $G_A G_E S_C S_F = H$. Again max $|S_X^{b1,\ b2}| = 1.0$, $S_R = S_C = Q$.

Hence, a high-quality bandpass filter is realizable by this method with only three active UGA's, two capacitors, three resistors, and the spread of element values is reasonably low. Alternatively, if one gets rid of amplifier K_3 and inserts an inverting GVUGA between Y_C and Y_E in Fig. (2.10), one has correspondingly parallel results for all three kinds of filters. However, in this case, one more GVUGA is needed at the output terminal for isolation purposes if cascading of several sections is desired.

2.4 *SYNTHESIS OF GROUNDED DRIVING-POINT ADMITTANCE FUNCTIONS*

By a simple and basic configuration one can relate the synthesis of a grounded driving-point admittance to that of a voltage transfer function. Since any voltage transfer function of a ratio of real-rational polynomials can be realized with high accuracy by using state-variable techniques as illustrated previously, any grounded driving-point admittance of the same nature is readily obtained. Consider the configuration as shown in Fig. (2.11) [9], [10]. The input admittance is given by $Y_{in} = I_1/V_1 = Y(1 - t_V)$. (2.19)

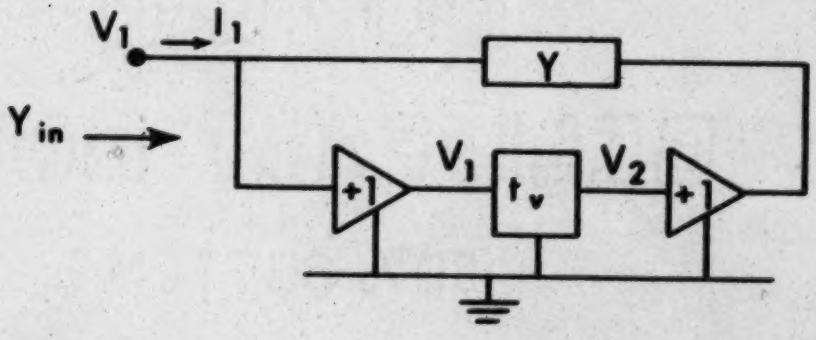

Figure (2.11) Synthesis of grounded driving-point admittance from t_V ($t_V = V_2/V_1$).

Therefore, for any specified Y_{in} one has only to realize the corresponding t_V by assuming a convenient Y. The restriction in Hilberman's case [10] that the UGA's must not be grounded is relaxed here as shown in Fig. (2.11). (Only one kind of UGA's, the non-inverting VUGA, is used in his case.) Furthermore, in order to realize the driving-point admittance of a ratio of real-rational polynomials by his method, one

has to realize the voltage transfer function as a ratio of two driving-point admittances first, $t_V = Y'/Y''$ [10] where Y' and Y" are realized respectively by a sum of parallel-connected driving-point admittances, and then to go through the procedure in Fig. (2.11), viz. $Y_{in}=Y(1 - t_V)$. This obviously requires an excessive number of both active and passive elements. An example will demonstrate the simplicity and ease of applying the state-variable technique to realize a grounded driving-point admittance as the following:

Suppose one is given for realization $Y_{in} = (4p^2 - 5)/(4p^2 - 3)$. For convenience, let Y = 1.0. From (2.19), $t_V = V_2/V_1 = 2/(4p^2 - 3)$. The required Y_{in} is realized in Fig. (2.12).

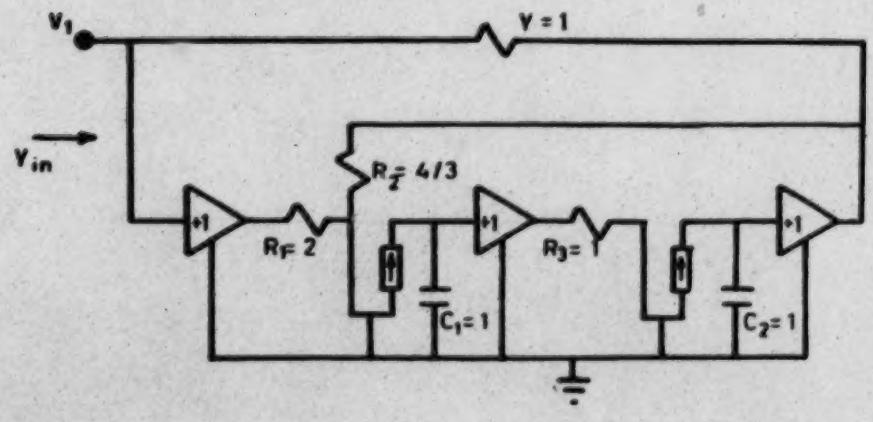

Figure (2.12) Realization of $Y_{in} = (4p^2 - 5)/(4p^2 - 3)$ by $t_V = 2/(4p^2 - 3)$ and Y = 1.

2.4.1 Realizing A Grounded Inductance

This has been treated using UGA's [9], [46]. Simulation of a grounded inductance in this dissertation is a special case of the method

just discussed. Consider the configuration shown in Fig. (2.13). The input admittance is calculated as

$$Y_{in} = \left(\frac{1}{R_5} - \frac{K_{456}R_3}{R_4R_5}\right) + \frac{K_{12345}R_3}{C_1R_1R_2R_5P}$$

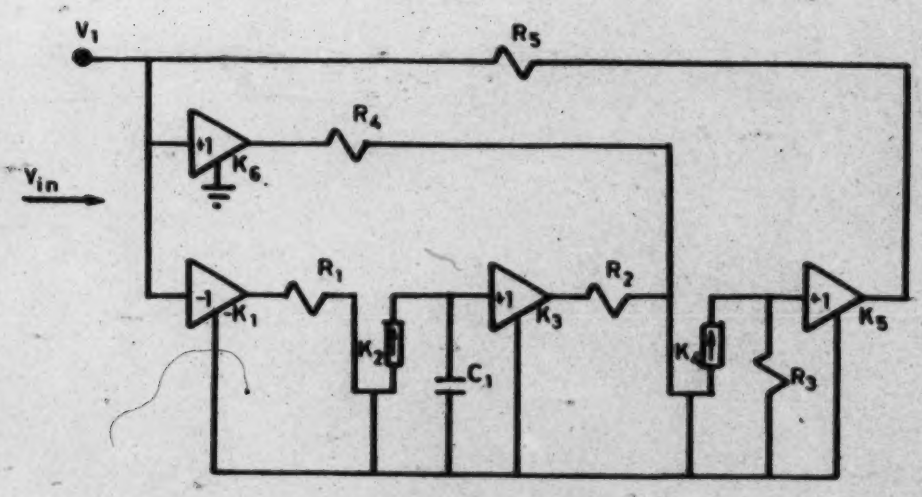

Figure (2.13) Simulation of a grounded inductance.

which gives the admittance function of a pure inductor when the real term is set to vanish. In other words, the element values must satisfy $R_3 = R_4$, $R_3/(C_1R_1R_2R_5) = 1/L$ (L: desired value in henrys); then $Y_{in} = 1/LP$. Sensitivity analysis indicates that in order to have accurate results, R_5 should be made as large as possible. It is, therefore, a question of a compromise between accuracy of the simulated inductance and spread of element values or a matter of high-frequency accuracy against the value of inductance desired (the higher the inductance, the more critical the realization would be in terms of frequency

response and spread of element values).

2.4.2 Realizing Grounded One-Port Negative R-L-C

The circuit shown in Fig. (2.14) has the driving-point admittance of $Y_{in} = -\frac{Y_C}{Y_B}Y$ (2.20) where $Y_A = Y_C + Y_B$.

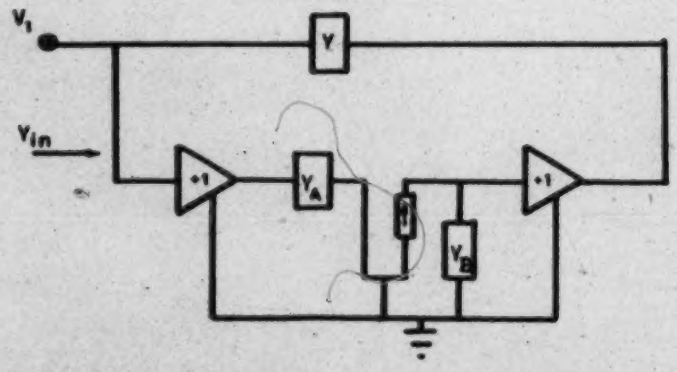

Figure (2.14) Simulation of grounded one-port negative R-L-C.

Equation (2.20) indicates that from Fig. (2.14) one can realize grounded one-port negative values of R-L-C by properly arranging various admittances concerned. If one chooses $Y_C = Y = 1.0$, then $Y_{in} = -\frac{1}{Y_B}$ and $Y_A = 1 + Y_B$; furthermore, letting $Y_B = G_B$, one then has a negative resistance at the input $R_{in} = -G_B$ where $Y_A = 1 + G_B$, $Y_C = Y = 1.0$.

If one chooses $Y_C = Y_B$, $Y = C_C P$, then $Y_{in} = -C_C P$ where $Y_A = 2Y_B$. Similarly, supposing $Y_C = Y = 1.0$ and $Y_B = C_B P$; one has a negative inductance given by $Y_{in} = -\frac{1}{C_B P}$ where $Y_A = 1 + C_B P$.

2.5 *SYNTHESIS OF THE SECOND-ORDER BAND-PASS FILTER FROM A PASSIVE CONFIGURATION*

With reference to the passive configuration in Fig. (2.15), one has for the voltage transfer function

$$\frac{V_{out}}{V_{in}} = \frac{P/C_X R_X}{P^2 + P/C_X R_X + 1/C_X L_X} \qquad (2.21)$$

Equation (2.21) is the transfer function of a second-order, Butterworth, band-pass filter which will be realized by inductorless design.

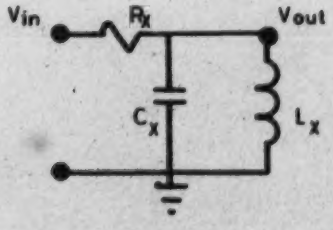

Figure (2.15) A passive Butterworth second-order band-pass filter.

One can first simulate the parallel-connected pair L_X and C_X by using UGA's as shown in Fig. (2.16).

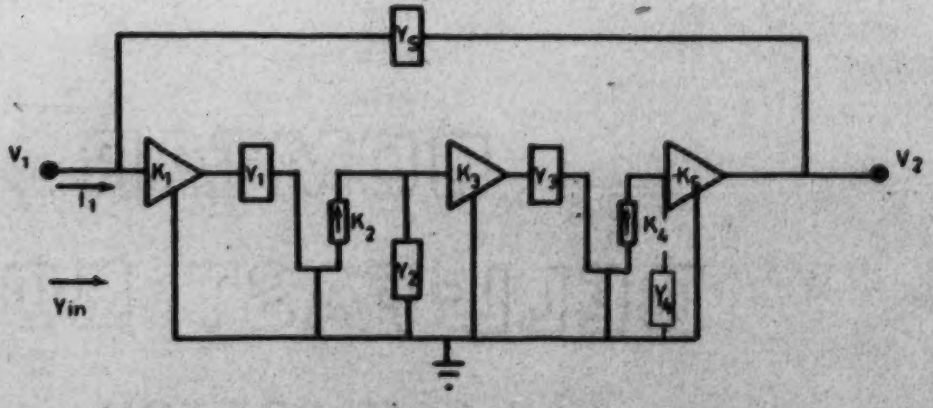

Figure (2.16) Simulation of L_X and C_X in parallel.

Figure (2.16) yields

$$\frac{V_2}{V_1} = K_{12345}\frac{Y_1Y_3}{Y_2Y_4} \quad \text{and} \quad Y_{in} = \frac{I_1}{V_1} = Y_5 + K_{12345}\frac{Y_1Y_3Y_5}{Y_2Y_4} \qquad (2.22)$$

Choosing $Y_2 = C_2P$, $Y_4 = C_4P$, $Y_5 = C_5P$, $Y_1 = G_1$, $Y_3 = G_3$, equation (2.22) becomes

$$Y_{in} = C_5P + K_{12345}\frac{C_5G_1G_5}{C_2C_4P}$$

which is the admittance of a parallel combination of an inductor and a capacitor. One can, therefore, assign

$$L_X = \frac{C_2C_4}{K_{12345}\,C_5G_1G_3} \quad , \quad C_X = C_5 \quad .$$

To complete the design, as shown in Fig. (2.17), one can take the signal right after the first amplifier (K_1) as the actual output of the filter for the purpose of cascading with the following sections.

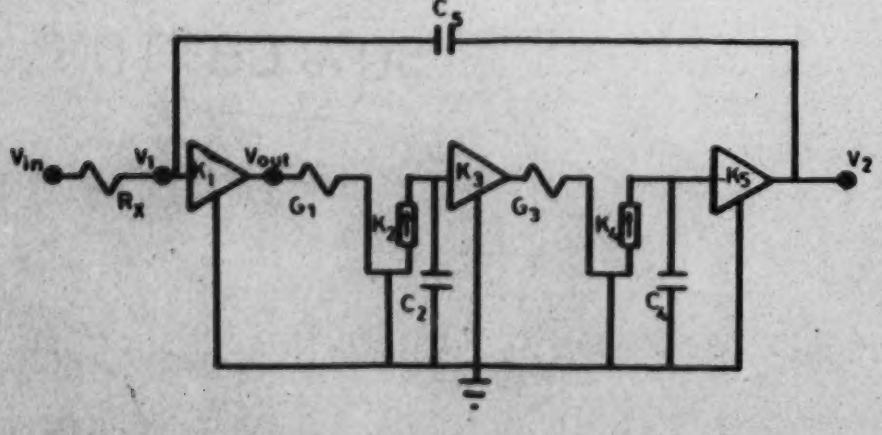

Figure (2.17) An active second-order Butterworth band-pass filter.

From Fig. (2.17), the voltage transfer function is given as

$$\frac{V_{out}}{V_{in}} = \frac{K_1 P/C_5 R_X}{P^2 + P/C_5 R_X + K_{12345}\, G_1 G_3/C_2 C_4} \qquad (2.23)$$

Equation (2.23) indicates that this circuit has a low-sensitivity result as the normalized coefficient sensitivities of the denominator polynomial with respect to all the passive elements and gains of amplifiers are unity in absolute value. Letting $C_2 = C_4 = C_5 = G_1 = G_3 = 1.0$, $R_X = Q$, one has for the spread of element values $S_C = 1$, $S_R = Q$ which are as low as those by the state-variable design in (2.24). Thus, high-Q realization is possible. The center frequency and quality factor are also independently adjustable.

Comparing with the method of design using Calahan's optimal decomposition of the denominator polynomial in Section (2.3.1), one has, in this case, to use one more unity-gain amplifier, but the advantages are: smaller S_R, the possibility of independent adjustment of Q and ω_0, and no cancellation of the unwanted zero. Also, in Fig. (2.17) the signal after amplifier (K_3) has a low-pass frequency characteristic.

2.6 *EXPERIMENTAL CIRCUITS FOR SYNTHESIZING SECOND-ORDER BAND-PASS FILTERS*

Of all the methods proposed so far using only UGA's, the state-variable technique is chosen to be implemented in practice. Better experimental results are measured on circuits designed via the method of Section (2.5) by using the CUGA and operational amplifiers in combination.

2.6.1 Transistor Circuitry Using State-Variable Technique

Figure (2.18) shows a complete schematic diagram of a second-order, Butterworth, band-pass, active filter designed according to the state-variable technique using discrete components only. It realizes a band-pass filter with a Q of 30 at a centre frequency of $\omega_0 = 10^5$rad/sec ($f_0 = 15.9$ KHz). The fact that both positive and negative supply voltages of fifteen volts are used and the way the circuit is laid out enables direct-coupling between successive stages. Resistors are of ± 5%, capacitors ± 10% tolerances. D. C. biasing voltages as actually measured are indicated as numbers within parentheses in the diagram. The first stage consisting of transistors Q1, Q2, and Q3 is a conventional design for a simple operational amplifier circuit. The second (Q4, Q5, Q6, Q7) and third (Q8, Q9, Q10, Q11) stages are the current unity-gain amplifiers and buffers. Transistor Q4 is basically of a common-base configuration with high input and low output admittances. Q9 and Q5 are constant current sources. Resistors 6.8K, 15K, 6.8K serve as a voltage-divider to supply proper bias voltages for Q4 and Q5. Q6 and Q7 are merely buffers. An arrangement like this is basically D. C. open-loop unstable. However, due to the negative feedback characteristic of the closed-loop response, this circuit as a whole is D. C. stable. To adjust for proper biasing voltages, one can close the inner loop first and vary R_b to yield a zero D. C. voltage at V_B; then adjust R_{bb} for zero output at Q11 when the outer loop is also closed. In the A. C. case, tuning is also quite simple. With the component values as chosen, R_3 is adjusted for an exact resonant frequency of $\omega_0 = 10^5$ rad/sec. Then, R_2 is adjusted to give Q = 30 as desired.

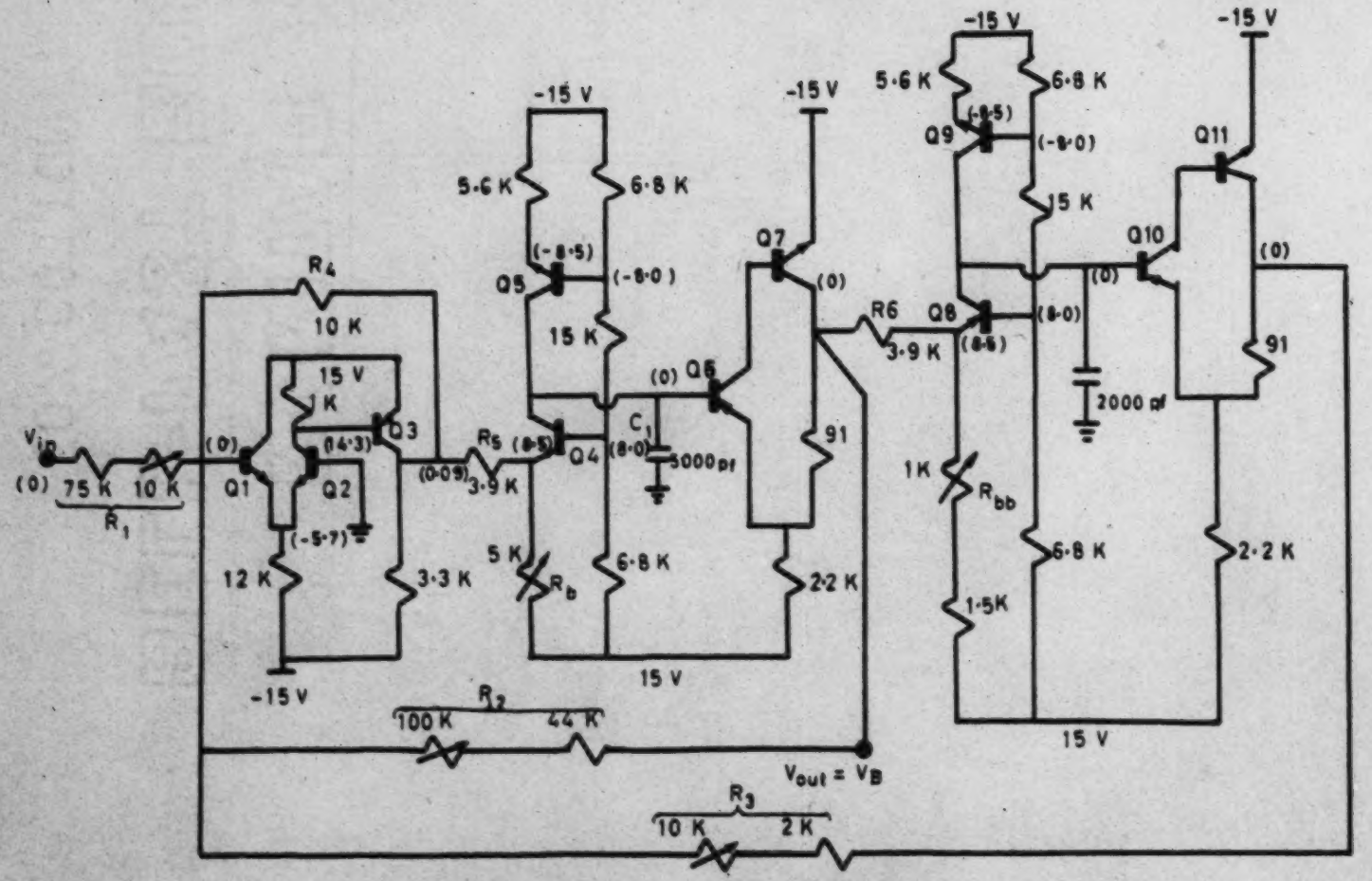

TRANSISTORS: NPN 2N4401

PNP 2N3906

Fig. (2.18) Schematic transistor circuit of band-pass filter for $Q = 30$, $\omega_0 = 10^5$ rad/sec.

The gain at resonance can be varied by changing R_1. Experimental measurement of frequency response is given in Fig. (2.19) and Fig. (2.20) and compared with the theoretical case. They are shown to be very close. Harmonic distortions at some typical frequencies are measured, and tabulated in Appendix A.

The ability of the above circuit to resonate at a higher frequency with a much higher Q can be demonstrated by the next experiment. The objectives are Q = 200 and f_0 = 200 K Hz. The circuit is the same as the one in Fig. (2.18) except the following changes: R_1 = 430 K + 10 K (pot), R_2 = 200 K + 100 K (pot), R_3 = 2 K + 10 K (pot), R_4 = 2 K, C_1 = 300 pf, C_2 = 200 pf. Also, it is found experimentally that a very small capacitor of 5 pf (10%) must be added in parallel with R_4. Adjustments are the same as before both in D. C. and A. C. cases. The experimental result is measured to be close to the theoretical one as given in Fig. (2.21) and (2.22). Averaging over six measurements gives Q = 200.27, f_0 = 200.041 K Hz. Errors are 0.14% and 0.02% respectively. The resonant frequency is found experimentally to go up as high as around 400 K Hz and the maximum Q around one thousand. However, due to reasons which will be discussed later, practical stable Q values are estimated to be limited to no more than several hundred.

2.6.2 Experimental Second-Order Band-Pass Filter Synthesis Using A CUGA and Riordan's Gyrator

The Riordan's gyrator [4] has been used by Orchard and Sheahan [21] for realizing floating inductors in their active filter design. In the same paper, this circuit has also been thoroughly analyzed with reference to sensitivity and noise.

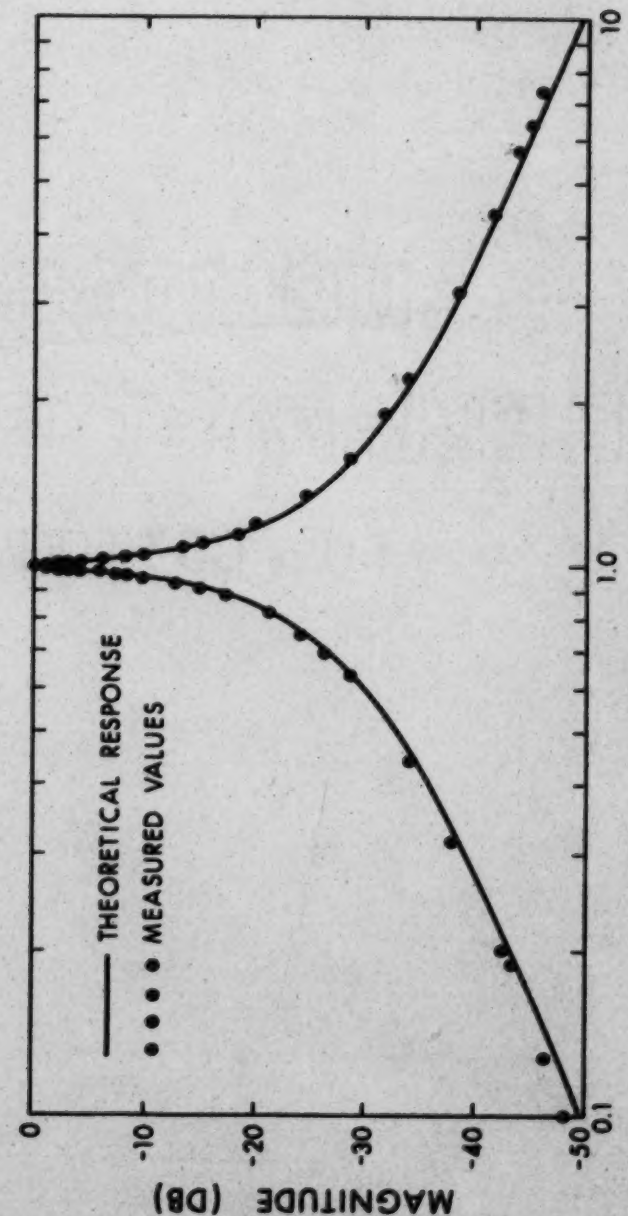

Figure (2.19) Frequency response of the second-order Butterworth band-pass active filter with a Q of 30, center frequency of 10^5 rad/sec.

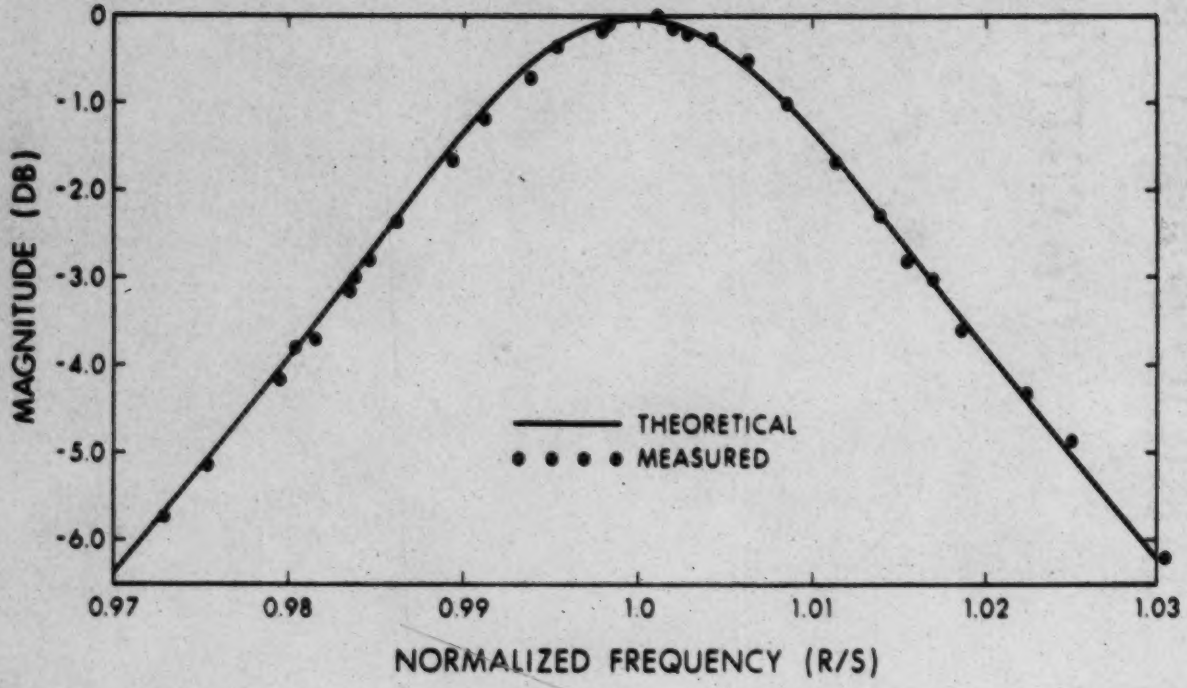

Figure (2.20) Frequency response of the second-order band-pass filter with a Q of 30, center frequency of 10^5 rad/sec in the neighborhood of resonance.

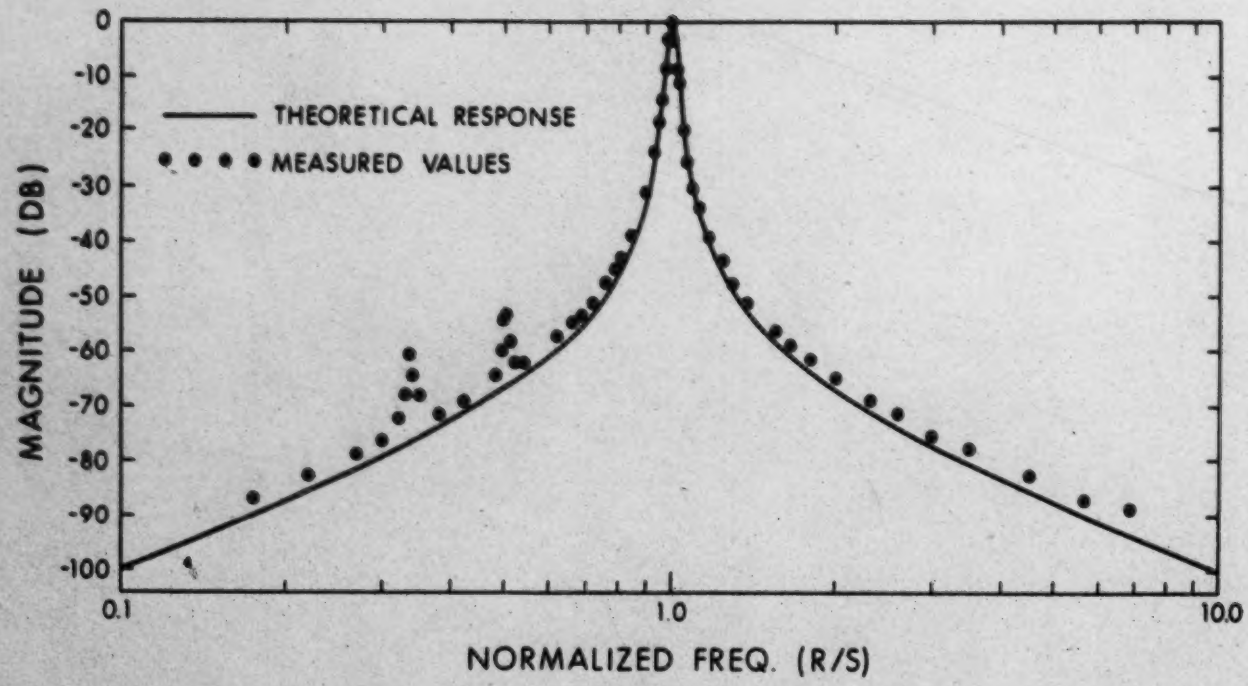

Figure (2.21) Frequency response of the second-order Butterworth band-pass active filter with a Q of 200, center frequency of 200 K Hz.

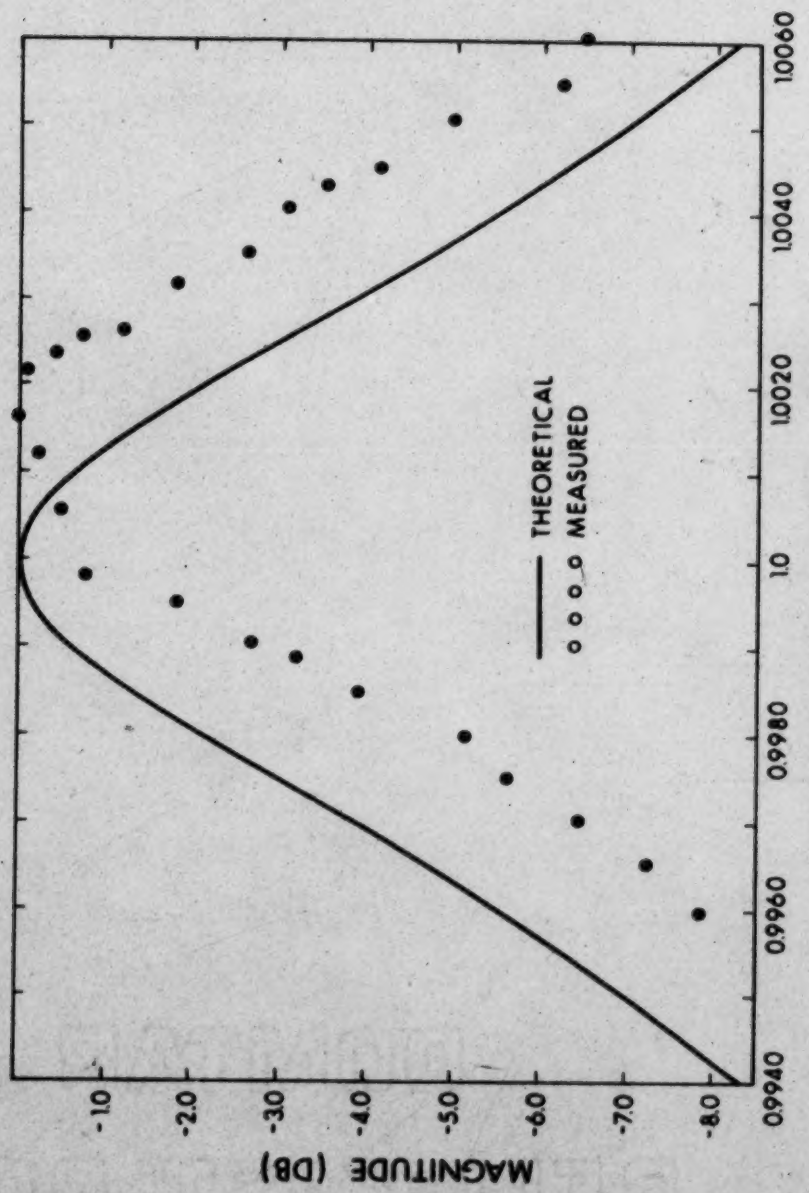

Figure (2.22) Frequency response of the second-order band-pass filter with a Q of 200, center frequency of 200 KHz in the neighborhood of resonance.

The circuit as discussed in Section (2.6.1) is capable of having Q values of no more than a few hundred. The reason for this is that due to the appearance of amplifier gains in the last coefficient of the denominator polynomial of the voltage transfer function the normalized sensitivity of V_{out}/V_{in} at resonance is equal to Q; i.e.

$$| S_K^{V_{out}/V_{in}(P = j1.0)} | = Q \quad .$$

Usually the gains of current amplifiers are more temperature dependent than other factors as a result of variations in β of transistors. These are the gains, for example, K_1, K_2, K_3, K_4, K_5 in equation (2.23). Although $| S_K^Q | = 1.0$, the resulting output wave-form as observed on the oscilloscope for very high Q is shifting up and down randomly in time. One way to get around this problem is to synthesize the filter so that the gains of the CUGA's do not appear in the last coefficient of the denominator polynomial; i.e. they are not included in the feedback loop. In other words, one should arrange that the gains appear only as a multiplying factor of the whole transfer function in the following way. Consider Fig. (2.23).

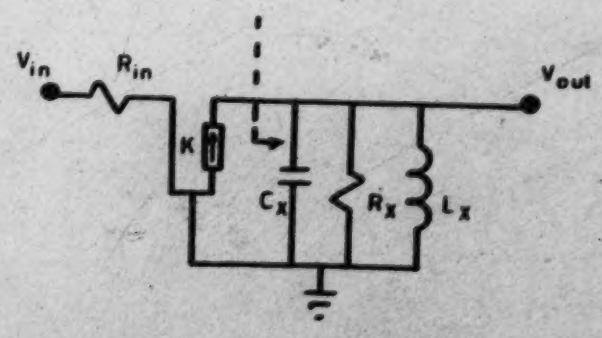

Figure (2.23) Very high-Q band-pass filter.

Straight-forward analysis yields

$$V_{out}/V_{in} = \frac{KP/C_X R_{in}}{P^2 + P/C_X R_X + 1/L_X C_X}$$

Note that the gain of current amplifier, K, appears as a multiplying factor only. There are three ways to simulate the parallel combination of L_X, C_X, R_X by using two operational amplifiers as shown in Fig. (2.24). Fig. (2.24c) uses most passive elements among the three, yet it has the desired advantages that the spread of capacitor values is unity and that ω_0, Q of the resulting filter are independently adjustable. The complete schematic diagram is shown in Fig. (2.25).

The construction of the CUGA is different from the previous one. Since it is used only in an open-loop fashion, one more transistor QX is added to stablize the circuit D. C. wise by negative feedback. In tuning this circuit, D. C. voltage of the output of second operational amplifier can be set to zero by adjusting R_b. A. C. wise, one can set R_3 for an approximate value of Q; then, R_5 is adjusted for exact ω_0; finally, exact Q can be obtained by varying R_X. For actual experiment, the objectives are Q = 500, $\omega_0 = 10^4$ rad/sec. Using a decade resistance box, R_X is found to be 228 KΩ. Results are plotted in Fig. (2.26), (2.27). Finally, by adjusting R_X alone to get very high Q values at the same resonant frequency, a stable wave-form is observed at a Q of about four thousand. No other attempt is made to try even higher values of Q.

Changing the power supply voltages by as much as ± 50% does not affect the performance significantly. Other measured data are given in Appendix B.

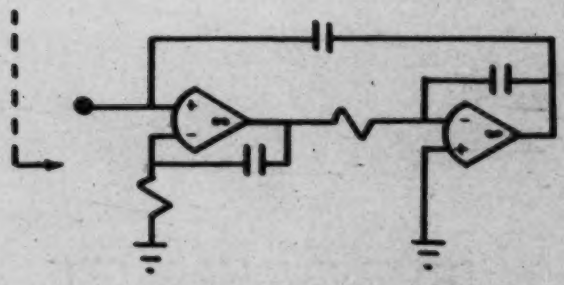

Figure (2.24a) Simulation of L_X, C_X, P_X; $S_C = S_R = Q$.

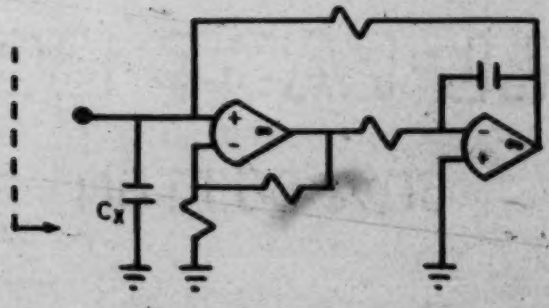

Figure (2.24b) Simulation of L_X and R_X; $S_C = \sqrt{Q}$, $S_R = Q$.

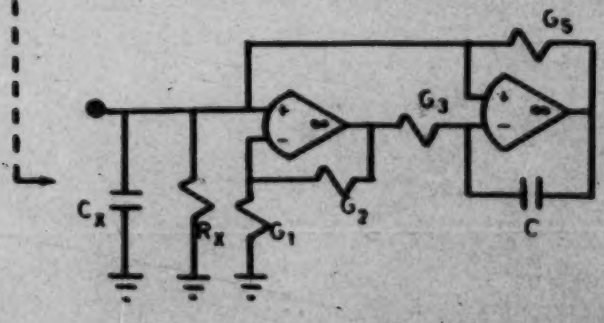

Figure (2.24c) Riordan's gyrator to simulate L_X; $S_C = 1$, $S_R = Q$, $L_X = G_2C/G_1G_3G_5$.

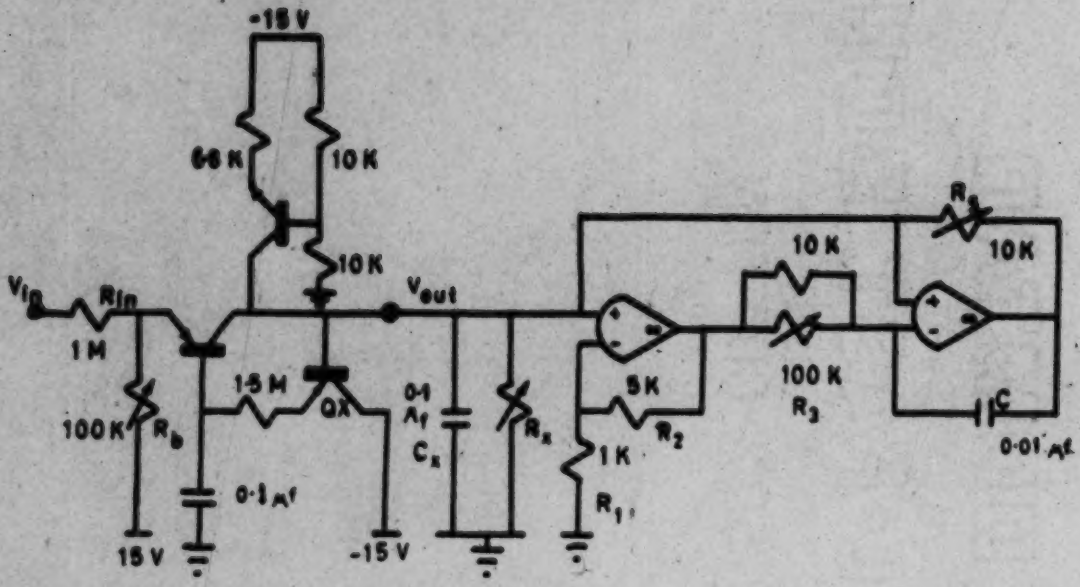

OPERATIONAL AMPLIFIERS : NATIONAL SEMICONDUCTORS LTD.
MODEL LM 301A

Figure (2.25) Schematic diagram for very high-Q band-pass filter.

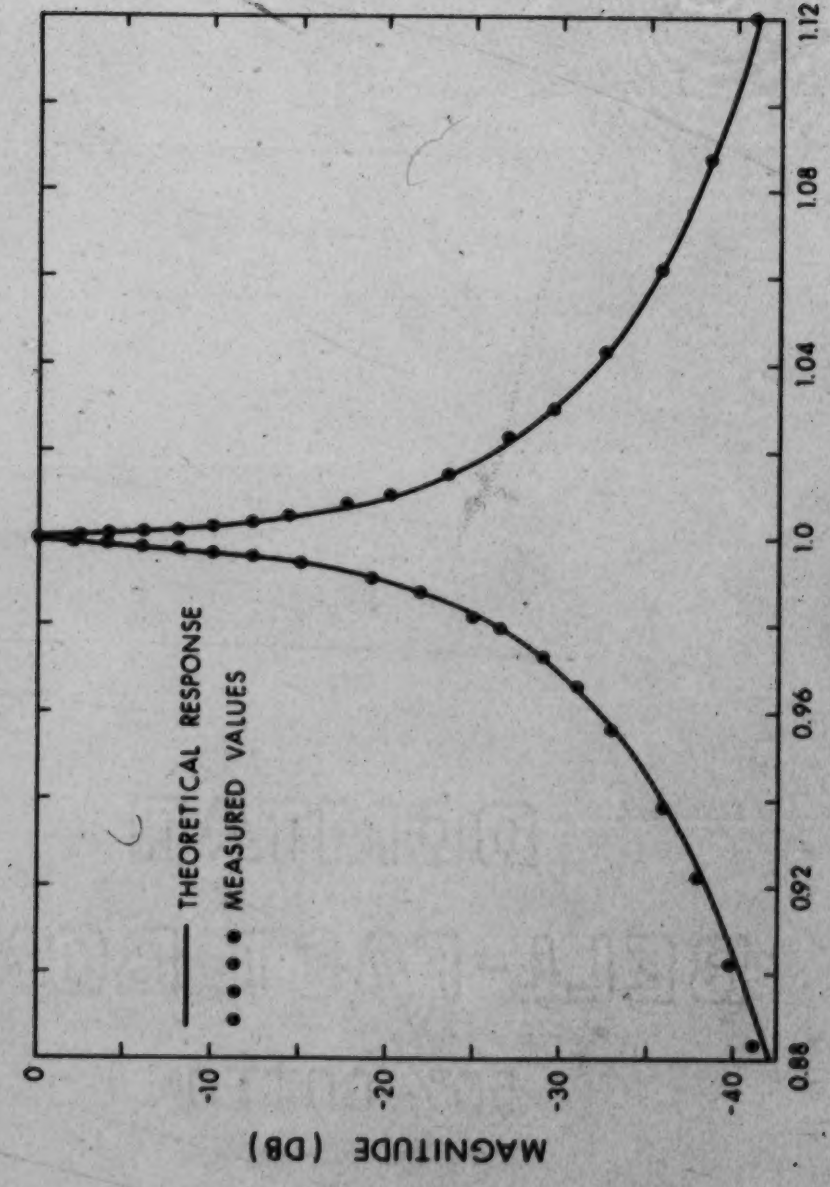

Figure (2.26) Frequency response of filter using Riordan's gyrator for $Q = 500$, $\omega_0 = 10^4$.

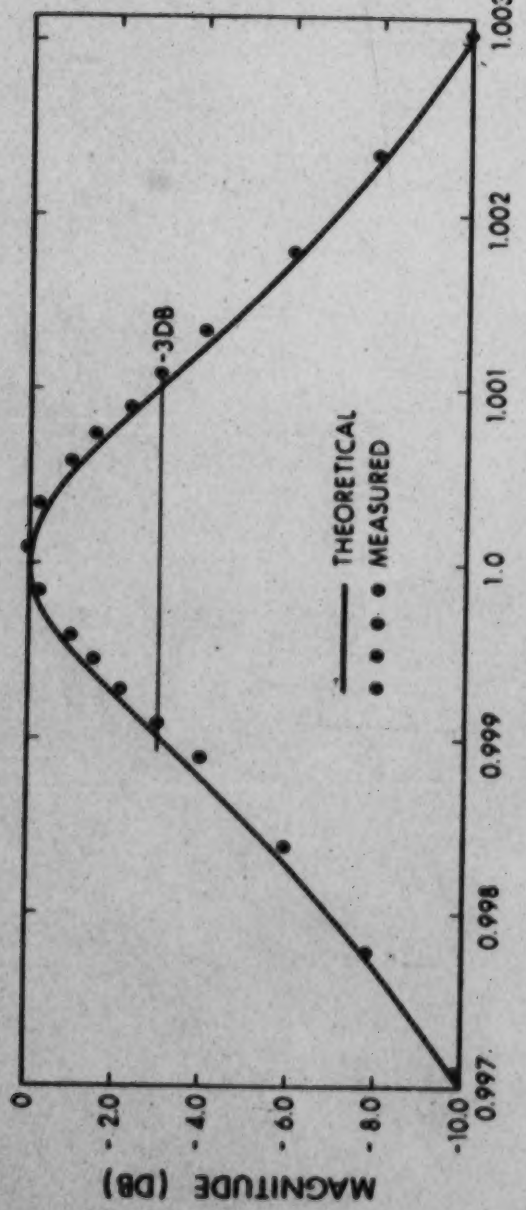

Figure (2.27) Frequency response of filter in the neighborhood of resonance.

CHAPTER III

HIGH-ORDER INDUCTORLESS FILTERS SYNTHESIZED BY NEGATIVE IMMITTANCE INVERTERS (NIV'S)

3.1 *BACKGROUND*

Most of the design methods available in the field of active filter synthesis are based on the approach of realizing second-order complex pole-pairs. To realize a high-order filter such sections would be connected in cascade. It is proved by Holt and Lee [28] that the circuit derived by direct synthesis of doubly terminated L-C filters has less sensitivity than that by cascading synthesis. On the other hand, the former method will normally require more passive and active components as a result of the complexity of filter structure of high-order transfer functions.

In an attempt to realize a high-order transfer function directly, one naturally starts from the passive R-L-C configuration chosen to meet all the necessary requirements of the design. Conventional methods of filter design are well developed, and are usually arranged in a convenient manner for the designers. All the necessary data including the final realization configuration and component values are generally well documented in numerous reference books such as [52] - [57]. One of the most complete is "Handbook of Filter Synthesis" by Zverev [52].

Given such a passive R-L-C filter configuration, the final

inductorless realization can be achieved by simulating all the inductors in the passive design by R-C and active components. Orchard and Sheahan [21] introduced two methods by which a high-order band-pass passive configuration can be rearranged to contain grounded inductors and negative capacitors, or , by means of impedance transformations, to contain ¶ - sections of inductors. Two gyrator circuits by Riordan were connected back-to-back through a ¶ network of resistors to simulate a ¶ of inductors. These two methods depended on an approximation procedure and subtraction of component values. The number of active devices used was no fewer than the order of functions. A novel method is presented in the following by which high-order filters can be realized with fewer active components.

3.2 *SIMULATION OF THE FLOATING INDUCTOR BY NIV'S*

Among the various kinds of active devices, the negative immittance inverter (NIV) is found useful in realizing the floating inductor. A NIV is defined as an active component which has the following two-port open-circuit impedance parameters:

$$Z_{11} = Z_{22} = 0 \quad , \quad Z_{12} = Z_{21} = \pm K \text{ (where K is a constant).}$$

The types of NIV's used in this work are the reciprocal, resistive two-port networks as illustrated in Figure (3.1).

Figure (3.1) Two reciprocal, resistive NIV networks.

With a load of Y_L connected to one port, the other port sees an input admittance of its negative reciprocal multiplied by the factor G^2; namely, $Y_{in} = -G^2/Y_L$. Thus, by cascading two sections of such networks and a negative capacitor together one can simulate a floating inductor with a slight modification.

The NIV's in Fig. (3.1) are represented by some simpler two-port notations as given in Fig. (3.2) where $J_\chi = G_\chi$.

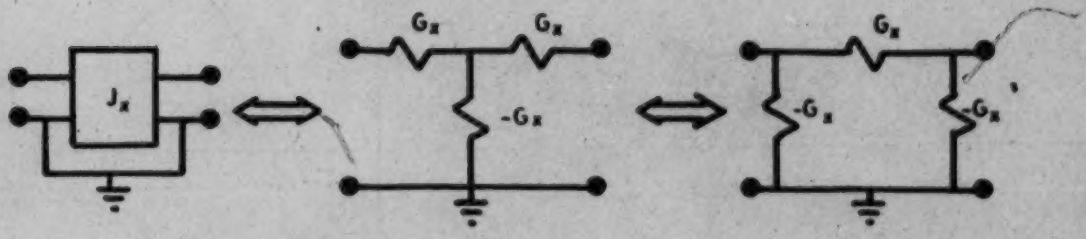

Figure (3.2) A simpler notation for NIV.

The Y matrix derived from the circuit in Figure (3.3) is given by

$$Y = \begin{bmatrix} -\frac{J_1^2}{Y_y} & -\frac{J_1 J_2}{Y_y} \\ -\frac{J_1 J_2}{Y_y} & -\frac{J_2^2}{Y_y} \end{bmatrix} . \qquad (3.1)$$

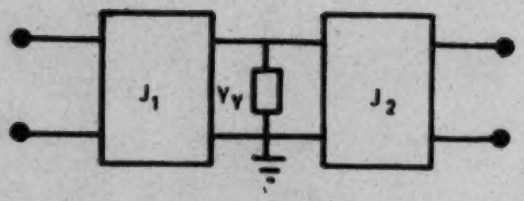

Figure (3.3) Cascading two NIV's.

On the other hand, cascading an admittance Y_X and an inverse-polarity ideal transformer with turns-ratio N as given in Fig. (3.4) has the following Y matrix

$$\underline{Y} = \begin{bmatrix} Y_X & Y_X N \\ Y_X N & Y_X N^2 \end{bmatrix} \qquad (3.2)$$

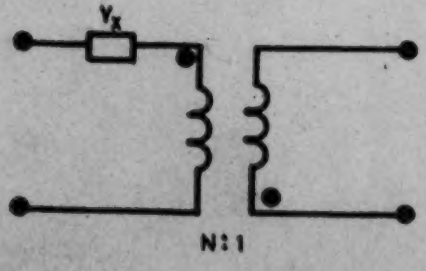

Figure (3.4) An admittance in cascade with an ideal transformer.

By making $Y_X = -J_1^2/Y_Y$ and $N = J_2/J_1$ the two matrices can be made identical. In other words, the circuits in Fig. (3.3) and Fig. (3.4) are equivalent two-port networks. In particular, a floating inductor of $Y_X = 1/L_X P$ and an ideal transformer with proper turns-ratio is realized by putting a negative capacitor of $Y_Y = -C_Y P$ between two NIV's. The simulated floating inductance is given by $L_X = C_Y/G_1^2$.

3.3 *REALIZING HIGH-ORDER TRANSFER FUNCTIONS BY NIV'S*

Nth-order polynomial low-pass filters realized by conventional technique with R-L-C elements can be represented by the configuration in Figure (3.5) [52].

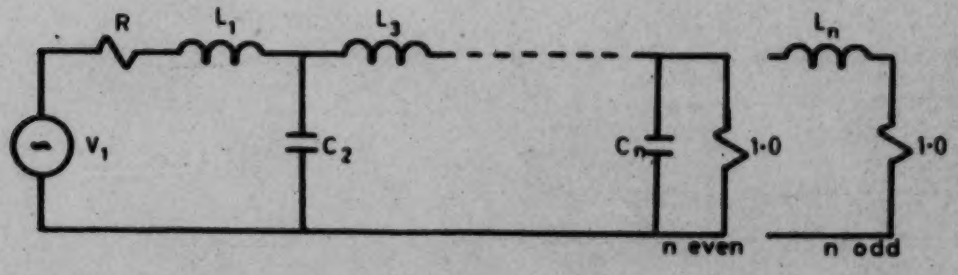

Figure (3.5) Nth-order polynomial filters.

The floating inductors in Fig. (3.5) are to be replaced by using NIV's, negative capacitors and ideal transformers in accordance with the following method. The four circuits in Fig. (3.6) are all equivalent two-port networks.

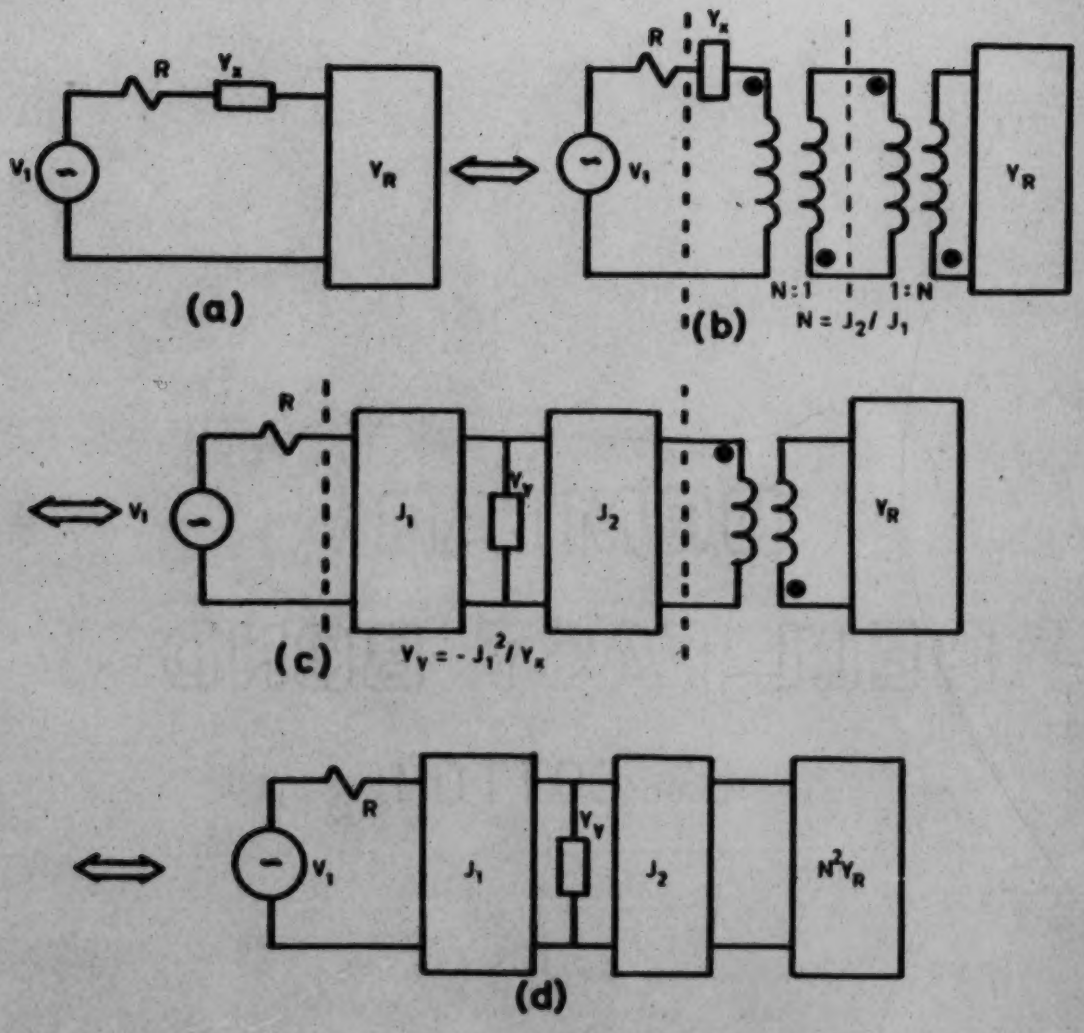

Figure (3.6a, b, c, d) Four equivalent two-port networks.

Network (a) is transformed into (b) by inserting two inverse-polarity ideal transformers in cascade. The dotted portion of (b) is replaced by the NIV's and a grounded Y_y in (c). The second ideal transformer is

absorbed into the remaining admittance Y_R by proper admittance scaling. At this point, it should be pointed out that voltages and currents associated with the remaining network N^2Y_R have changed polarity once. The same process can be applied to N^2Y_R and its remaining one repeatedly until all the floating admittances are replaced by their grounded negative reciprocals. In particular, floating inductors L_1, L_3, etc., in Fig. (3.5) are replaced by resistive NIV's and grounded negative capacitors. The resulting output voltage changes sign only when there is an odd number of floating inductors in the original passive configuration. For convenience, it is simpler to assume the J's on each section, J_1, J_2, etc., to be identical; i. e., the same positive and negative resistance values are used for the two NIV's in the active realization. Or, in other words, all ideal transformers have unity turns-ratio. Thus a polynomial low-pass filter of arbitrary order can be realized by means of resistive NIV's and negative grounded capacitors.

3.3.1 Realizing The Negative Resistance In The NIV By Operational Amplifier

The negative grounded resistances in the NIV can be realized by using operational amplifiers as given in Fig. (3.7) where $Y_{in} = -G_1G_3/G_2$.

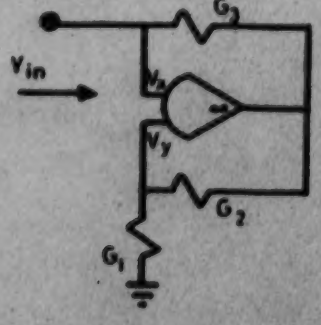

Figure (3.7) An operational-amplifier circuit to simulate a negative grounded resistance.

Usually one can assign $G_1 = G_2$ for convenience. The circuit in Fig. (3.7) is input conditional stable. Depending on the choice of V_X and V_Y as the positive or negative differential input for the operational amplifier, the input port can be made conditional short-circuit stable [50]. Stability can be investigated by assuming a one-pole approximation for the non-ideal model of the operational amplifier. The Thevenin equivalent impedance presented by the remaining filter circuit and seen by each of the above negative-resistance circuits at its input port as the series impedance,determines whether it should be input open-circuit or short-circuit stable. This, though being theoretically possible, is a time-consuming process for a complex filter structure. As a general rule of thumb, one can arrange the negative-resistance operational-amplifier circuit for an input open-circuit stable condition with positive feedback when the input port sees a series impedance; and for an input short-circuit stable condition with negative feedback when there is some parallel impedance connected to the input port. This arrangement is found suitable in several experimental circuits which will be discussed later.

3.4 *SYNTHESIS OF A SIXTH-ORDER CHEBYSHEV LOW-PASS FILTER*

The synthesis procedure discussed in Section (3.3) is applied to realize a sixth-order Chebyshev low-pass filter in the following. For the design objectives of :

Low-pass filter

Chebyshev

Sixth-order

pass-band ripple = 0.1 db

Half-power frequency = f_{-3db} = 795.774 Hz (5×10^3 r/s),

one is given the passive R-L-C configuration in Fig. (3.8) [52].

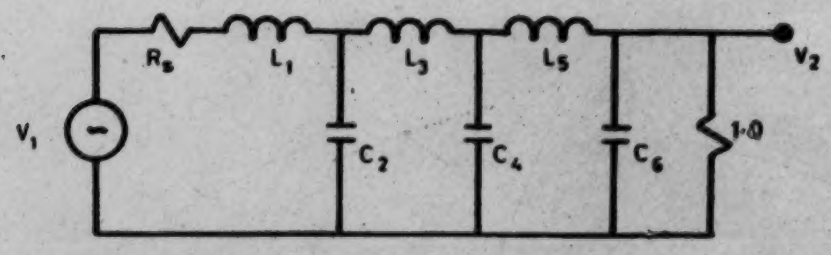

Figure (3.8) A passive R-L-C sixth-order Chebyshev low-pass filter.

Normalized element values are :

R_S = 1/1.3554, L_1 = 0.9419, C_2 = 2.0797, L_3 = 1.6581

C_4 = 2.2473, L_5 = 1.5344, C_6 = 1.2767.

Transforming all the floating inductors into negative grounded capacitors by NIV's results in a circuit given in Fig. (3.9) where

$$C_1 = L_1G_1^2, \quad C_3 = L_3G_2^2, \quad C_5 = L_5G_3^2 .$$

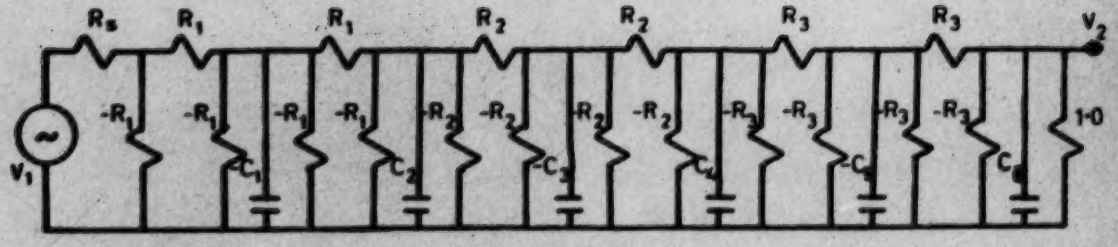

Figure (3.9) Transformation by NIV's.

Note that there is a sign change for the output voltage as a result of simulating three floating inductors. There is no impedance scaling due to the use of unity-turns-ratio transformers. Combining parallel-connected resistances and applying Thevenin's technique at the input port simplifies the filter circuit into a form given by Fig. (3.10).

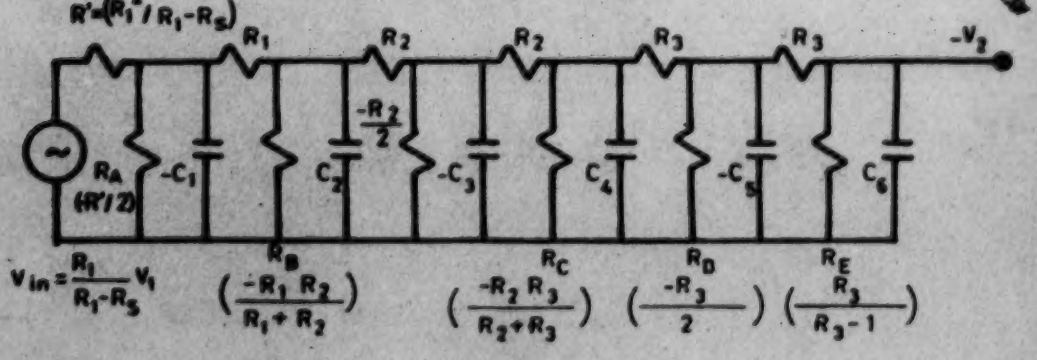

Figure (3.10) Simplification of Fig. (3.9).

Choosing $R_1 = R_2 = R_3 = 1.0$ in normalized values gives the following values :

$$V_{in} = 3.814\ V_1 \ , \quad R' = 3.814 \ , \quad R_A = R_B = R_C = R_D = -0.5,$$
$$R_F = \infty \ , \quad C_1 = 0.9419 \ , \quad C_3 = 1.6581 \ , \quad C_5 = 1.5344 \ .$$

The spread of element values in this case is quite low :

$$S_R = 8.1 \ , \qquad S_C = 2.4 \ .$$

With magnitude scaling of 10K the final realization by operational amplifiers is given in Fig. (3.11). Resistors are given in KΩ and capacitors in nf and both are within ± 1% tolerances. Operational amplifiers realizing negative R-C are arranged with either negative or positive feedback as discussed before. Six inexpensive operational operational amplifiers (1741c) are used including one for the buffer at the output. Experimental results are measured with temperature as a parameter. Measured data are very close to the expected theoretical response and this circuit is relatively insensitive to temperature variations. Results are presented in Figure (3.12), and (3.13). Other measurements are given in Appendix C. Tuning of this filter is quite simple. The input resistor (38.14 K) is replaced by a variable one by which the correct half-power frequency is set. With no further tuning , the half-power frequency is measured to be $f_{-3db} = 795.43$ Hz which has the negligible inaccuracy of - 0.043 % .

The same method can be directly applied to synthesizing any type of polynomial filters of arbitrary order as they all have basically the same passive R-L-C configuration.

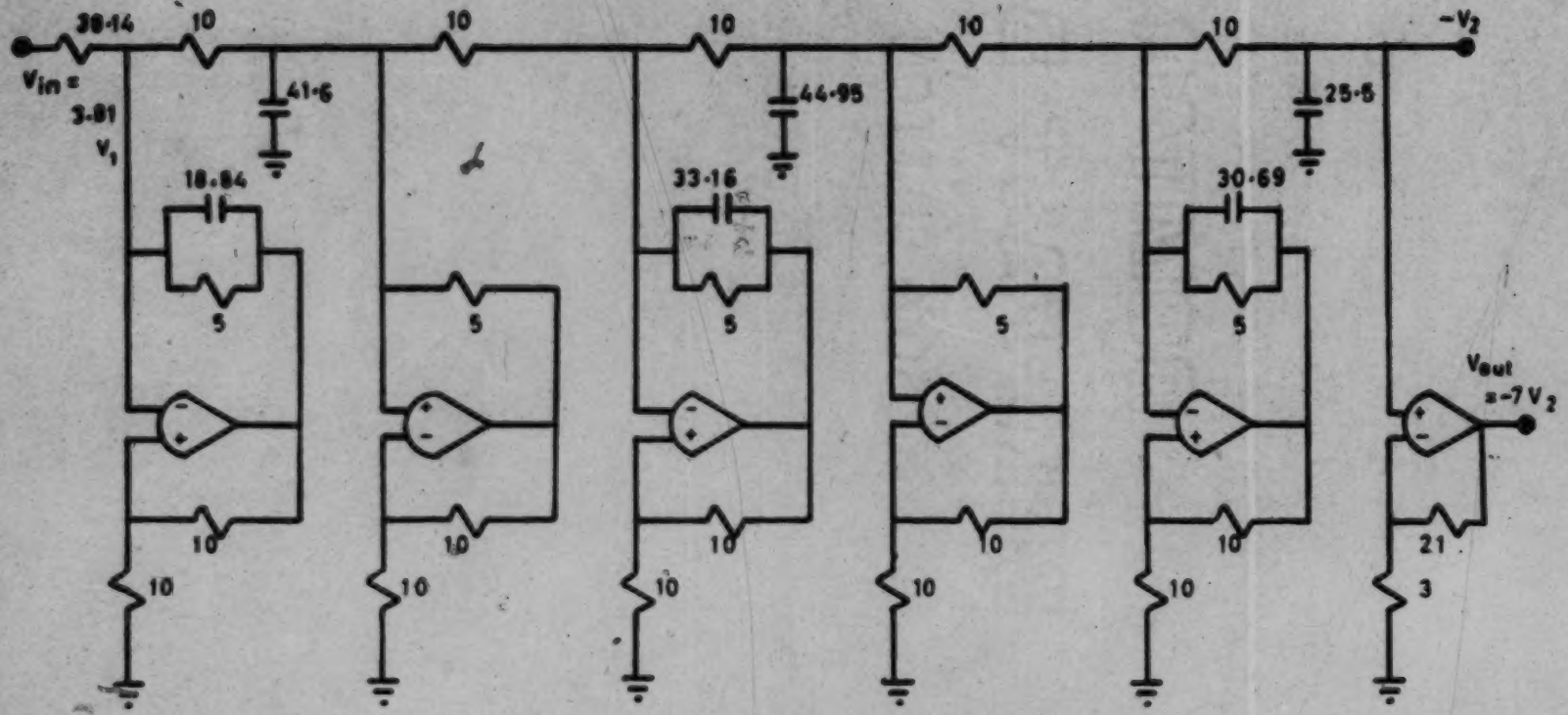

Figure (3.11) An active sixth-order Chebyshev low-pass filter;

f_{-3db} = 795.774 Hz.

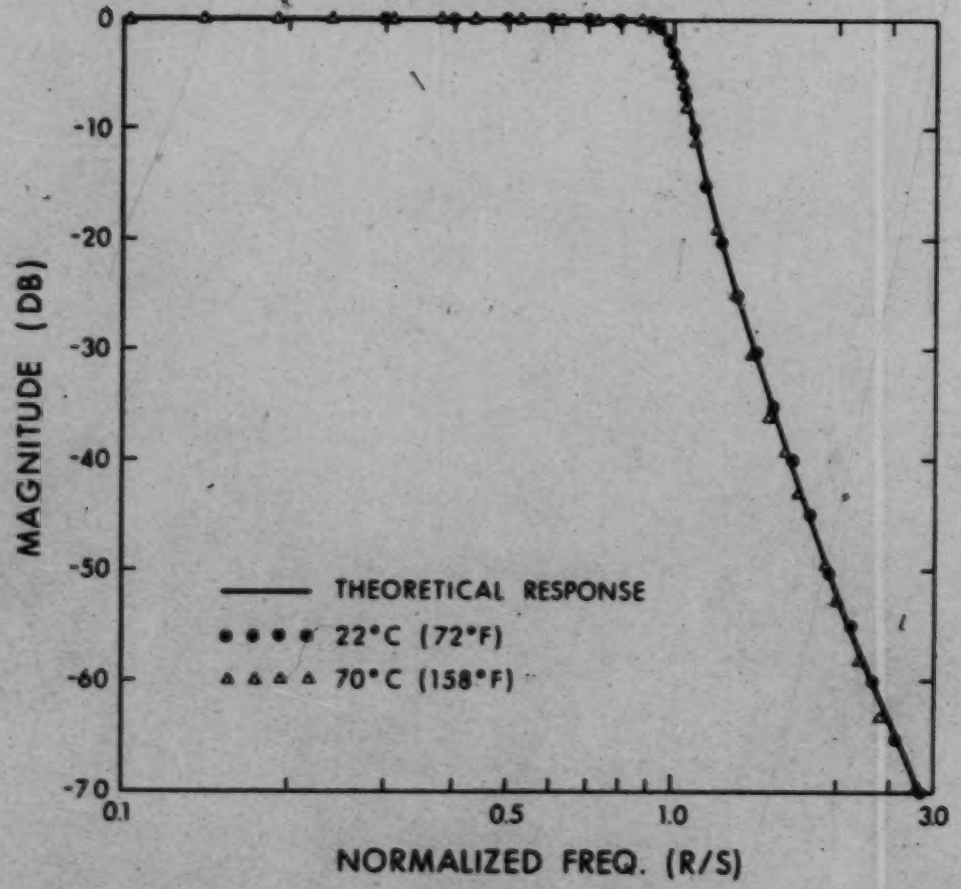

Figure (3.12) Frequency response of the active sixth-order Chebyshev low-pass filter; f_{-3db} = 795.774 Hz.

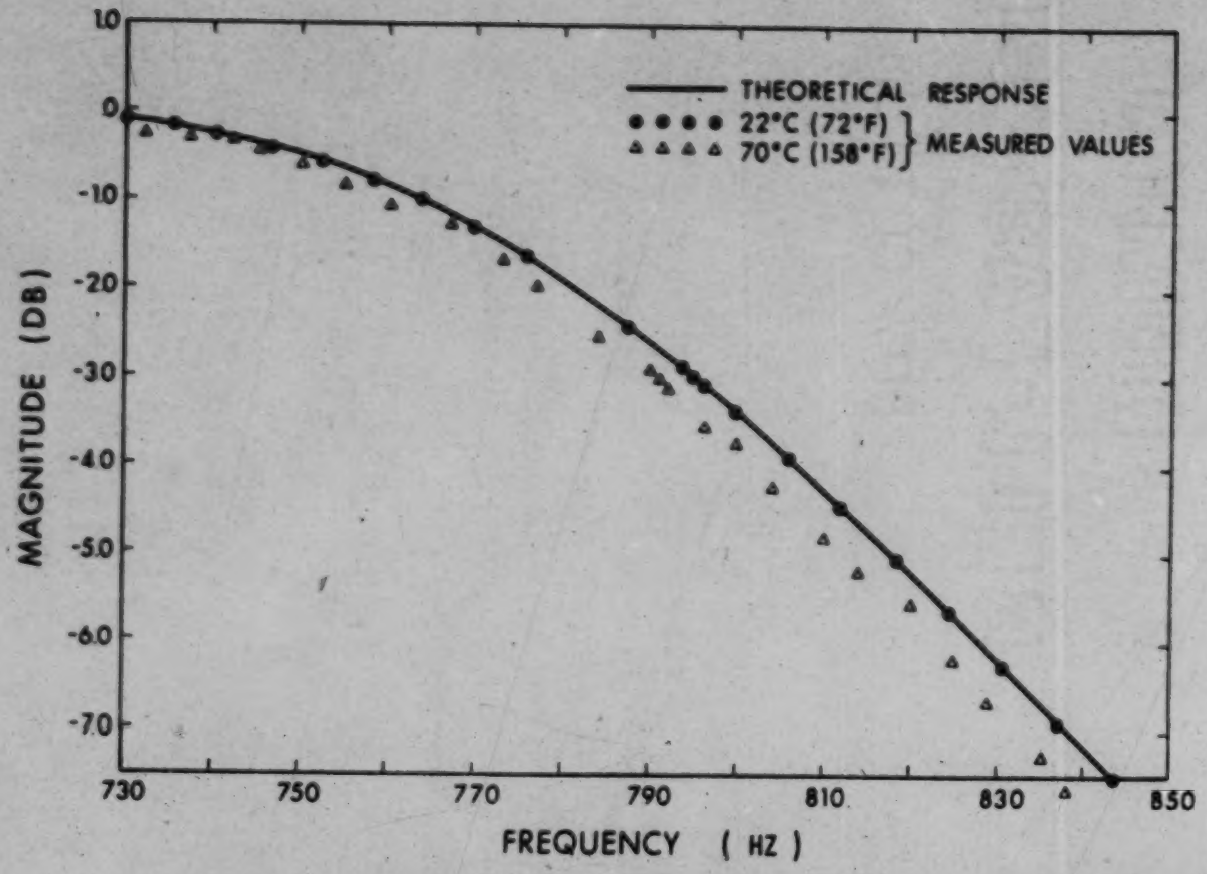

Figure (3.13) Frequency response of the sixth-order Chebyshev low-pass filter in the neighborhood of the half-power point f_{-3db} = 795.774 Hz.

3.5 *REALIZING A GROUNDED INDUCTOR BY A NIV*

Terminating the NIV with a negative grounded capacitor at one port gives an admittance of a grounded inductor at the other port, $Y_{in} = G^2/CP$, as given in Fig. (3.14) where $G_1 = G_2 = G_3 = G$.

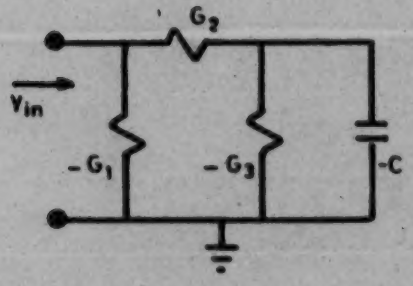

Figure (3.14) Simulating a grounded inductor.

A non-ideal inductor due to unequal resistances, G_1, G_2, G_3, results in a one-port network containing three parallel-connected branches as shown in Fig. (3.15). For given component tolerances of ± 1%, simple analysis of the various impedances in the three branches reveals that, in order to have a more accurate simulation, one should use a large value for the product of CR and match the values G_1 and G_2 as close as possible, where R is the nominal value of R_1, R_2, R_3.

Practical results in the circuits to follow using two operational amplifiers in the NIV circuit for realizing a grounded inductor prove that the above approximation is close enough to be used in the direct synthesis of high-order functions.

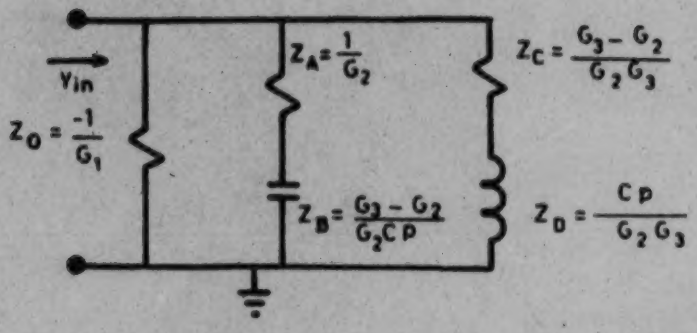

Figure (3.15) Non-ideal realization of a grounded inductor.

3.6 *SYNTHESIS OF FOURTH-ORDER BUTTERWORTH BAND-PASS FILTERS*

The application of NIV's in the synthesis of high-order polynomial band-pass filters is obvious and straight forward when a band-pass passive configuration is obtained from the corresponding low-pass one by frequency transformation. Both the floating and grounded inductors in the band-pass filter are to be replaced by NIV circuits in the following examples.

A second-order, low-pass, Butterworth filter is given in Fig. (3.16) with a voltage transfer function of

$$\frac{V_2}{V_1} = \frac{1}{P^2 + \sqrt{2}P + 1} \quad .$$

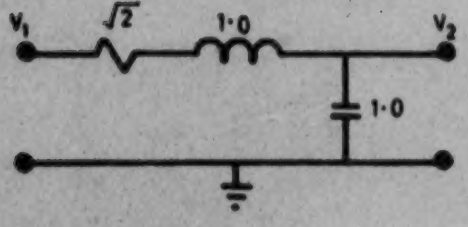

Figure (3.16) A second-order Butterworth low-pass filter.

After frequency transformation, a corresponding fourth-order band-pass filter is shown in Fig. (3.17), where the transfer function is

$$\frac{V_2}{V_1} = \frac{P^2/Q^2}{P^4 + P^3\sqrt{2}/Q + P^2(2 + 1/Q^2) + P\sqrt{2}/Q + 1}$$

where Q = 1/bandwidth.

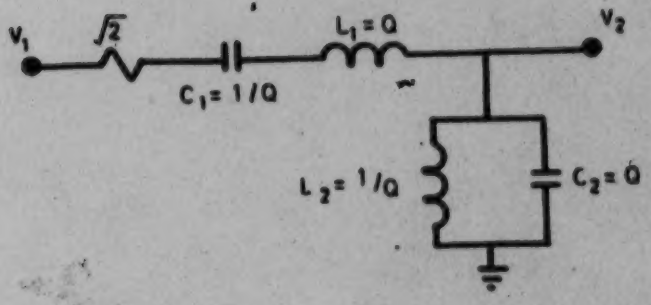

Figure (3.17) A fourth-order Butterworth band-pass filter.

At this point, the methods previously discussed can be applied directly to simulate the floating and grounded inductors, L_1 and L_2. After some simplication, one has an equivalent filter circuit as in Fig. (3.18). The parallel-connected negative R-L-C can be simulated by a NIV with negative elements as shown in Fig. (3.19), where

$$Y_{in} = -1/QP - P/Q - 2/Q.$$

This circuit can be simulated by using only one operational amplifier as given in Fig. (3.20).

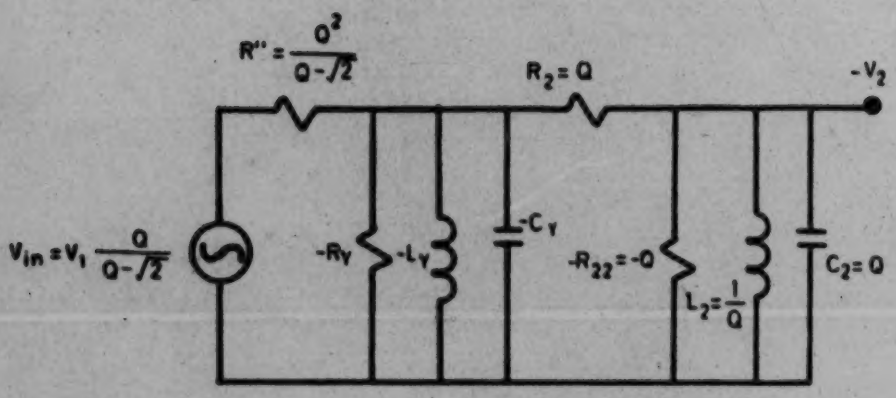

Figure (3.18) An equivalent fourth-order band-pass filter ($- R_y = - Q/2$, $- C_y = - 1/Q$, $- L_y = - Q$).

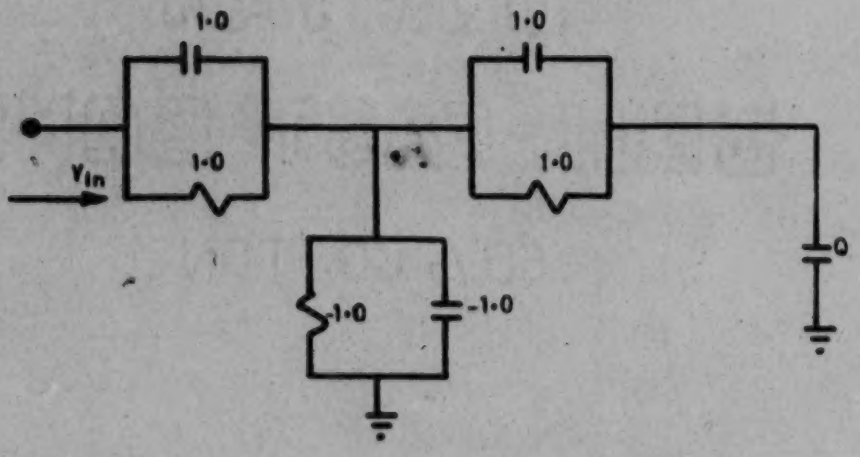

Figure (3.19) Simulation of negative R-L-C in parallel.

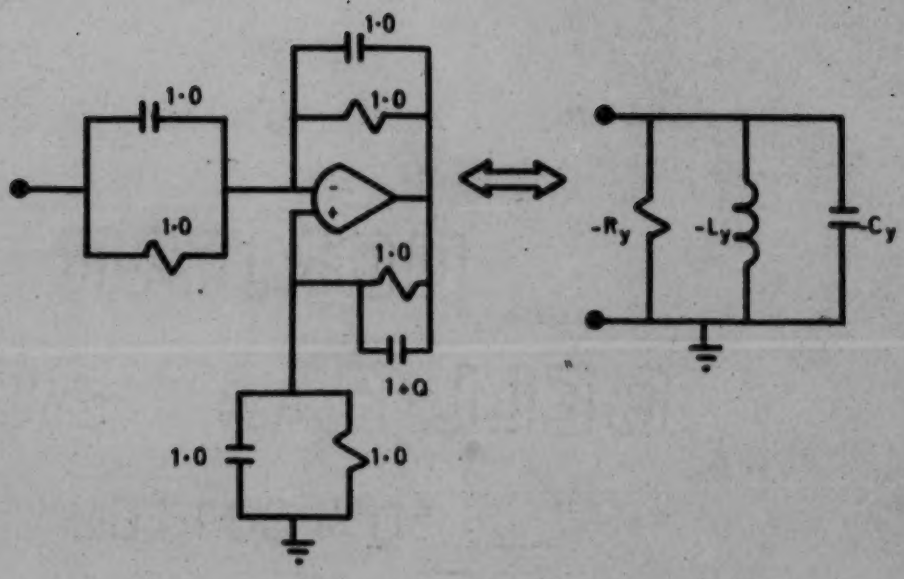

Figure (3.20) Simulation of parallel-connected R-L-C by one operational amplifier.

For the design objectives of f_0 = 795.774 Hz and Q = 5.0 , the final active realization using only three amplifiers is given in Figure (3.21).

Tuning of this filter is carried out by the following procedure. The circuit is disconnected at the point D. With reference to Fig. (3.18) and Fig. (3.21), the transfer function is a second-order band-pass one:

$$t_V(P) = \frac{-P/C_yR''}{P^2 + P(1/C_yR_y - 1/C_yR'') + 1/L_yC_y} .$$

Thus, the resonant frequency of the first stage, $\omega_0 = 1/\sqrt{L_yC_y}$, can be checked by finding the frequency for a sharp peak of resonance. The

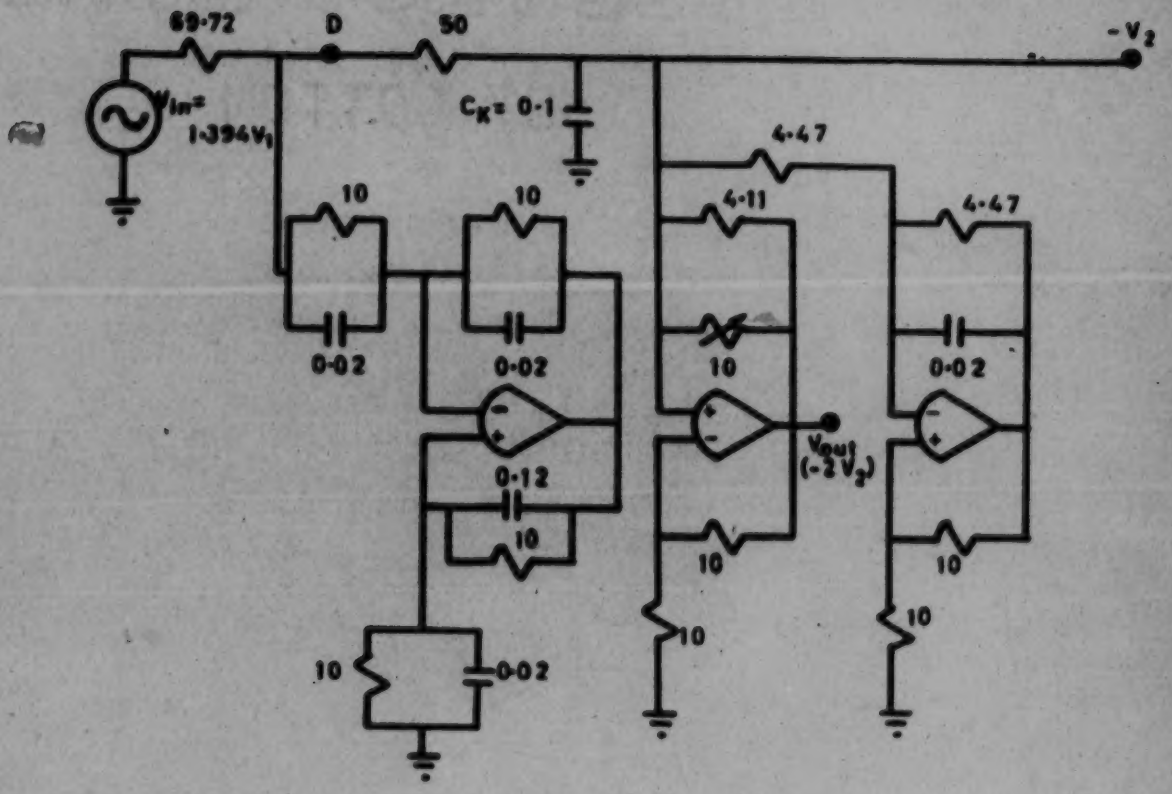

Figure (3.21) Active fourth-order Butterworth band-pass filter, f_0 = 795.774 Hz, Q = 5.0 .

transfer function of the second stage is given by

$$t_v(P) = \frac{P/C_2R_2}{P^2 + P/C_2(1/R_2 - 1/R_{22}) + 1/L_2C_2} .$$

Since $R_2 = R_{22}$, trimming the 10 K variable resistor in Fig. (3.21), one can adjust for the proper value of R_{22} by setting the poles on the

imaginary axis. The correct resonant frequency, $\omega_0 = 1/\sqrt{L_2C_2}$, can be set by varying C_K in Fig. (3.21).

Resonant frequency f_0 and Q are measured to be f_0 = 806 Hz (1.26 %) and Q = 4.835 (- 3.3 %) respectively. Frequency response and other measured data are given in Fig. (3.22), Fig. (3.23), and Appendix D.

Next, an attempt is made to realize a high-Q circuit meeting the design objectives of $\omega_0 = 5\times10^3$ rad/sec (f_0 = 795.774 Hz) and $Q = \sqrt{1000} = 31.6228$. The same design method is used and the final active realization is given in Fig. (3.24).

Resistor and capacitor values in Fig. (3.21) and Fig. (3.24) are within ± 1% accuracy of their nominal values and the operational amplifiers used are 1741's.

The same procedure is carried out for tuning. The resonant frequency and system Q are measured to be f_0 = 795.776 Hz (- 0.22%), Q = 31.76 (0.43 %). Note that the Q measured above is associated with the high-order system; Q's for the individual complex pole-pairs may be much higher. Much higher system Q's can be achieved for the above filter resonating at the same frequency. By varying R" in Fig. (3.24), experiment indicates that one can achieve a stable Q value of about three hundred. However, the wave-form as observed on the oscilloscope is drifting by 1db when the system is set to resonate with a Q of six hundred. It is, therefore, estimated that the practical system Q of this filter is limited to about three hundred. It should be pointed out that, in the above high-Q settings, the resonant frequency is measured to vary by no more than one half percent. Other measurements are given in Fig. (3.25), Fig. (3.26) and Appendix D.

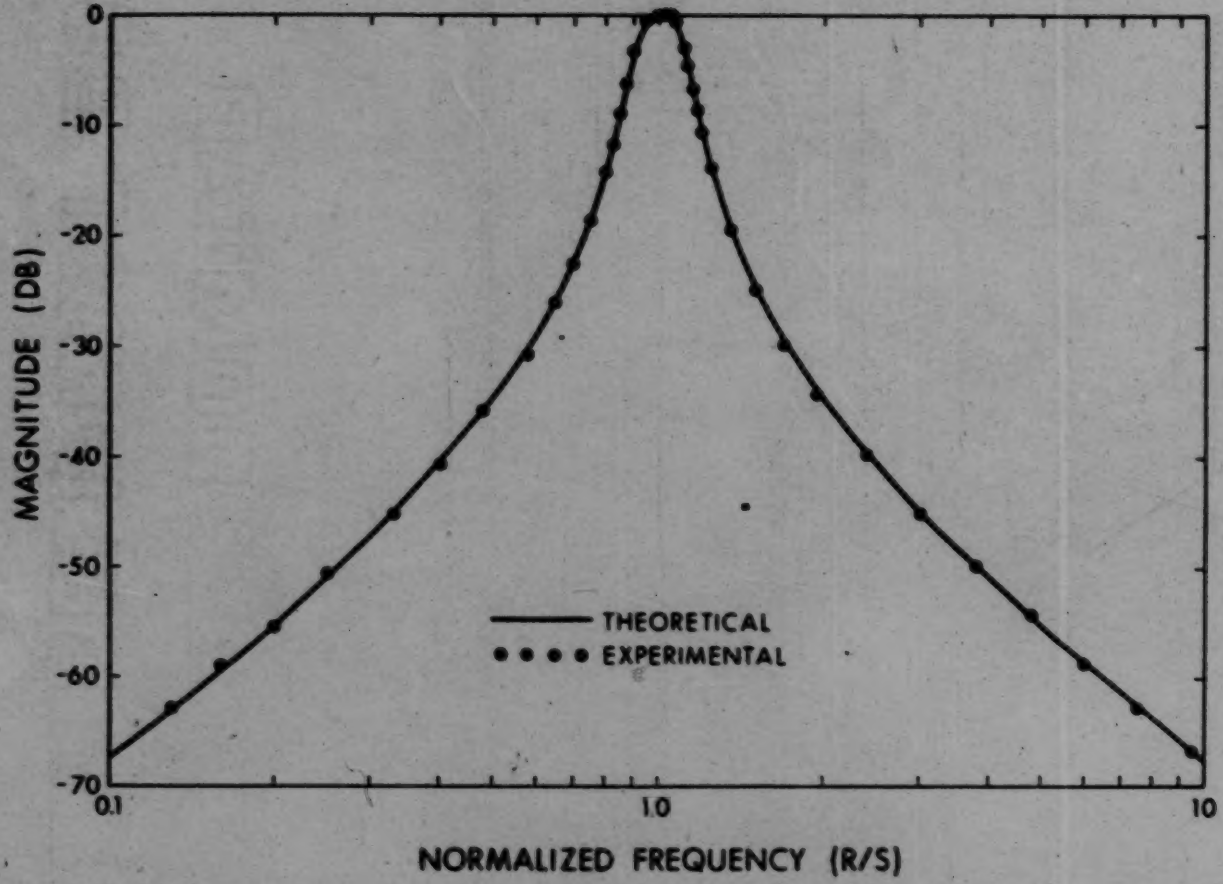

Figure (3.22) Frequency response of a fourth-order Butterworth band-pass filter; Q = 5.0, f_0 = 795.774 Hz.

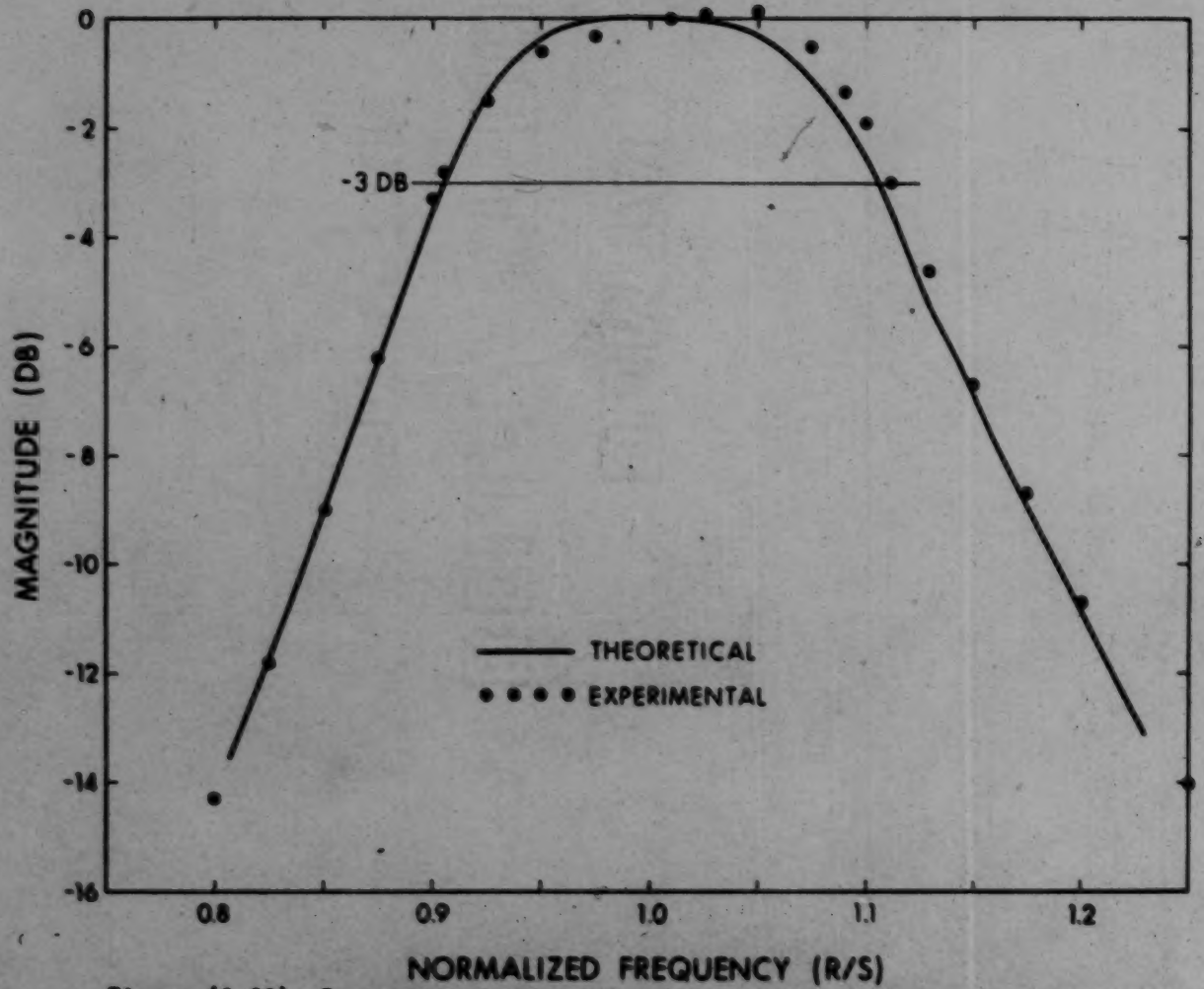

Figure (3.23) Frequency response of a fourth-order Butterworth band-pass filter in the pass-band region ; Q = 5.0, f_0 = 795.774 Hz.

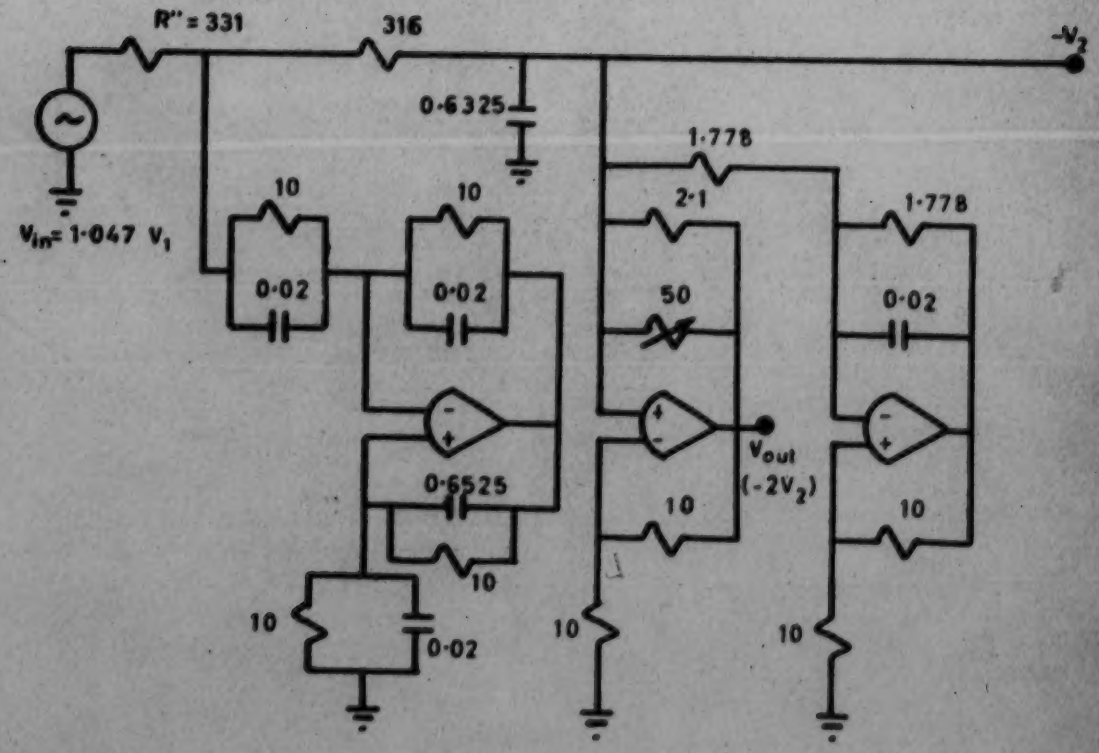

Figure (3.24) An active fourth-order Butterworth band-pass filter; $Q = 31.6$, $\omega_0 = 5\times10^3$.

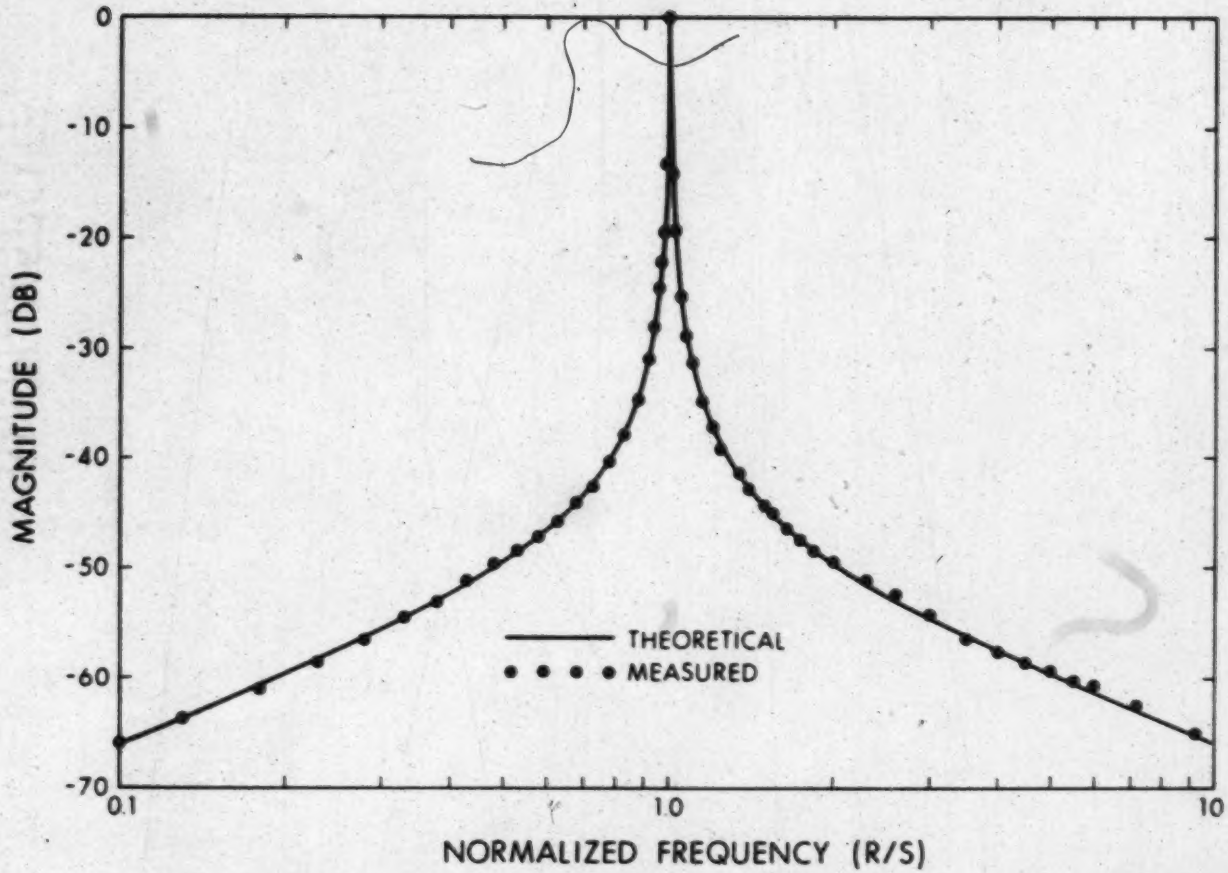

Figure (3.25) Frequency response of a fourth-order Butterworth band-pass filter ; $Q = 31.6$, $\omega_0 = 5\times10^3$.

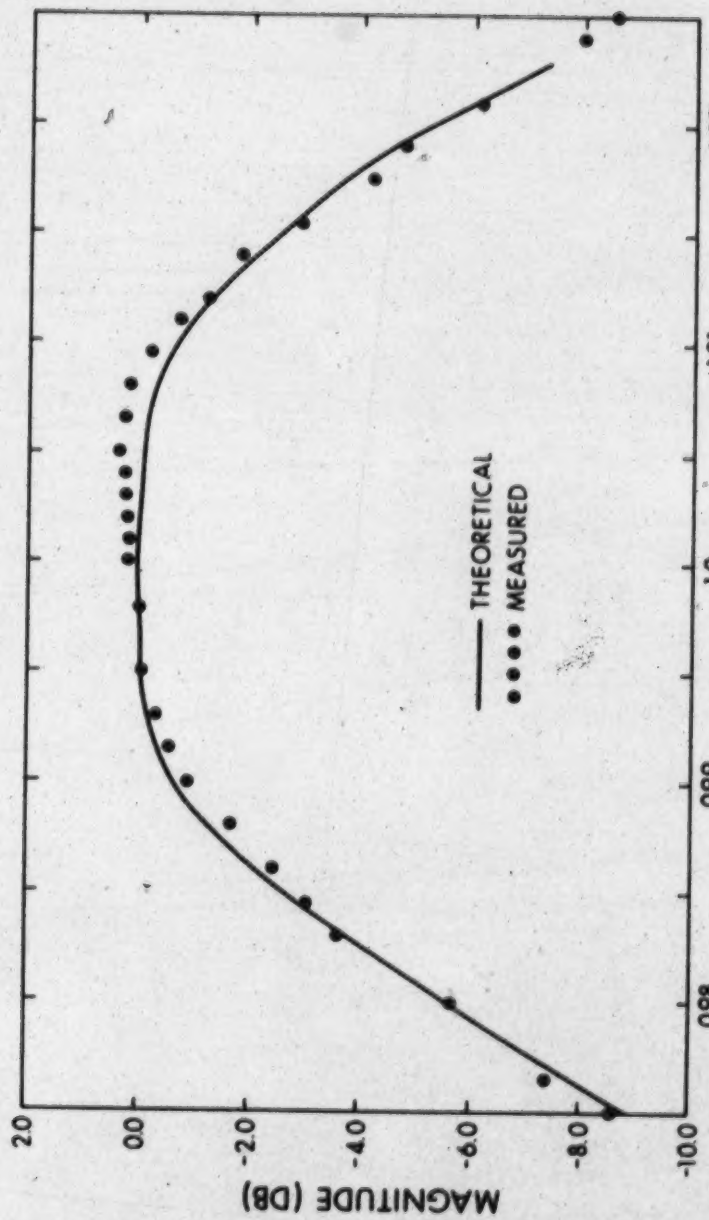

Figure (3.26) Frequency response of a fourth-order Butterworth band-pass filter in the pass-band region ; $Q = 31.6$, $\omega_0 = 5 \times 10^3$.

3.7 *A TWELFTH-ORDER BUTTERWORTH BAND-PASS FILTER REALIZED BY NIV'S*

The success of construction of the fourth-order band-pass filters discussed in Section (3.6) leads to a more ambitious attempt of synthesis. A twelfth-order Butterworth band-pass filter using the NIV's is realized in the following.

A sixth-order Butterworth low-pass passive R-L-C filter as shown in Fig. (3.8) is chosen from [52] and its element values are

$R_S = 1.0$, $L_1 = 0.5176$, $C_2 = 1.4142$, $L_3 = 1.9319$,

$C_4 = 1.9319$, $L_5 = 1.4142$, $C_6 = 0.5176$.

The low-pass filter is frequency-transformed into a corresponding twelfth-order band-pass filter in Fig. (3.27).

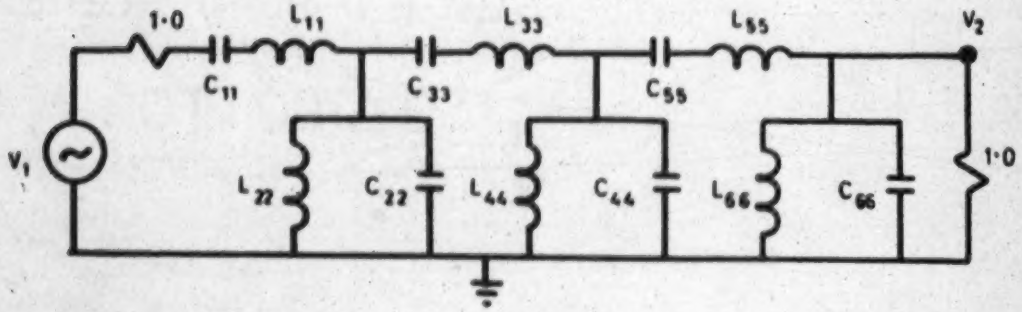

Figure (3.27) A twelfth-order Butterworth band-pass filter.

The element values of the band-pass filter are

$C_{11} = 1/L_1Q$, $C_{22} = C_2Q$, $C_{33} = 1/L_3Q$, $C_{44} = C_4Q$,

$C_{55} = 1/L_5Q$, $C_{66} = C_6Q$, $L_{11} = L_1Q$, $L_{22} = 1/C_2Q$,

$L_{33} = L_3Q$, $L_{44} = 1/C_4Q$, $L_{55} = L_5Q$, $L_{66} = 1/C_6Q$.

Transformation of the passive band-pass filter by NIV's results in a circuit shown in Fig. (3.28) with the following element values

$$C_A = G_1^2 L_1 Q \ , \quad L_A = 1/C_A \ , \quad C_B = G_2^2 L_3 Q \ ,$$
$$L_B = 1/C_B \ , \quad C_C = G_3^2 L_5 Q \ , \quad L_C = 1/C_C \ .$$

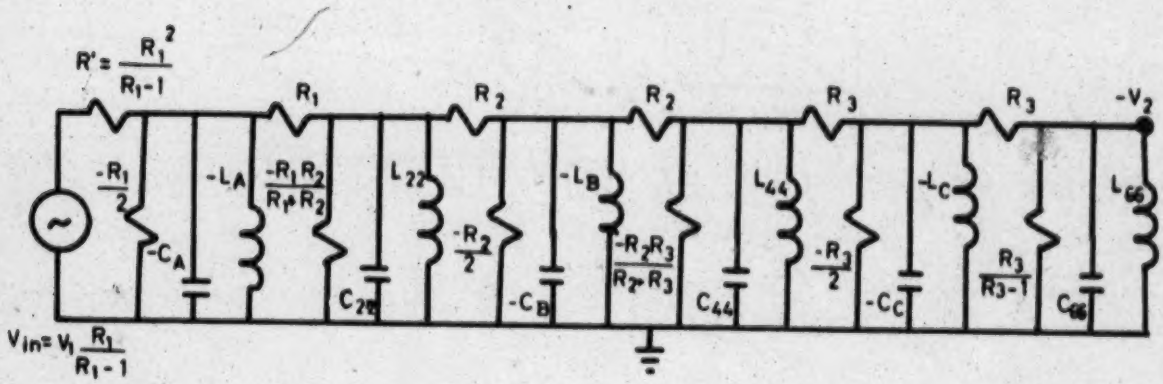

Figure (3.28) A twelfth-order Butterworth band-pass filter realized by NIV's.

Using the same method as before for simulating negative parallel grounded R-L-C's and grounded inductors, one arrives at the final circuit of active realization as given in Fig (3.29) where passive components are of ± 1% accuracy, and in units of KΩ, μf, and the operational amplifiers used are 1741C's.

Tuning of this filter follows basically the same procedure as before. The complete filter can be broken down into six second-order sections, all the resonant frequencies of which can be checked to be about 796 Hz . It is found experimentally that by replacing the

series resistor of 282.8 KΩ in the last section by a parallel combination of a 40 pf capacitor and two resistors of 262K+50K(variable), one can adjust for a correct system Q and smooth the frequency response around the region of the higher 3db point. Frequency response is given in Fig. (3.30) and Fig. (3.31).

The resonant frequency and Q are measured to be

$$f_0 = 799.233 \text{ Hz } (0.435\%) , \quad Q = 9.8915 \ (- 1.085\%) .$$

Effects due to temperature variation are also measured and shown in the above two figures to be relatively insignificant. Other measured data are given in Appendix E. Compared with the design method of realizing the same filter by the state-variable technique by Kerwin, Huelsman, and Newcomb [6] one can save no fewer than nine operational amplifiers by using NIV's in this case.

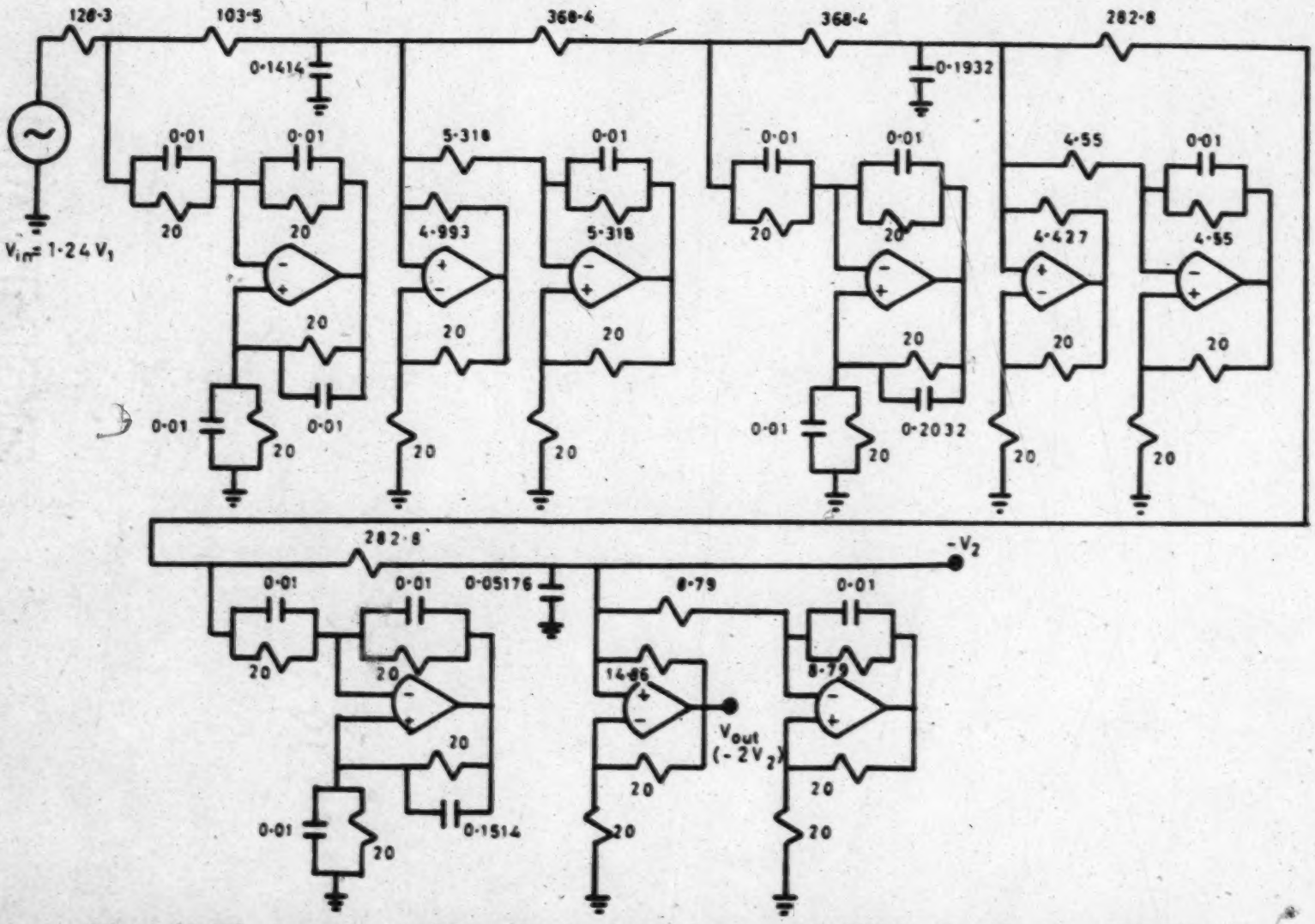

Figure (3.29) An active twelfth-order band-pass Butterworth filter, Q = 10 , f_0 = 795.774.

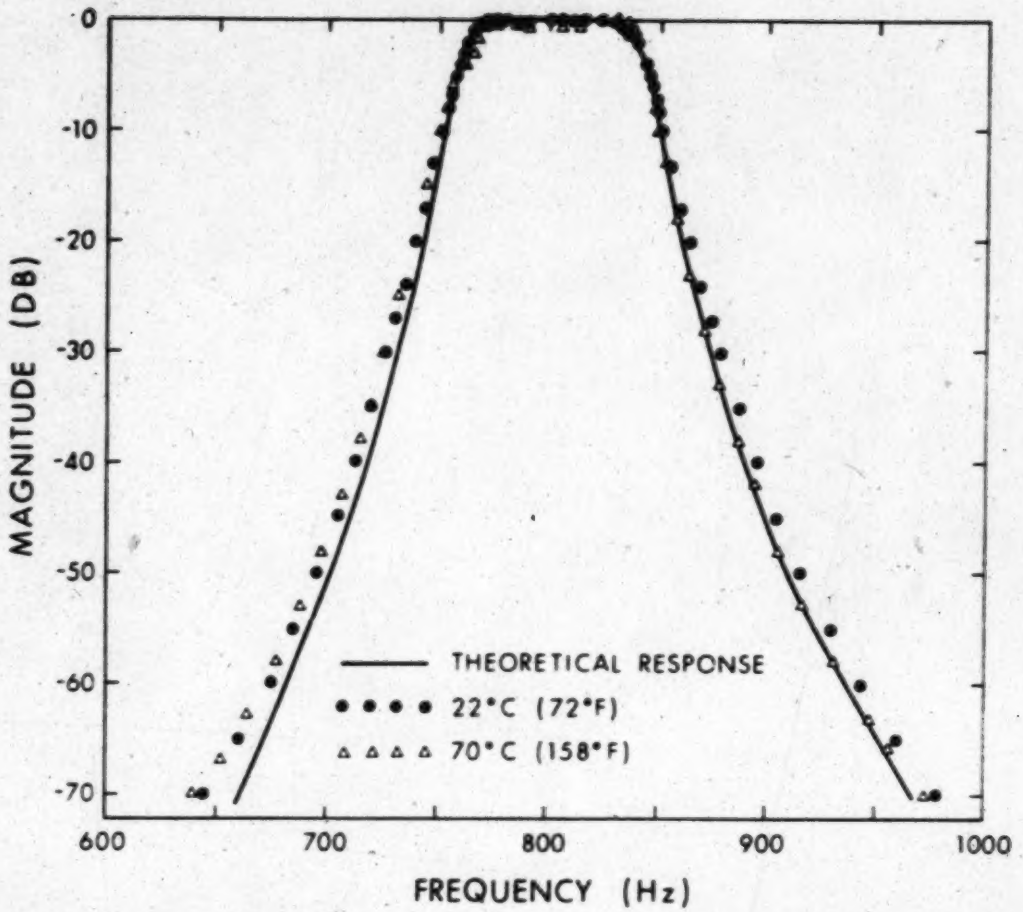

Figure (3.30) Frequency response of the active twelfth-order band-pass Butterworth filter;Q=10,f_0=795.774Hz.

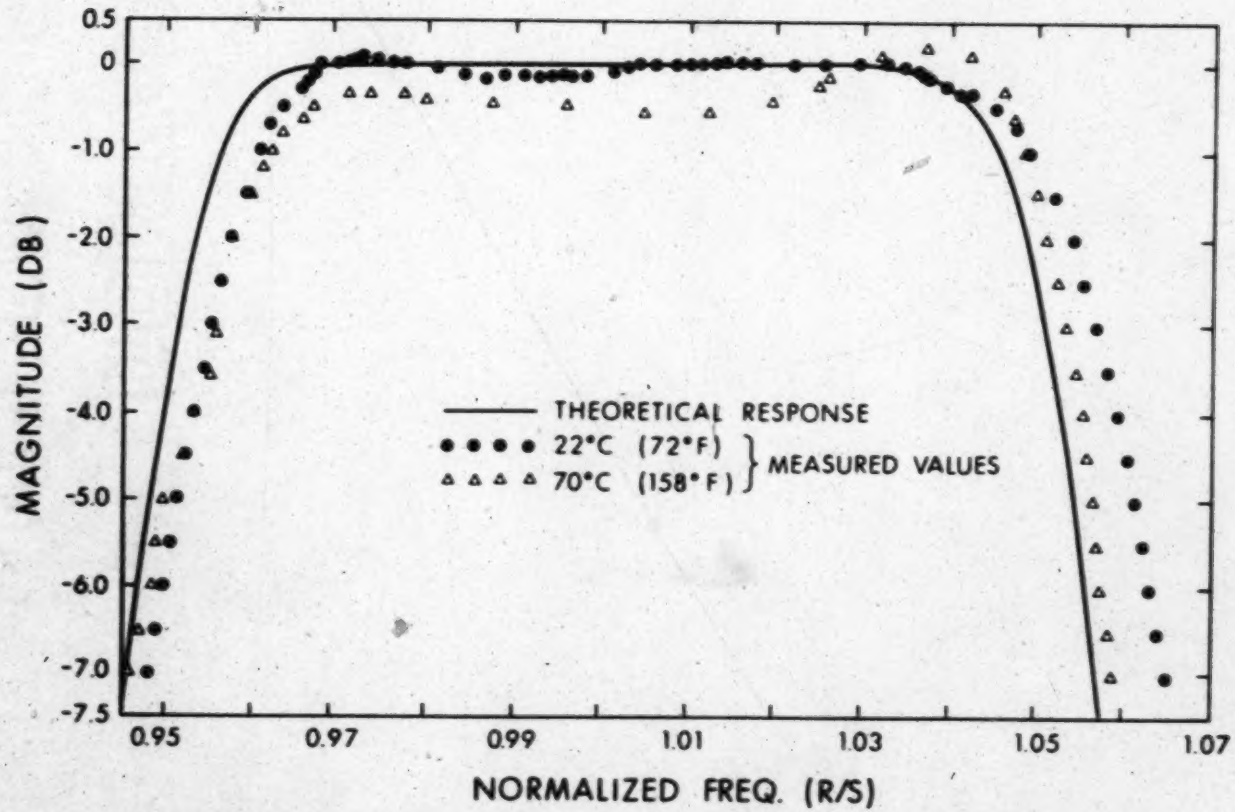

Figure (3.31) Frequency response of the active twelfth-order band-pass Butterworth filter in the pass-band region; Q = 10 , f_0 = 795.774 Hz.

CHAPTER IV

ACTIVE INDUCTORLESS CAUER FILTERS

4.1 *BACKGROUND*

Among the various types of generally used filters, the Cauer filter may be the most effective one in providing very sharp frequency cutoff with relatively low-order functions. Due to its general structure, the Cauer filters are usually more difficult to realize by active inductorless design. The idea initiated by Bruton [7], [12] of using frequency-dependent negative-resistance element for realization proved very effective in realizing high-order Cauer low-pass filters. This method was later extended to the case of realizing high-order band-pass filters by Antoniou [25].

Consider the operational amplifier circuit given in Fig. (4.1).

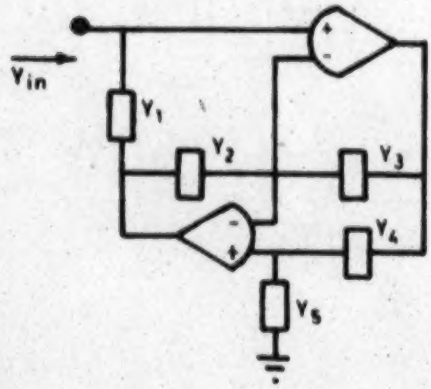

Figure (4.1) The frequency-dependent negative-resistance (conductance) element realized by two operational amplifiers.

The positive imittance-converter-type network has an input admittance of $Y_{in} = Y_1Y_3Y_5/Y_2Y_4$. This expression is derived by assuming no other approximations than that the operational amplifiers are ideal with infinite gain, input impedance and output admittance. By assigning the various admittances to be either capacitances or conductances, two very useful elements can be realized; i.e., the frequency-dependent negative-resistance element (FDNR), $Z(P)=K_1P^2$, and the frequency-dependent negative-conductance element (FDNC), $Y(P) = K_2P^2$, where K_1, K_2 are positive constants. These two elements are to be applied to the synthesis of Cauer, low-pass, and band-pass filters.

A Cauer low-pass filter of arbitrary order is realized in Fig. (4.2) with passive R-L-C elements.

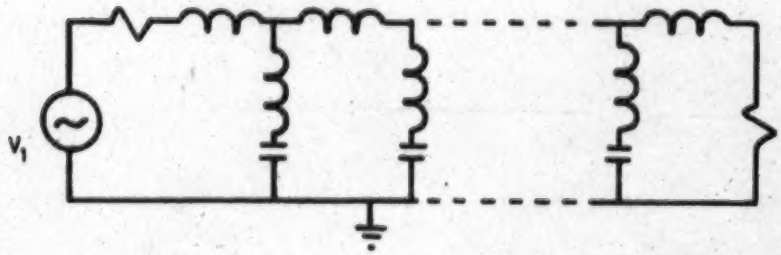

Figure (4.2) A Cauer low-pass filter.

The voltage transfer function remains unchanged when the admittance of each branch of the filter is multiplied by P ($P = j\omega$). The

R-L-C elements are transformed into C-R-FDNC, respectively. The transformed filter circuit is shown in Fig. (4.3) with symbol of ⫩ denoting a FDNC element.

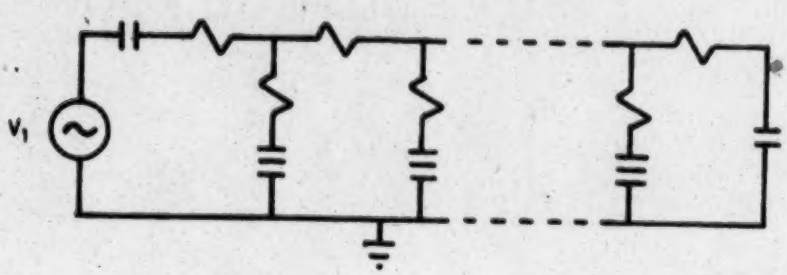

Figure (4.3) A Cauer low-pass filter using FDNC's.

The circuit in Fig. (4.1) can then be directly applied to realize FDNC elements for the transformed low-pass filter. Thus, a Cauer, high-order, low-pass filter is realized by using a small number of operational amplifiers.

For the direct synthesis of band-pass Cauer filters, the low-pass, passive configuration is re-arranged so that the input-series resistor disappears. This can be done in most practical cases as will be discussed in the next section. The standard technique of frequency-transformation converts a grounded FDNC element into a parallel combination of a resistor, a FDNC element, and a FDNR element denoted by the symbol ⊠. The corresponding band-pass filter transformed from the low-pass one by the above methods is given in Fig. (4.4).

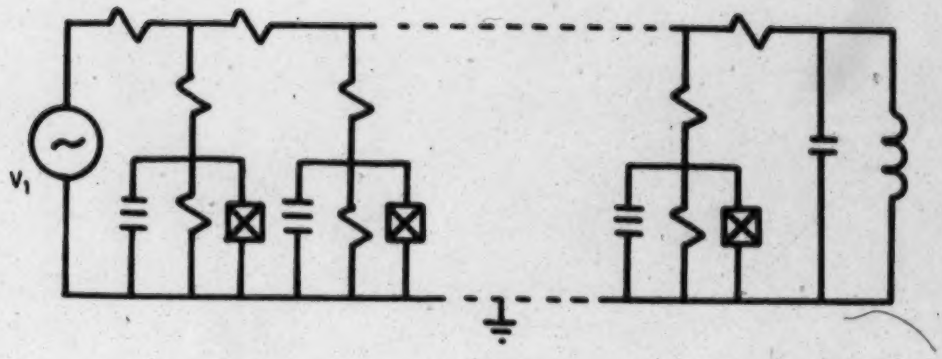

Figure (4.4) A Cauer band-pass filter by using FDNC and FDNR elements.

The band-pass synthesis is complete when the FDNC and FDNR elements are realized by using the circuit in Fig. (4.1).

These methods are considered very efficient and easy to apply for practical filter synthesis. A small number of active elements are required; e.g., only seven operational amplifiers are necessary to realize a sixth-order Cauer band-pass filter with sharp frequency roll-offs.

However, the realization of a Cauer, band-stop filter proves to be a much more difficult problem because a grounded FDNC element is transformed from the low-pass configuration to the band-stop configuration into a series combination of a resistor, a FDNC and a FDNR element. In this case, either the FDNC or the FDNR element must be realized in a floating manner. Two ideas were suggested by Antoniou [25]. The floating FDNC or FDNR element can be realized by using two identical generalized immittance converters in Riordan's floating-

inductance configuration. The other method requires a three-terminal gyrator terminated by the dual of the series elements which is a parallel combination of the three elements concerned. Both methods require additional active elements; furthermore, the first method needs identical active elements which must be critically matched. However, no details of these two methods are given, nor any experimental circuits are reported.

4.2 *ACTIVE SYNTHESIS OF HIGH-ORDER CAUER BAND-STOP FILTERS*

The general procedure of realizing high-order, band-stop filters by active elements follows from the low-pass configuration shown in Fig. (4.3). The corresponding band-stop filter after frequency-transformation is given in Fig. (4.5), where the filter is designed with a series element at the input port.

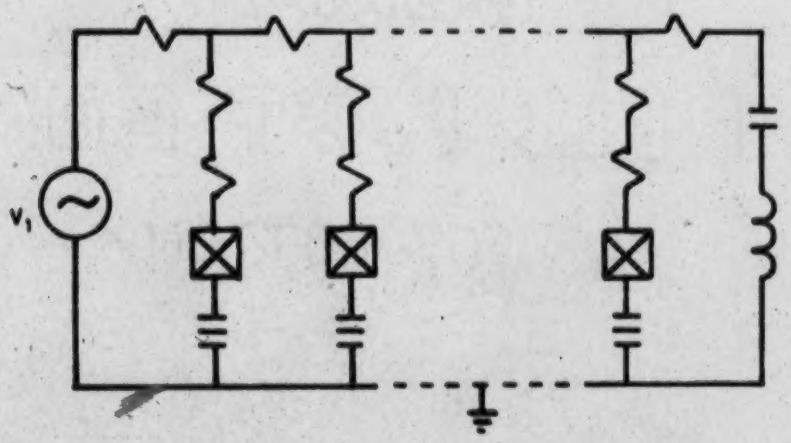

Figure (4.5) A Cauer band-stop high-order filter using FDNC and FDNR elements.

The series arrangement of a resistor, a FDNC, and a FDNR element is to be realized by the following method. Consider the circuit in Fig. (4.6) where five operational amplifiers are employed. Each of the input admittances as seen by V_2 and V_4 is a grounded FDNR element realized by two operational amplifiers in each stage; i.e.,

$$Y_1 = \frac{G_1 G_3 G_5}{C_2 C_4 P^2} \quad \text{and} \quad Y_{11} = \frac{G_{11} G_{33} G_{55}}{C_{22} C_{44} P^2} .$$

The voltage transfer functions in these two sections are given by

$$\frac{V_3}{V_2} = 1 - \frac{G_3 G_5}{C_2 C_4 P^2} \quad \text{and} \quad \frac{V_5}{V_4} = 1 - \frac{G_{33} G_{55}}{C_{22} C_{44} P^2} .$$

For simplicity, one can assign $C_2 C_4 R_3 R_5 = C_{22} C_{44} R_{33} R_{55} = 1.0$. Therefore, the above circuit can be replaced by its equivalent using the controlled-sources representation in Figure (4.7).

One can, then, very easily arrive at the following expressions

$$\frac{V_2}{V_1} = \frac{G_X P^2}{G_1 + G_X P^2} , \quad \frac{V_3}{V_2} = \frac{P^2 - 1}{P^2} ,$$

$$\frac{V_4}{V_3} = \frac{G_{XX} P^2}{G_{11} + G_{11} P^2} , \quad \frac{V_5}{V_4} = \frac{P^2 - 1}{P^2} .$$

The overall voltage transfer function is, therefore, given by

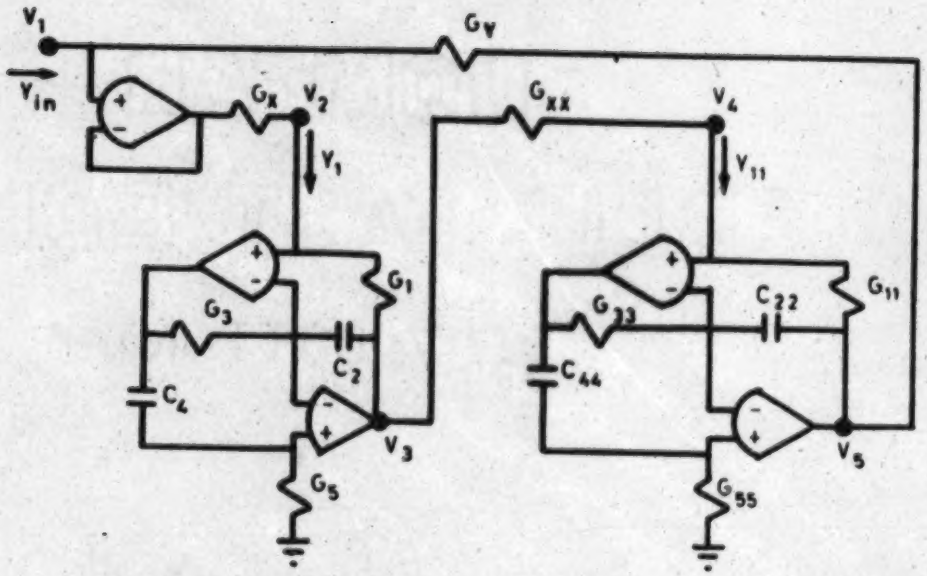

Figure (4.6) Realization of a series combination of a resistor, a FDNC and a FDNR element by realizing two FDNR elements.

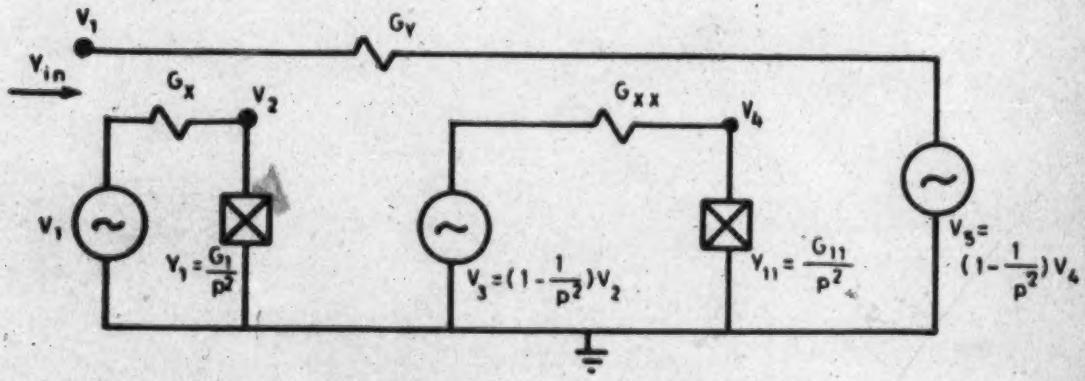

Figure (4.7) An equivalent circuit to that in Fig. (4.6).

$$\frac{V_5}{V_1} = \frac{(P^2 - 1)^2}{(P^2 + 1)^2} = \frac{P^4 - 2P^2 + 1}{P^4 + 2P^2 + 1}$$

after the assumption is made for $G_X = G_1$, $G_{XX} = G_{11}$. The resulting input admittance is given by

$$Y_{in} = (1 - \frac{V_5}{V_1})\, G_Y = \frac{1}{R_Y/4\ (P^2 + 2 + 1/P^2)}$$

which is the admittance of a grounded, series combination of a resistor, a FDNR and a FDNC element transformed from a grounded FDNC element in the low-pass case. The value of the feedback resistor, R_Y, can be adjusted to meet the requirement of the band-stop system Q .

An alternate method is given in Fig. (4.8) and Fig. (4.9) where realization of two FDNC elements by five operational amplifiers leads to the same final result. The same assumption is made for the time constants; i.e., $C_3C_5R_2R_4 = C_{33}C_{55}R_{22}R_{44} = 1.0$. The input admittance functions seen by V_2 , V_4 , and the voltage transfer function are respectively

$$Y_1 = G_1P^2 \ , \ Y_2 = G_{11}P^2 \ , \ \frac{V_2}{V_1} = \frac{1}{1 + P^2} \quad (\text{where } G_X = G_1) \ ,$$

$$\frac{V_3}{V_2} = 1 - P^2 \ , \ \frac{V_4}{V_3} = \frac{1}{1 + P^2} \quad (\text{where } G_{XX} = G_{11}) \ , \ \frac{V_5}{V_1} = 1 - P^2 \ .$$

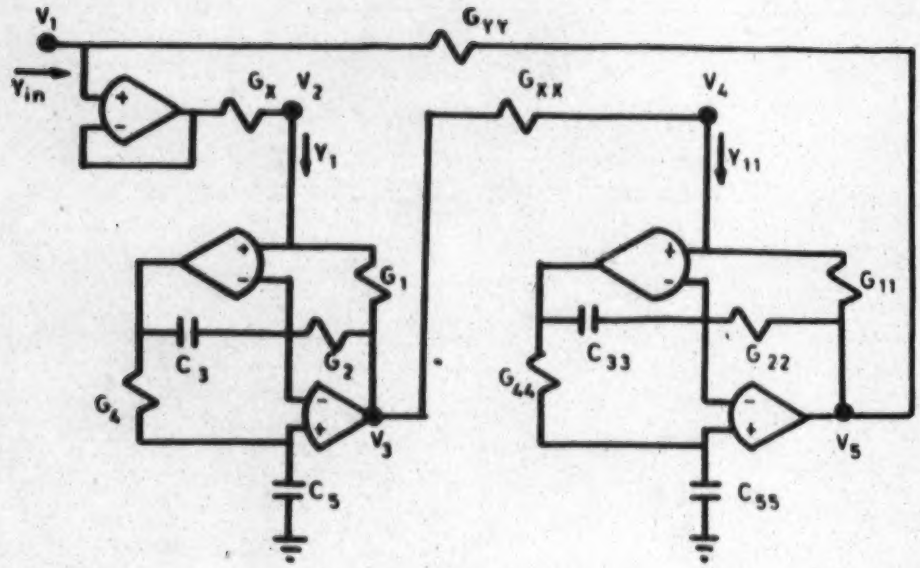

Figure (4.8) Realization of a series combination of a resistor, a FDNC and a FDNR element by realizing two FDNC elements.

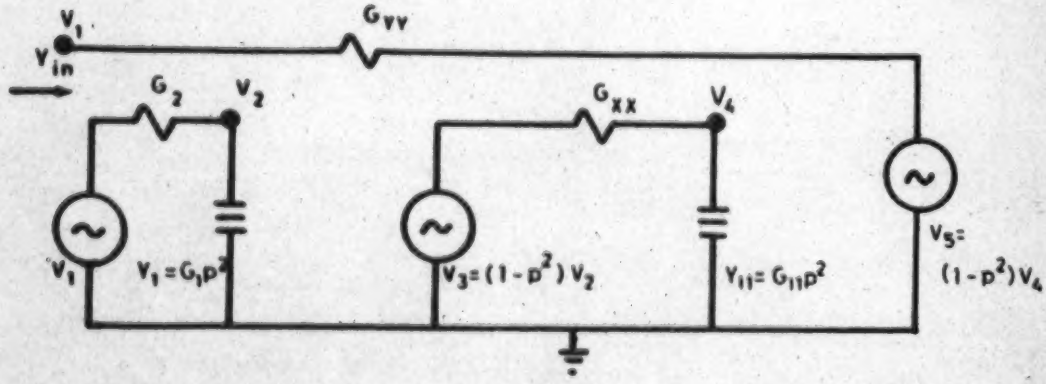

Figure (4.9) An equivalent circuit to that in Fig. (4.8).

The overall transfer function and the input admittance function are, then, given by

$$\frac{V_5}{V_1} = \frac{(1 - P^2)^2}{(1 + P^2)^2} = \frac{1 - 2P^2 + P^4}{1 + 2P^2 + P^4} \quad , \quad Y_{in} = \frac{1}{R_{yy}/4\ (P^2 + 2 + 1/P^2)} \quad .$$

Thus, two methods have been presented for the realization of the series R-FDNC-FDNR arrangement by using only five operational amplifiers in each case. The final realization of a high-order, Cauer, band-stop filter is complete when either of the above two circuits is used in Fig. (4.5). The number of operational amplifiers used per each series R-FDNC-FDNR realization is one more than that required for realizing the corresponding parallel elements in the case of band-pass realization by Antoniou [25]. However, this extra amplifier is used to realize a highly stable buffer for the purpose of isolating the following stages. The number of amplifiers required, N_1, and the order of the corresponding low-pass filter, N_2, are given in the following for N_2 between three and seven: $N_2 = 3, 4, 5, 6, 7$ corresponding to $N_1 = 8, 13, 13, 18, 18$ respectively. It is, therefore, more economical to realize the band-stop filter with odd number of orders for the corresponding low-pass case.

4.3 *REALIZING A SIXTH-ORDER CAUER BAND-STOP FILTER*

An experimental circuit using one of the methods discussed in Section (4.2) is constructed in this section to illustrate the technique of synthesis. The problems were encountered by a local company where a voice channel carried frequency shift keyed (FSK) information as well. In order to filter out the FSK signals at frequencies of 2100 Hz and 2300 Hz , a band-stop filter of sufficiently sharp frequency-cutoff characteristic is needed. The filtering of the signals with frequencies between these two did not reduce the effectiveness of the voice channel appreciably.

A sixth-order, Cauer band-stop filter was chosen with the two zero frequencies falling at 2100 and 2300 Hz . A corresponding third-order low-pass filter was chosen from page 179 of [52] as shown in Fig. (4.10) with a pass-band ripple of 1.25db and a minimum attenuation of 30db in the stop-band. The center frequency was f = 2197.7 Hz and the system Q was 5.587.

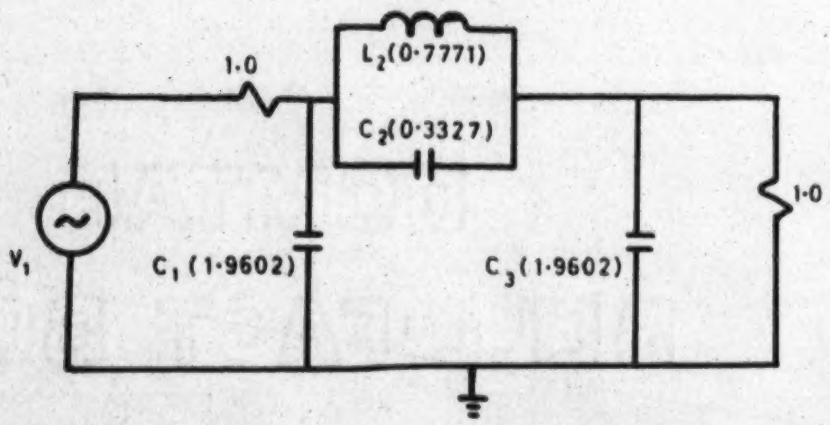

Figure (4.10) A Cauer third-order low-pass filter.

This filter with an equivalent transfer function but a zero input resistor is shown in Fig. (4.11).

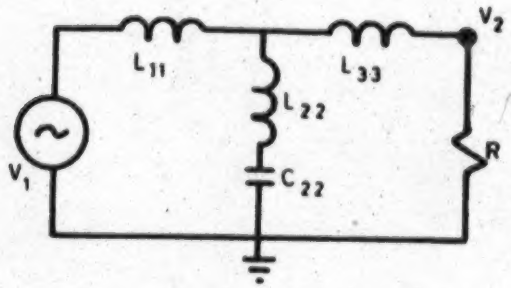

Figure (4.11) An equivalent circuit to that in Fig. (4.10).

The condition that must be satisfied for the component values to be positive in the equivalent circuit is $C^2 > L_2C_2$ (where $C_1 = C_3 = C$) . This condition is found to be satisfied by most filters contained in [52]. The component values are given by $R = 2.0$, $L_{11} = 2.8691953015$, $L_{22} = 0.486981571681$, $C_{22} = 0.530905449066$, $L_{33} = 1.8283046985$. The transformed circuit has twice the output voltage at low frequencies as compared to the original one. Multiplying the admittance of each branch by P (where $P = j\omega$) results in an equivalent circuit containing a grounded FDNC element as shown in Fig. (4.12).

The low-pass filter is further transformed into a band-stop one as shown in Fig. (4.13) by applying the standard technique of frequency transformation, i.e.,

$$P = \frac{1}{Q(P + 1/P)} .$$

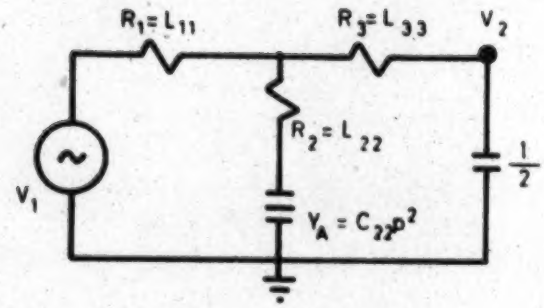

Figure (4.12) The equivalent low-pass filter containing a FDNC element.

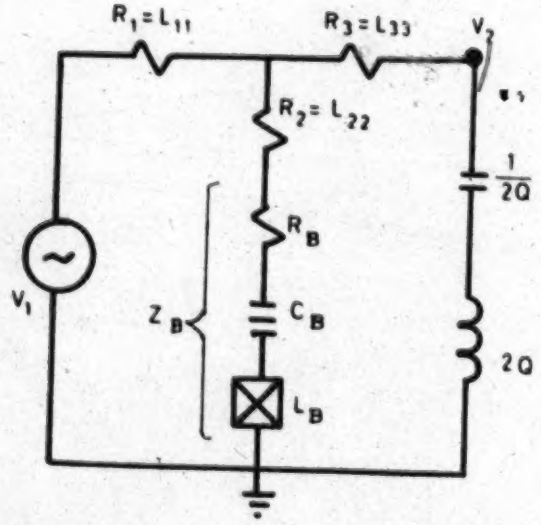

Figure (4.13) A sixth-order Cauer band-stop filter.

The FDNC element, $Y_A = C_{22}p^2$, is transformed into a series R-FDNC-FDNR combination, the impedance of which is given by

$$Z_B = R_B + L_B p^2 + \frac{1}{C_B p^2} = \frac{2Q^2}{C_{22}} + \frac{Q^2}{C_{22}} p^2 + \frac{Q^2}{C_{22} p^2} \quad .$$

The grounded inpedance Z_B is to be realized by using the second method containing FDNC elements as discussed in the last section, and the grounded inductance of 2Q by NIV's. The final circuit realization using only eight operational amplifiers is given in Fig. (4.14). Measured data are very close to the theoretical ones: f_0 = 2183 Hz (- 0.67 %); two zero frequencies f_A = 2083 (- 0.81 %), f_B = 2286 (- 0.61 %); magnitude response is - 31.6db at f = 2300; Q = 5.55 (- 0.673 %). Other details of measurement are given in Appendix F. Capacitor and resistor values are of ± 1% accuracy and in units of nano-farads and kilo-ohms. The amplifiers used are 1741C's. Frequency response with respect to temperature variations is plotted in Fig. (4.15). Measured data as compared to the theoretical response indicate that the objectives of design have been fulfilled and the filter performance is relatively insensitive to temperature changes.

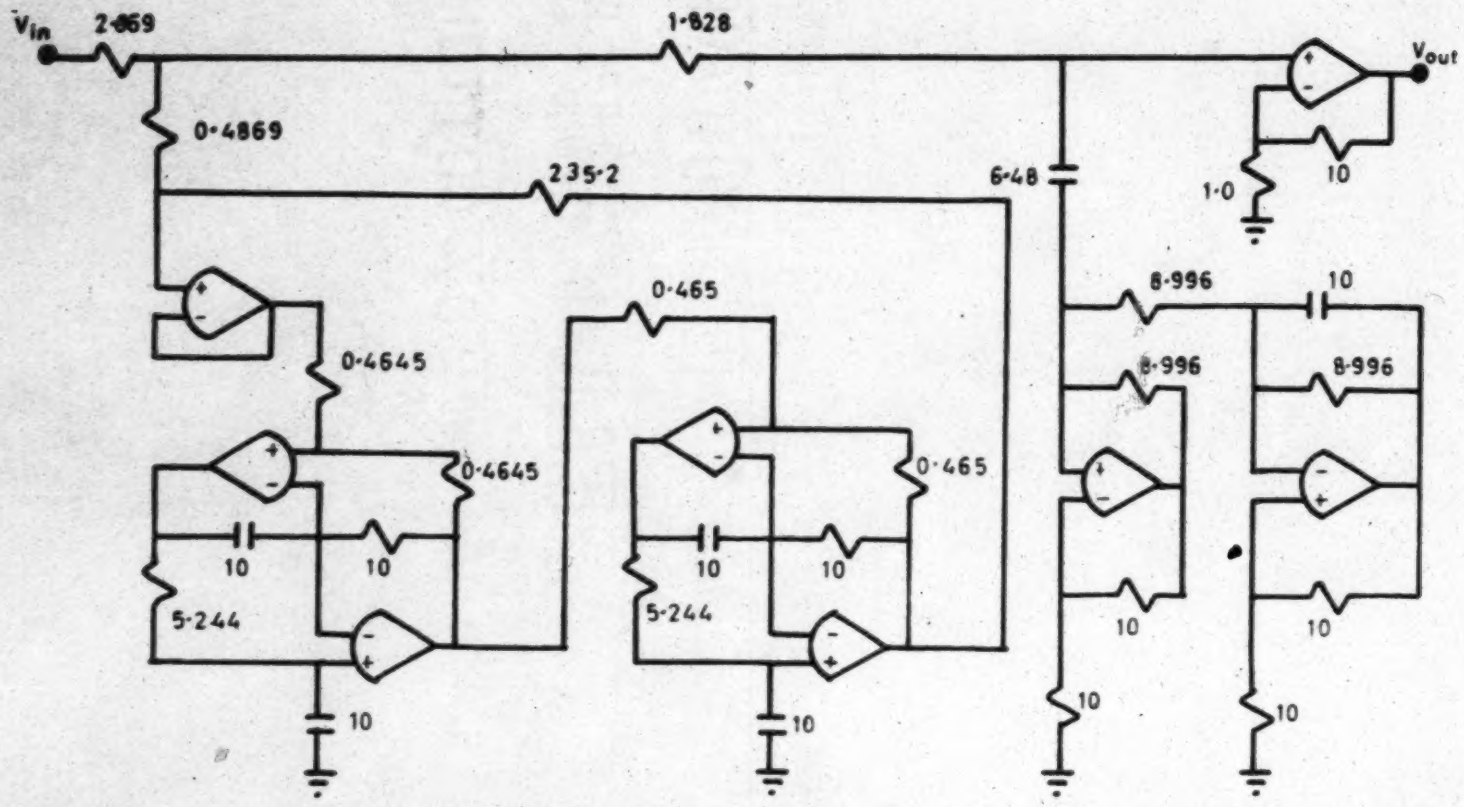

Figure (4.14) The active sixth-order Cauer band-stop filter for a minimum attenuation of 30db between f = 2100 and 2300 Hz.

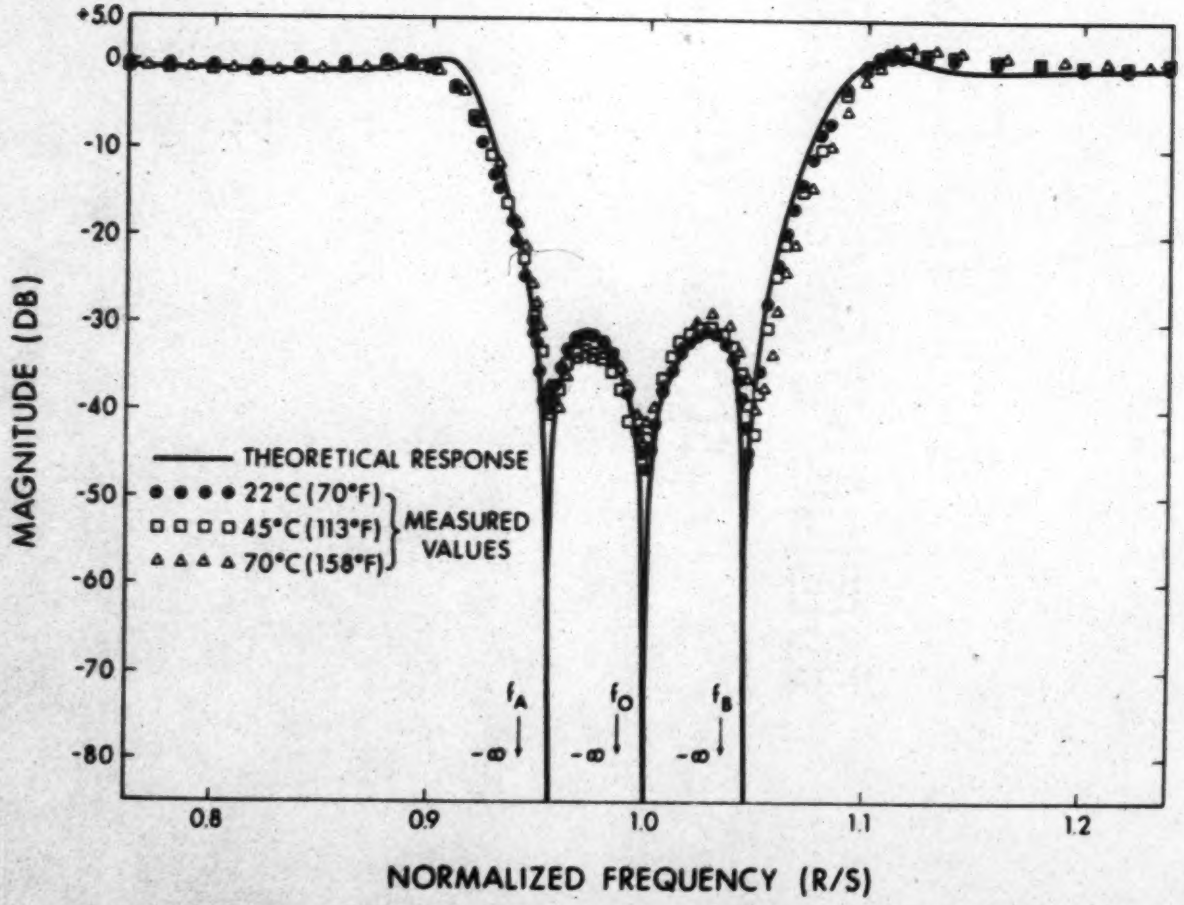

Figure (4.15) Frequency response of the band-stop filter with respect to temperature variations.

CHAPTER V

CONCLUDING REMARKS

5.1 *CONCLUSIONS*

Two approaches to the synthesis of inductorless active filter synthesis have been discussed in this dissertation. Various methods are investigated to realize a second-order voltage transfer function using unity-gain amplifiers. Sensitivity to parameter variations in most cases is minimized. Some experimental prototypes using transistors and operational amplifiers are built according to the proposed theoretical schemes of design. Results obtained for narrow and very narrow bandwidth are shown to be very close to the theoretical ones. The Riordan's gyrator is found suitable for realizing a grounded inductor in the case of very high-Q requirements.

Extensive use is made of the resistive negative-immittance-inverters to replace floating inductors in the direct approach to high-order-function synthesis. The design procedure is a general one applicable to all polynomial types of filters. The problem of realizing Cauer band-stop filters is solved by using only five operational amplifiers to simulate a series combination of a resistor, a frequency-dependent negative resistance, and a frequency-dependent negative-conductance element. The fact that relatively low-cost operational amplifiers are used in the practical constructions indicates that the design methods are not critical at all. The methods proposed are very economical,

as only a small number of active devices are required. Temperature variations are found to be relatively insignificant in the performance of the high-order filters realized by these methods. Thus, direct filter synthesis is possible in integrable, hybrid, or discrete forms.

It is, therefore, concluded that in the audio frequency range it is practical and economical to solve the problem of filter synthesis by the proposed inductorless active arrangements using either the approach of cascading second-order realizations, or that of direct synthesis.

5.2 *SUGGESTIONS FOR FURTHER RESEARCH*

In the practical realization by integrated-circuit frabrication, improvements can be found in the circuits using state-variable technique and grounded-inductor simulation discussed in Chapter II if one can construct the unity-gain amplifiers by using NPN transistors only. High-quality PNP transistors are usually more difficult to fabricate in integrated form.

Direct synthesis of high-order filters, using linear active devices, and possessing desirable properties of independently adjustable center frequency and Q by varying some resistances is certainly an area that calls for further research in the near future. This will not probably be achieved by using more amplifiers. However, due to the trend of continuous reduction in costs of operational amplifiers in integrated forms, the penalty one pays for using more active devices

will not be severe.

In addition, research in active filter synthesis should also be directed towards the goal of a higher frequency range of operation. This probably calls for design techniques that will solve the problem of stray capacitances in both the passive and active components. Compensation techniques may be found to take care of the problem of phase shift introduced in the active devices for high frequency cases.

However, the design objectives for filters will continue to be a relatively high stability margin, low sensitivity to active and passive components and temperature variations, the use of canonic numbers of capacitors, low spread of passive element values, the use of non-critical active devices, and high useful dynamic range.

BIBLIOGRAPHY

[1] R. P. Sallen, E. L. Key, "A Practical Method of Designing RC Active Filters", IRE Trans. Circuit Theory, Vol. CT-2, pp. 74-85, Mar. 1955.

[2] S. S. Haykim, "RC Active Filters Using An Amplifier as the Active Element", Proc. IEE, Vol. 112, No. 5, pp. 901-912, May 1965.

[3] W. J. Kerwin, L. P. Huelsman, "The Design of High-Performance Active RC Band-Pass Filters", IEEE Int. Conv. Rec. Vol. 14, Part 10, pp. 74-80, 1966.

[4] R. H. S. Riordan, "Simulated Inductors Using Differential Amplifiers, Electronics Letters, Vol. 3, No. 2, pp. 50-51, Feb. 1967.

[5] G. J. Deboo, "Application of a Gyrator-Type Circuit to Realize Ungrounded Inductors", Trans. Circuit Theory, pp. 101-102, Mar. 1967.

[6] W. J. Kerwin, L. P. Huelsman, R. W. Newcomb, "State-Variable Synthesis for Insensitive Integrated Circuit Transfer Functions", IEEE J. Solid-State Circuits, Vol. CS-2, pp. 87-92, Sept. 1967.

[7] L. T. Bruton, "Frequency Selectivity Using Positive Impedance Converter-Type Networks", Proc. IEEE, Vol. 56, pp. 1378-1379, Aug. 1968.

[8] P. R. Geffe, "RC-Amplifier Resonators for Active Filters", IEEE Trans. Circuit Theory, Vol. CT-15, pp. 415-419, Dec. 1968.

[9] D. Hilberman, R. D. Joseph, "Analysis and Synthesis of Admittance Matrices of RLC: VGUGA Common-Ground Networks", IEEE Trans. Circuit Theory, Vol. CT-15, No. 4, pp. 426-430, Dec. 1968.

[10] D. Hilberman, "Synthesis of Rational Transfer and Admittance Matrices with Active RC Common-Ground Networks Containing Unity-Gain Voltage Amplifiers", IEEE Trans. Circuit Theory, Vol. CT-15, No. 4, pp. 431-440, Dec. 1968.

[11] W. H. Holmes, W. E. Heinlein, "Sharp-Cutoff Low-Pass Filters Using Floating Gyrators", IEEE J. Solid-State Circuits, Vol. SC-4, pp. 38-50, Feb. 1969.

[12] L. T. Bruton, "Network Transfer Functions Using the Concept of Frequency-Dependent Negative Resistance", IEEE Trans. Circuit Theory, Vol. CT-16, pp. 406-408, Aug. 1969.

[13] J. Tow, "A Step-By-Step Active-Filter Design", IEEE Spectrum, Vol. 6, pp. 64-68, Dec. 1969.

[14] S. K. Mitra, "Filter Design Using Integrated Operational Amplifiers", Wescon Tech. Papers, Session 4, 1969.

[15] M. A. Soderstrand, S. K. Mitra, "Low Sensitivity Canonic Active RC Filters", IEEE Int. Symp. Circuit Theory, Symp. Dig., p.24, 1969.

[16] G. S. Moschytz, "The Operational Amplifier in Linear Active Networks", IEEE Spectrum, vol. 7, pp. 42-50, Jan. 1970.

[17] L. K. Cheung, "Synthesis of RC Active Filters Using Controlled Sources", Proc. IEE, Vol. 117, No. 3, pp. 539-544, Mar. 1970.

[18] G. S. Moschytz, "Fcn Filter Design Using Tantalum and Silicon Integrated Circuits", Proc. IEEE, Vol. 58, pp.550-566, Apr. 1970.

[19] A. Antoniou, "Novel RC-Active-Network Synthesis Using Generalized-Immittance Converters", IEEE Trans. Circuit Theory, Vol. CT-17, pp. 212-217, May 1970.

[20] P. R. Geffe, "Toward High Stability in Active Filters", IEEE Spectrum, Vol. 7, pp. 63-66, May 1970.

[21] H. J. Orchard, D. F. Sheahan, "Inductorless Bandpass Filters", IEEE J. Solid-State Circuits, Vol. SC-5, pp. 108-118, June 1970.

[22] R. M. Inigo, "Active Filter Realization Using Finite-Gain Voltage Amplifiers", IEEE Trans. Circuit Theory, Vol. CT-17, pp.445-448, Aug. 1970.

[23] R. Tarmy, M. S. Ghausi, "Very High-Q Intensitive Active RC Networks", IEEE Trans. Circuit Theory, Vol. CT-17, pp.358-366, Aug. 1970.

[24] G. S. Moschytz, "Second-Order Pole-Zero Pair Selection for Nth-Order Minimum Sensitivity Networks", IEEE Trans. Circuit Theory, Vol. CT-17, pp. 527-534, Nov. 1970.

[25] A. Antoniou, "Band-Pass Transformation and Realization Using Frequency-Dependent Negative-Resistance Elements", IEEE Trans. Circuit Theory, Vol. CT-18, pp. 297-299, Mar. 1971.

[26] L. C. Thomas, "The Biquad: Part 1- Some Practical Design Considerations", IEEE Trans. Circuit Theory, Vol. CT-18, pp. 350-357, May 1971. "The Biquad: Part 2- A Multipurpose Active Filtering System, IEEE Trans. Circuit Theory, Vol. CT-18, pp. 358-361, May 1971.

[27] T. A. Hamilton, A. S. Sedra, "Some New Configurations for Active Filters", IEEE Trans. Vol. CT-19, No. 1, pp. 25-33, Jan. 1972,

[28] A. G. J. Holt, M. R. Lee, "Sensitivity Comparison of Active-Cascade and Inductance-Simulation Schemes", Proc. IEE, Vol. 119, No. 3, Mar. 1972.

[29] L. T. Bruton, "Electronically Tunable Analog Active Filters", IEEE Trans. CT-19, No. 3, pp. 299-301, May 1972.

[30] L. Mattera, "Active Filters Get More of the Action", Electronics, Vol. 45, No. 13, pp. 104-109, June 19, 1972.

[31] E. H. C. Cheng, K. A. Stromsmoe, "Synthesis of Integrable High-Q Filters Using Grounded Unity-Gain Amplifiers", Int. J. Electronics, Vol. 33, No. 6, pp. 665-676, 1972.

[32] S. S. Haykim, "A Synthesis Procedure of RC Active Filters Using Unity-Gain Current and Voltage Amplifiers", Int. J. Control, Vol. 3, No. 6, pp. 553-564, 1966.

[33] D. Hazony, "Ground RC Unity-Gain Amplifier Transfer Vector Synthesis", IEEE Trans. Circuit Theory, Vol. CT-14, No. 1, pp. 75-76, Mar. 1967,

[34] G. S. Moschytz, "Sallen and Key Filter Networks with Amplifier Gain Larger Than or Equal to Unity", IEEE Journal of Solid-State Circuits, Vol. SC-2, No. 3, pp. 114-116, Sept. 1967.

[35] Y. F. Zai, "RC Active Filters Using Unity-Gain Amplifiers", Electronics Letters, Vol. 3, No. 10, pp. 461-462, Oct. 1967.

[36] D. F. Berndt and S. C. Dutta Roy, "Inductor Simulation Using a Single Unity-Gain Amplifier", IEEE J. of Solid-State Circuits, Vol. SC-4, No. 3, pp. 161-162, June 1969.

[37] D. Hazony, R. D. Joseph, "Transfer Matrix Synthesis with RC Networks", J. Siam Appl. Math., Vol. 14, No. 4, pp. 739-761, July 1966.

[38] J. Millman, Electronic Devices and Circuits, New York: McGraw-Hill, p. 353, 1967.

[39] A. J. Cote, Jr., J. B. Oakes, Linear Vacuum-Tube and Transistor Circuits, New York: McGraw-Hill, pp. 154-155, 1961,

[40] D. A. Calahan, "Restrictions on the Natural Frequencies of an RC-RL Network", J. Franklin Inst., Vol. 272, No. 2, pp. 112-133, Aug. 1961.

[41] D. A. Calahan, "Sensitivity Minimization in Active RC Synthesis", IRE. Trans. Circuit Theory, Vol. CT-9, No. 1, pp. 38-42, Mar. 1962.

[42] I. M. Horowitz, "Optimization of Negative Impedance Concersion Methods of Active RC Synthesis", IRE Circuit Theory, Vol. CT-6, No. 3, pp. 296-303, Sept. 1959.

[43] D. A. Calahan, "Notes on the Horowitz Optimization Procedure", IRE Circuit Theory, Vol. CT-7, No. 3, pp. 352-354, Sept. 1960.

[44] L. P. Huelsmen, "Active RC Synthesis with Prescribed Sensitivities", Proc. Nat. Electron Conf., Vol. 16, pp. 412-426, 1960.

[45] L. P. Huelsman, Theory and Design of Active RC Circuits, New York: McGraw-Hill, 1968.

[46] K. R. Rao, S. Venkateswaran, "Synthesis of Inductors and Gyrators with Voltage-Controlled Voltage Sources", Electronics Letters, Vol. 6, No. 2, pp. 29-30, Jan. 22, 1970.

[47] R. E. Bach, Jr., "Selecting R-C Values for Active Filters", Electronics, Vol. 33, pp. 82-85, May 13, 1960.

[48] L. J. Sevin, Field Effect Transistors, New York: McGraw-Hill, p. 105, 1965.

[49] R. W. Newcomb, Active Integrated Circuit Synthesis, New Jersey: Prentice-Hall, 1968.

[50] S. K. Mitra, Analysis and Synthesis of Linear Active Networks. New York: John Wiley & Sons, 1969.

[51] K. L. Su, Active Network Synthesis, New York: McGraw-Hill, 1965.

[52] A. I. Zverev, Handbook of Filter Synthesis, New York: John Wiley & Sons, 1967.

[53] E. Christian, E. Eisenmann, Filter Design Tables and Graphs , New York: John Wiley & Sons, 1966.

[54] J. L. Herrero, G. Willoner, Synthesis of Filters , Toronto: Prentice-Hall", 1966.

[55] J. W. Craig, Design of Lossy Filters , Cambridge, Massachusetts: The M.I.T. Press, 1970.

[56] G. E. Hamsell, Filter Design and Evaluation , New York: Van Nostrand Reinhold, 1969.

[57] Y. J. Lubkin, Filter Systems and Design , Massachusetts: Addison-Wesley, 1970.

APPENDIX A

Realizing an Inverse-L and a ¶ of Inductors

In synthesizing high-order polynomial band-pass filters transformed from the corresponding low-pass ones, one has to realize sections of inductors in the shape of an inverse-L. The short-circuit admittance parameters derived from the networks, shown in Fig. (A.1), are identical as given by

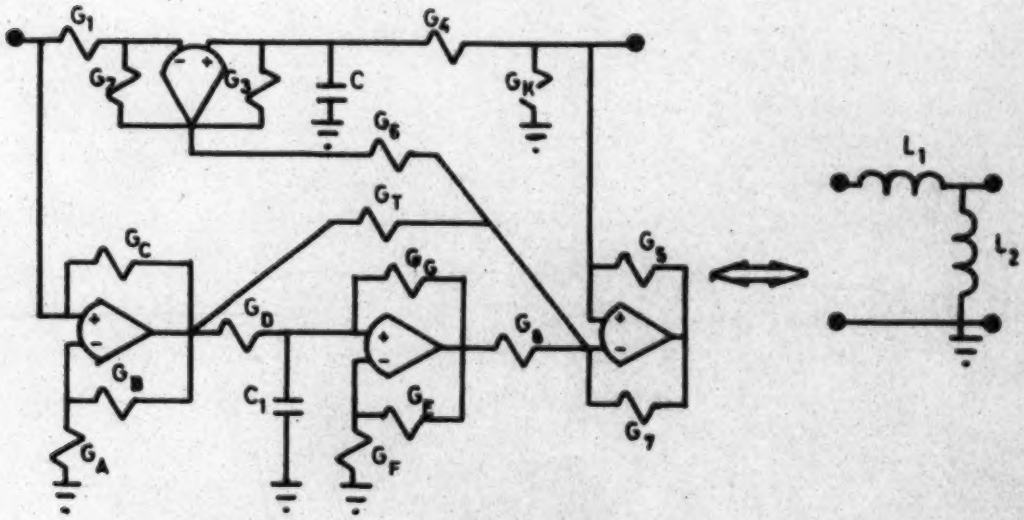

Figure (A.1) Realizing an inverse-L of inductors.

$$Y_{11} = \frac{G_1G_2(G_4 + CP)}{G_2CP + G_2G_4 - G_1G_3} - \frac{G_AG_C}{G_B} = \frac{G_1G_4}{CP} + G_1 - \frac{G_AG_C}{G_B} = \frac{1}{L_1P} ,$$

$$- Y_{12} = \frac{G_1G_4}{CP} = \frac{1}{L_1P} ,$$

$$- Y_{21} = \frac{1}{CP} \left[\frac{G_1G_5G_6}{G_2G_7}(G_3 + G_4) - \frac{G_1G_3G_4}{G_2} - (1 + \frac{G_F}{G_E})(1 + \frac{G_A}{G_B}) \frac{G_5G_8G_DG_C}{G_7C_1} \right]$$

$$+ \frac{G_1G_5G_6}{G_2G_7} - \frac{G_5G_T}{G_7}(1 + \frac{G_A}{G_B}) = \frac{1}{L_1P} ,$$

$$Y_{22} = \frac{1}{CP} \left[\frac{G_1G_4G_5G_6}{G_2G_7} + \frac{G_4G_5G_6}{G_7} - \frac{G_1G_3G_4}{G_2} \right] + G_4 + G_K - \frac{G_5}{G_7}(G_8 + G_T + G_6)$$

$$= \frac{1}{L_1P} + \frac{1}{L_2P} ,$$

provided $G_1 = G_2 = G_3 = G_4 = G_5 = G_7 = G_A = G_B = G_C = G_D = G_E = G_F = G_G = G$,

$$G_6 = G_8 = G(1 + \frac{1}{2K}) , \quad G_T = \frac{G}{2}(1 + \frac{1}{2K}) ,$$

$$G_K = \frac{G}{2}(3 + \frac{5}{2K}) , \quad C = L_1G^2 ,$$

$$C_1 = 4CK(1 + \frac{1}{2K}) , \text{ where } L_2 = KL_1 .$$

This circuit has been used to realize a fourth-order, band-pass, Butterworth filter for $Q = 5.0$, $\omega_0 = 5\times10^3$ rad/sec . Due to the great difference in magnitude in the order of Q^2 between L_1 and L_2 , the filter was found sensitive to passive component values and was shelved, although other conditions such as stability were satisfied. However, this circuit may find application in a design where approximately equal values of L_1 and L_2 are required.

The simulation of a π of inductors will be illustrated by the following two methods. It will find application at least in Orchard and Sheahen's design [21] where high-order Cauer band-pass filter can be realized by synthesizing sections of π's of inductors.

The two two-port networks as shown in Fig. (A.2) are equivalent with their short-circuit admittance parameters given by

$$Y_{11} = \frac{1}{P}\left(\frac{G_1G_4}{C} + \frac{G_AG_TG_Z}{G_WC_9}\right) + \left(G_1 - G_A\frac{C_B}{C_9}\right) = \frac{1}{L_1P} + \frac{1}{L_3P} ,$$

$$-Y_{12} = \frac{G_1G_4}{CP} = \frac{1}{L_1P} ,$$

$$-Y_{21} = \frac{1}{CP}\left[\frac{G_1G_5G_6}{G_2G_7}(G_3 + G_4) - \frac{G_1G_3G_4}{G_2} - \frac{G_AG_5G_8C}{G_7C_9}\right] + \frac{G_1G_5G_6}{G_2G_7} - \frac{G_5G_8}{G_7}$$

$$= \frac{1}{L_1P} ,$$

$$Y_{22} = \frac{1}{CP}\left[\frac{G_1G_4G_5G_6}{G_2G_7} + \frac{G_4G_5G_6}{G_7} - \frac{G_1G_3G_4}{G_2}\right] + G_4 + G_K - \frac{G_5G_8}{G_7} - \frac{G_5G_6}{G_7}$$

$$= \frac{1}{L_1P} + \frac{1}{L_2P} \quad ,$$

provided $G_1 = G_2 = G_3 = G_4 = G_5 = G_7 = G_A = G_W = G_Z = G$,

$G_6 = G_8 = G\left(1 + \frac{1}{2K}\right)$, $G_K = G\left(1 + \frac{1}{K}\right)$, $G_T = \frac{KG(1 + 1/2K)}{K'}$,

$C = L_1G^2$, $C_B = C_9 = L_1G^2K(1 + 1/2K)$,

where $L_2 = KL_1$, $L_3 = K'L_1$.

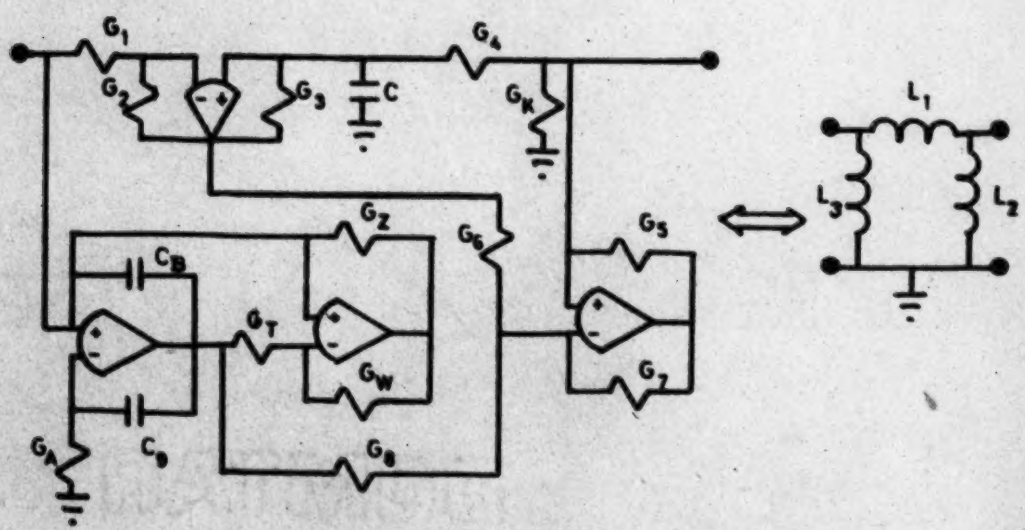

Figure (A.2) Realizing a ↕ of inductors.

The second method which makes use of the resistive NIV can be illustrated by the two equivalent two-port networks as shown in Fig. (A.3).

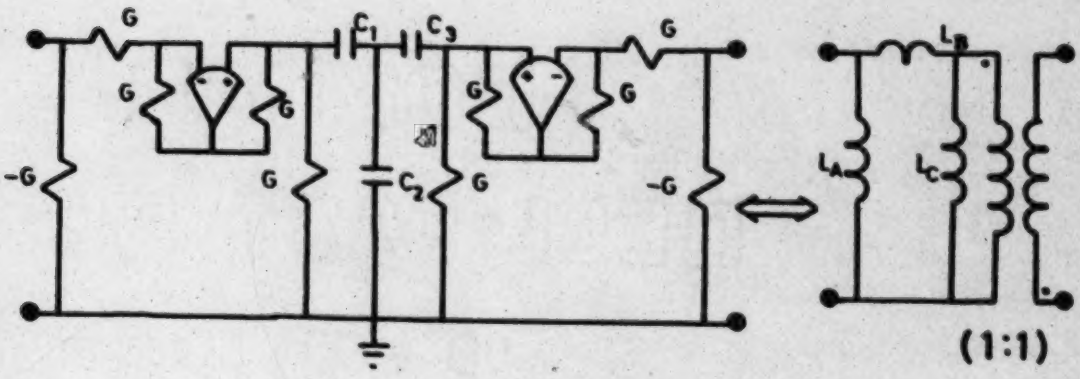

Figure (A.3) Realizing a 1 of inductors and an inverse-polarity ideal transformer by NIV's.

The short-circuit admittance parameters are given by

$$Y_{11} = G^2\left(\frac{1}{C_1P} + \frac{1}{C_2P}\right) = \frac{1}{L_AP} + \frac{1}{L_BP} ,$$

$$Y_{12} = Y_{21} = \frac{G^2}{C_2P} = \frac{1}{L_BP} ,$$

$$Y_{22} = G^2\left(\frac{1}{C_2P} + \frac{1}{C_3P}\right) = \frac{1}{L_BP} + \frac{1}{L_CP} .$$

APPENDIX B

Realizing a Second-Order Polynomial Band-Pass Filter

The circuit in Fig. (A.4) yields a voltage transfer function of

$$\frac{V_2}{V_1} = \frac{P/CR}{P^2 + P/CR + 1/LC} \quad , \text{ where } L = CR_1^2 \ .$$

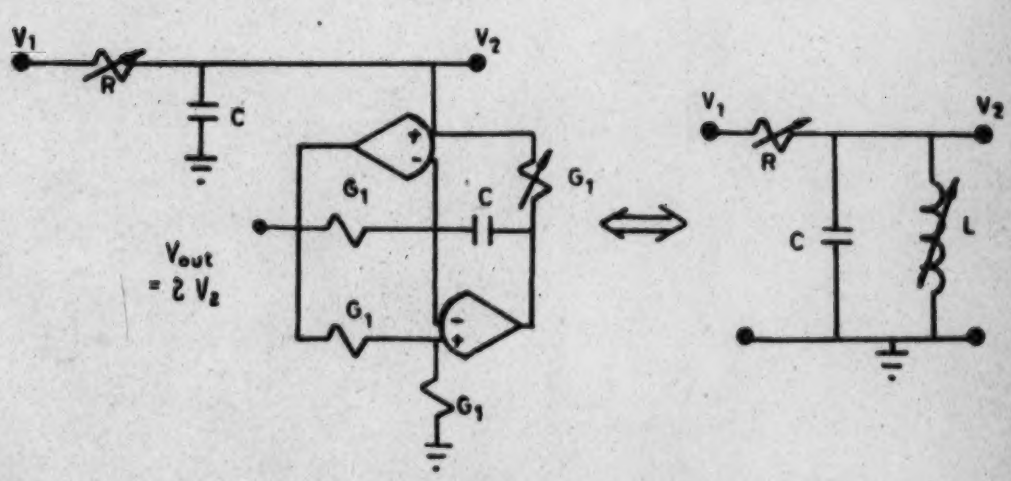

Figure (A.4) A second-order polynomial band-pass filter.

The output can be taken from $V_{out} = 2V_2$ for isolation purposes and the filter has the advantage of independent adjustments of Q and ω_0 by trimming two resistors.

APPENDIX C

Harmonic Distortions of Filter Using State-Variable Technique

The percentage harmonic distortions of the second-order band-pass filter with Q = 30, $\omega_0 = 10^5$ rad/sec at some typical frequencies are measured by a DONNER'S Wave Analyzer (Model 2102) as below:

harmonics	center freq.		lower 3db point		higher 3db point	
	second	third	second	third	second	third
$V_0 = V_{in}$ = - 20 dbm at resonance						
V_{in}	0.055	0.02	0.075	0.03	0.075	0.03
V_{out}	0.063	0.03	0.2	0.1	0.13	0.11
$V_0 = V_{in}$ = - 1.85 dbm at resonance						
V_{in}	0.094	0.034	0.093	0.045	0.083	0.033
V_{out}	0.24	0.036	0.107	0.07	0.185	0.038

APPENDIX D

Measured Data of Very High-Q Band-Pass Filter

(A) The following data are taken for the specifications of Q = 500, f_0 = 1.5917 KHz.

(1) f_0 = 1.5917 KHz,
lower 3db point, f_1 = 1.5901 KHz,
higher 3db point, f_2 = 1.5933 KHz,
Q = 497.4 (- 0.52%).

(2) f_0 = 1.5916, f_1 = 1.5901, f_2 = 1.5933, Q = 497.4 .

(3) f_0 = 1.5919, f_1 = 1.5901, f_2 = 1.5933, Q = 497.4 .

(4) f_0 = 1.5916, f_1 = 1.5901, f_2 = 1.5933, Q = 497.4 .

(5) f_0 = 1.5917, f_1 = 1.5901, f_2 = 1.5933, Q = 497.4 .

(6) f_0 = 1.5919, f_1 = 1.5901, f_2 = 1.5933, Q = 497.4 .

(7) After four hours of continuous operation;
f_0 = 1.5916, f_1 = 1.5900, f_2 = 1.5932, Q = 497.4 .

(8) Power supply is switched off and on,
f_0 = 1.5917, f_1 = 1.5899, f_2 = 1.5931, Q = 497.4 .

(9) The circuit is turned on next day, after warming up for a few minutes;
f_0 = 1.5916, f_1 = 1.5902, f_2 = 1.5934, Q = 497.4 .

(B) Two measurements for very high-Q values are recorded by varying R_X only.

(1) V_{out} (resonance) = 0.5 v. (P-P),

$$Q = \frac{1.5915}{1.5919 - 1.5910} = 1768 \ .$$

(2) V_{out} (resonance) = 0.58 v. (P-P),

$$Q = \frac{1.5913}{1.5916 - 1.5912} = 3978 \ .$$

Both f_1 and f_2 are measured twice to be the same as those above, wave-form is very stable with no drifting at all.

(C) Measurements of Q and f_0 when power supply voltages (V^+ and V^-) vary.

(1) After measurement (B), filter is reset to have

$f_0 = 1.5912$,

$f_1 = 1.5928$,

$f_2 = 1.5896$,

$Q = 497.25$,

which are measured twice at

$V^+ = 14.99$ v,

$V^- = -14.99$v .

(2) Different supply voltages

$V^- = -14.99$

V^+	15.73	16.48	17.99	19.50	21.01	22.5	13.49	11.99	10.51	9.00	7.50
$\Delta V^+(\%)$	5	10	20	30	40	50	-10	-20	-30	-40	-50
f_0	1.5913	1.5913	1.5912	1.5911	1.5913	1.5911	1.5913	1.5912	1.5912	1.5912	1.5912
$\Delta f_0(\%)$	.0063	.0063	0	-.0063	.0063	-.0063	1.5913	1.5912	1.5912	1.5912	1.5912
f_2	1.5928	1.5927	1.5927	1.5928	1.5927	1.5927	1.5927	1.5928	1.5928	1.5928	1.5928
f_1	1.5895	1.5895	1.5894	1.5895	1.5895	1.5894	1.5895	1.5896	1.5896	1.5896	1.5896
Q	482.2	497.28	482.18	482.16	497.28	482.16	497.28	497.25	497.25	497.25	497.25
$\Delta Q(\%)$	-1.005	.006	-3.02	-3.02	.006	-3.02	.006	0	0	0	0

(3) $V^+ = 16.49\ (10\%)$,

$V^- = -\ 16.49\ (-\ 10\%)$;

$\frac{\Delta f_0}{f_0} = 0\%$,

$\frac{\Delta Q}{Q} = 0\%$.

(4) $V^+ = 16.48\ (10\%)$,

$V^- = -\ 13.49\ (10\%)$;

$$Q = \frac{1.5911}{1.5928 - 1.5897} = 513.26,$$

$\frac{\Delta f_0}{f_0} = -\ 0.0063\ \%$,

$\frac{\Delta Q}{Q} = 3.2\ \%$.

(5) $V^+ = 13.49\ (-\ 10\ \%)$,

$V^- = -\ 13.49\ (\ 10\ \%)$;

$$Q = \frac{1.5914}{1.5928 - 1.5898} = 530.5\ ,$$

$\frac{\Delta f_0}{f_0} = 0.0126\ \%$,

$\frac{\Delta Q}{Q} = 6.6\ \%$.

(6) $V^+ = 13.5\ (-\ 10\ \%)$, $V^- = -\ 16.49\ (-\ 10\ \%)$;

$$Q = \frac{1.5915}{1.5932 - 1.5899} = 482.3\ ,$$

$\frac{\Delta f_0}{f_0} = 0.0189\ \%$, $\frac{\Delta Q}{Q} = -\ 3.02\ \%$.

(7) After another three hours, the following data are recorded

$V^+ = 14.99$

V^-	-13.49	-12.0	-10.01	-8.99	-7.49	-16.5	-18.01	-19.5	-21.0	-22.5
$\Delta V^-(\%)$	10	20	33.3	40	50	-10	-20	-30	-40	-50
f_0	1.5915	1.5914	1.5914	1.5912	1.5913	1.5915	1.5915	1.5915	1.5916	1.5916
$\Delta f_0(\%)$	.0189	.0126	.0126	0	.0063	.0189	.0189	.0189	.0189	.0252
f_2	1.5930	1.5930	1.5929	1.5929	1.5928	1.5931	1.5932	1.5932	1.5932	1.5932
f_1	1.5897	1.5898	1.5898	1.5898	1.5897	1.5899	1.5899	1.5899	1.5899	1.5899
Q	482.3	497.23	513.35	513.29	513.32	497.23	482.3	482.3	482.33	482.33
$\Delta Q(\%)$	-3.02	.004	3.2	3.2	3.2	-.004	-3.02	-3.02	-3.02	-3.02

(8) $V^+ = 14.99$,

$V^- = -14.99$;

$f_0 = 1.5912$,

$$Q = \frac{1.5912}{1.5928 - 1.5896} = 497.3 .$$

APPENDIX E

Measurements of Sixth-Order Low-Pass Filter

(A) Measuring the 3db point in Hz ;

when V_{out} = 15 dbm (at low freq.)

V_{in} = 9.5 dbm ,

for V^+ = 15 v ,

V^- = - 15 v ,

six data are taken for the 3db point as below

f_{-3db} = 795.4, 795.5, 795.4, 795.5, 795.3, 795.5.

Therefore, f_{-3db} = 795.4333 (- 0.0427%) on the average.

(B) At different drive levels ;

(1) V_{out} = 5 dbm (at low freq.), V_{in} = - 0.5 dbm,

f_{-3db} = 795.3.

(2) V_{out} = - 5 dbm (at low freq.), V_{in} = - 10.5 dbm,

f_{-3db} = 795.5.

(C) Variations in power supply voltages when

V_{out} = 15 dbm (at low freq.), V_{in} = 9.5 dbm;

(1) V^+ = 20 v, V^- = - 20 v,

f_{-3db} = 795.4.

(2) V^+ = 20 v, V^- = - 10 v,

f_{-3db} = 795.5.

(3) V^+ = 10 v, V^- = - 20 v,

f_{-3db} = 795.3.

(4) V^+ = 10 v, V^- = - 10 v,

f_{-3db} = 795.4.

(D) The maximum drive level before the output amplifier saturates;

V_{out} = 18 dbm (6.1 v RMS),

V_{in} = 12 dbm (3.3 v RMS).

(E) D.C. power consumption;

with maximum drive level as in (D),

Power = 0.45 watts which includes power supply to the first buffer stage.

(F) Ripple in the pass-band is observed to be approximately 0.1 db.

(G) At Temp. = 70°C (158°F),

f_{-3db} = 791 Hz (- 0.558%).

APPENDIX F

Measurements of Fourth-Order Band-Pass Filters

(A) The following data are recorded for a band-pass filter of Q = 5, f_0 = 795.774 Hz.

(1) Maximum drive level before the first amplifier saturates is

V_{out} = 9.2 v (P-P),

V_{in} = 6.8 v (P-P).

(2) Frequency response in magnitude is plotted for

V_{out} = 8 dbm,

V_{in} = 4.8 d-m.

(3) Center and half-power frequencies;

f_1 = 718.3 Hz,

f_2 = 885.0 Hz,

f_0 = 806 Hz (1.26%),

Q = 4.835 (-3.3%).

(4) D.C. power consumption;

with input at maximum amplitude and without input signal,

Power = 0.270 watts

which includes the power supplied to the buffer stage.

(B) The following data are recorded for the same filter but with Q = 31.33.

(1) Center and half-power frequencies;

f_0(Hz)	f_2(Hz)	f_1(Hz)
794.2	808.5	783.5
794.1	808.4	783.5
794.0	808.4	783.4
794.1	808.6	783.4
793.9	808.5	783.4
794.0	808.5	783.4

f_0 (average) = 795.776 Hz (-0.217%),

Q (average) = 31.76 (0.43%).

(2) By varying R" only, several higher Q values are recorded;

$$Q_1 = \frac{793.7}{797.5 - 790.3} = 111.8,$$

$$Q_2 = \frac{795.7}{797 - 794.2} = 284.2,$$

$$Q_3 = \frac{795.7}{796.5 - 795.1} = 568.4.$$

However, at measuring Q_3, the output wave-form may drift about 1db at resonance, but the half-power points are quite stable.

(3) Maximum drive level is

V_{out} = 1.9 v (P-P) = - 0.6 dbm,

V_{in} = 1.3 v (P-P) = - 4.7 dbm.

(4) D.C. power consumption is 0.255 watts at resonance (V_{in} = - 6.4 dbm), or 0.241 watts for no input signal.

APPENDIX G

Measurements of a Twelfth-Order Band-Pass Filter

(A) Frequency response in magnitude is plotted for

V_{in} = 4.6 dbm,

V_{out} = 0 dbm, at resonances.

(B) Resonance is defined to be the case when V_{out} and V_{in} are exactly 180° out of phase.

(C) Center and half-power frequencies;

f_0 (Hz)	f_2 (Hz)	f_1 (Hz)
799.3	841.0	760.2
799.0	840.9	760.2
799.2	841.0	760.1
799.3	841.0	760.2
799.3	841.0	760.2
799.3	841.0	760.2

f_0 (average) = 799.233 Hz (0.435%),

Q (average) = 9.8915 (-1.085%).

(D) Different drive levels;

V_{in} = - 10 dbm,

f_0 = 799.3 Hz (0.44%),

$$Q = \frac{799.3}{841.1 - 760.2} = 9.88 \ (-1.2\%).$$

V_{in} = - 20 dbm,

f_0 = 799.3 (0.44%),

$$Q = \frac{799.3}{841.1 - 760.2} = 9.88 \ (-1.2\%)$$

(E) Variations in power supply voltages;

V_{out}(dbm)	0	- 10	- 10	- 10
V^+	20	20	10	10
V^-	- 20	- 10	- 20	- 10
f_0	799.8	798.8	799.8	798.8
Δf_0(%)	0.503	0.38	0.503	0.38
f_2	841.3	840.7	841.8	840.8
f_1	760.8	759.5	760.8	759.2
Q	9.94	9.84	9.87	9.8
ΔQ(%)	- 0.6	- 1.6	- 1.3	- 2.0

(F) Maximum drive level is

V_{in} = 6.8 dbm (4.8 v P-P).

(G) D. C. power consumption;

with maximum V_{in} and without input signal

Power = 0.555 watts (including power supplied to the buffer stage).

(H) For Temp. = 70°C (150°F);

if the same zero DB line on the graph for

T = 22°C is used,

$$Q = \frac{799.233}{842 - 764.3} = 10.28 \ (2.8\%);$$

if one uses (- 0.5 db) as the zero DB reference,

$$Q = \frac{799.233}{843 - 763} = 9.9904 \ (- 0.096\%) \ .$$

APPENDIX H

Measurements of the Sixth-Order Cauer Band-Stop Filter

(A) Maximum drive level is

V_{in} = 0.015 v (P-P).

(B) D. C. power consumption is

0.765 watts for maximum drive level at the stop-band, and

0.517 watts at the pass-band or without signal input.

(C) Different supply voltages;

for V^+ = 10 v, V^- = - 10 v,

f_0 = 2180 Hz (- 0.14%),

f_A = 2083 Hz (0%),

f_B = 2284 Hz (-0.092%),

Q = 5.55 (- 0.673%),

minimum attenuation is 31.3 db;

for V^+ = 18 v, V^- = - 18 v,

f_0 = 2183 Hz (0%),

f_A = 2083 Hz (0.048%),

f_B = 2289 Hz (0.13%),

Q = 5.5 (- 1.57%),

minimum attenuation is 31.0 db.

(D) D. C. offset voltage at the output is 28 mv.

(E) For Temp. = 45°C (113°F);

f_0 = 2175 Hz (- 0.37%),

f_A = 2084 Hz (0.048%),

f_B = 2289 Hz (0.13%),

Q = 5.5203 (- 1.2%).

(F) For T = 70°C(158°F);

f_0 = 2173 Hz (- 0.46%),

f_A = 2090 Hz (0.34%),

f_B = 2296 Hz (0.438%),

Q = 5.49 (-1.45%).

APPENDIX I

Experimental Apparatus

Voltmeter:	H. P., VTVM Model 400D
Digital Multimeter:	Fairchild, Model 7000
D. C. Power Supply:	Harrison, Model 6205A
Oscilloscope:	Tektronix, Type 546
Signal Generator:	H. P. Model 202C, 209A
Digital Frequency Counter:	G. R., Type 1151-A
Temperature Chamber:	Delta Design, Model MK 6300
Impedance Bridge:	G. R., Type 1650-A
Harmonic Distortion Analyzer:	Donner, Model 2102

In measuring effects due to temperature variations, only the filter circuit board was left inside the temperature chamber.

APPENDIX J

Operational Amplifier 741C Specifications

absolute maximum ratings

Supply Voltage	LM741	±22V
	LM741C	±18V
Power Dissipation (Note 1)		500 mW
Differential Input Voltage		±30V
Input Voltage (Note 2)		±15V
Output Short-Circuit Duration		Indefinite
Operating Temperature Range	LM741	-55°C to 125°C
	LM741C	0°C to 70°C
Storage Temperature Range		-65°C to 150°C
Lead Temperature (Soldering, 10 sec)		300°C

electrical characteristics (Note 3)

PARAMETER	CONDITIONS	LM741			LM741C			UNITS
		MIN	TYP	MAX	MIN	TYP	MAX	
Input Offset Voltage	$T_A = 25°C$, $R_S < 10 k\Omega$		1.0	5.0		1.0	6.0	mV
Input Offset Current	$T_A = 25°C$		30	200		30	200	nA
Input Bias Current	$T_A = 25°C$		300	500		200	500	nA
Input Resistance	$T_A = 25°C$	0.3	1.0		0.3	1.0		MΩ
Supply Current	$T_A = 25°C$, $V_S = ±15V$		1.7	2.8		1.7	2.8	mA
Large Signal Voltage Gain	$T_A = 25°C$, $V_S = ±15V$ $V_{OUT} = ±10V$, $R_L > 2 k\Omega$	50	160		25	160		V/mV
Input Offset Voltage	$R_S \leq 10 k\Omega$			6.0			7.5	mV
Input Offset Current				500			300	nA
Input Bias Current				1.5			0.8	μA
Large Signal Voltage Gain	$V_S = ±15V$, $V_{OUT} = ±10V$ $R_L > 2 k\Omega$	25			15			V/mV
Output Voltage Swing	$V_S = ±15V$, $R_L = 10 k\Omega$	±12	±14		±12	±14		V
	$R_L = 2 k\Omega$	±10	±13		±10	±13		V
Input Voltage Range	$V_S = ±15V$	±12			±12			V
Common Mode Rejection Ratio	$R_S < 10 k\Omega$	70	90		70	90		dB
Supply Voltage Rejection Ratio	$R_S < 10 k\Omega$	77	96		77	96		dB

Note 1: The maximum junction temperature of the LM741 is 150°C, while that of the LM741C is 100°C. For operating at elevated temperatures, devices in the TO-5 package must be derated based on a thermal resistance of 150°C/W, junction to case.

Note 2: For supply voltages less than ±15V, the absolute maximum input voltage is equal to the supply voltage.

Note 3: These specifications apply for $V_S = ±15V$ and $-55°C \leq T_A \leq 125°C$, unless otherwise specified. With the LM741C, however, all specifications are limited to $0°C \leq T_A \leq 70°C$ and $V_S = ±15V$.